DISK INCLUDED

SECOND EDITION

MECHANISM DESIGN

Analysis and Synthesis

VOLUME I

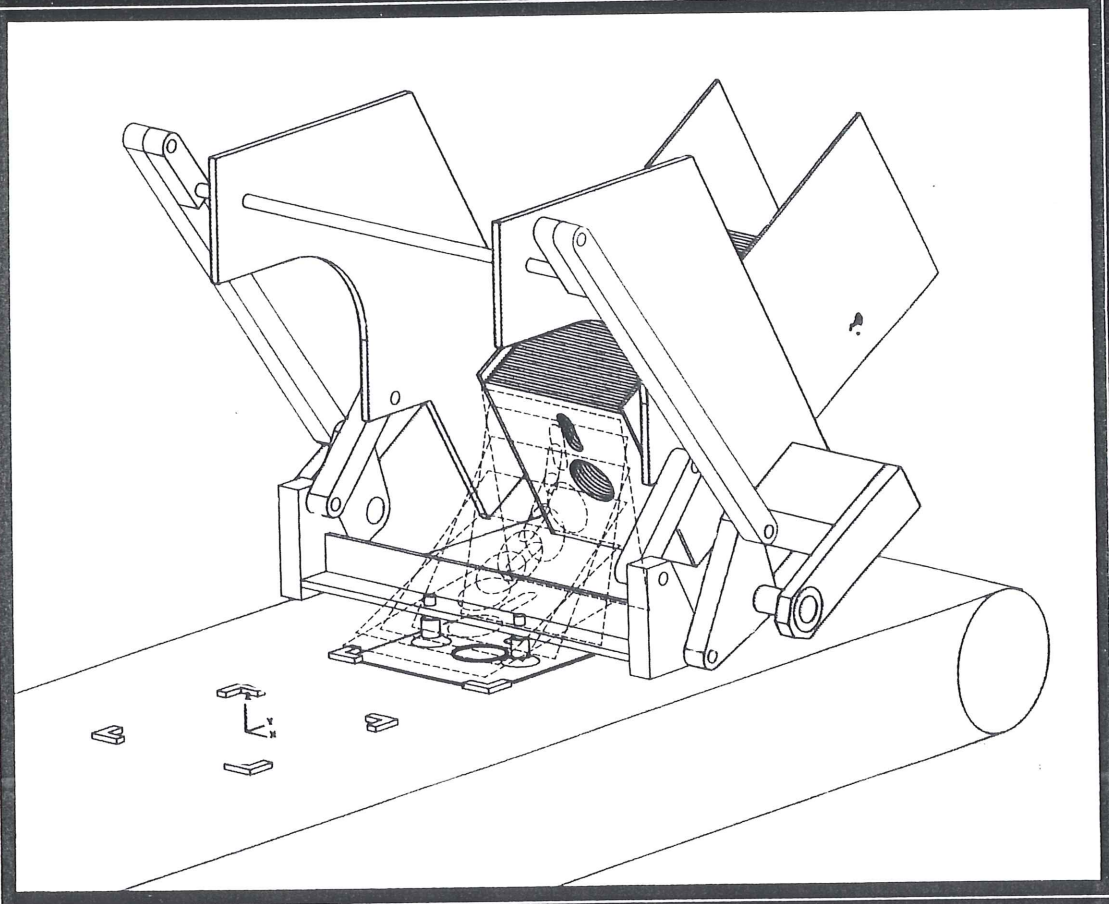

Arthur G. Erdman / George N. Sandor

chapter eight

Introduction to Kinematic Synthesis–Graphical and Linear Analytical Methods

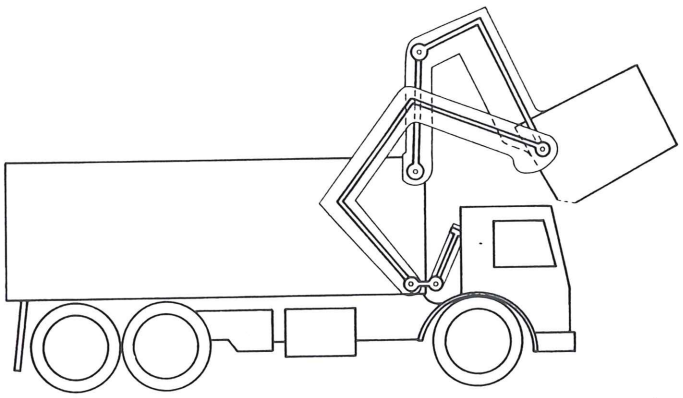

8.1 INTRODUCTION

Ampère defined kinematics as "the study of the motion of mechanisms and methods of creating them." The first part of this definition deals with kinematic *analysis*. Given a certain mechanism, the motion characteristics of its components will be determined by kinematic analysis (as described in Chap. 3). The statement of the task of analysis contains all principal dimensions of the mechanism, interconnections of its links, and the specification of the input motion or method of actuation. The objective is to find the displacements, velocities, accelerations, shock or jerk (second acceleration), and perhaps higher accelerations of the various members, as well as the paths described and motions performed by certain elements. In short, *in kinematic analysis we determine the performance of a given mechanism*. The second part of Ampère's definition may be paraphrased in two ways:

1. The study of methods of creating a given motion by means of mechanisms.
2. The study of methods of creating mechanisms having a given motion.

In either version, the *motion* is given and the mechanism is to be found. This is the essence of *kinematic synthesis*. Thus kinematic synthesis deals with the *systematic design of mechanisms for a given performance*.

The areas of synthesis may be grouped into two categories.

1. *Type synthesis*. Given the required performance, what type of mechanism will be suitable? (Gear trains? Linkages? Cam mechanisms?) Also: How many links should the mechanism have? How many degrees of freedom are required? What configuration is desirable? And so on. Deliberations involving the number of links and degrees of freedom are often referred to as the province of a subcategory of type synthesis called *number synthesis,* pioneered by Gruebler (see Chap. 1). One of the techniques of type synthesis which utilizes the "associated linkage" concept is described in Sec. 8.3.

2. *Dimensional synthesis*. The second major category of kinematic synthesis is best defined by way of its objective:

> Dimensional synthesis seeks to determine the significant dimensions and the starting position of a mechanism of preconceived type for a specified task and prescribed performance.

Principal or *significant dimensions* mean link lengths or pivot-to-pivot distances on binary, ternary, and so on, links, angle between bell-crank levers, cam-contour dimensions and cam-follower diameters, eccentricities, gear ratios, and so forth (Fig. 8.1). Configuration or *starting position* is usually specified by way of an angular position of an input link (such as a driving crank) with respect to the fixed link or frame of reference, or the linear distance of a slider block from a point on its guiding link (Fig. 8.2).

A *mechanism of preconceived type* may be a slider-crank, a four-bar linkage, a cam with flat follower, or a more complex linkage of a certain configuration defined topologically but not dimensionally (geared five-bar, Stevenson or Watt six-bar linkage, etc.), as depicted in Fig. 8.3.

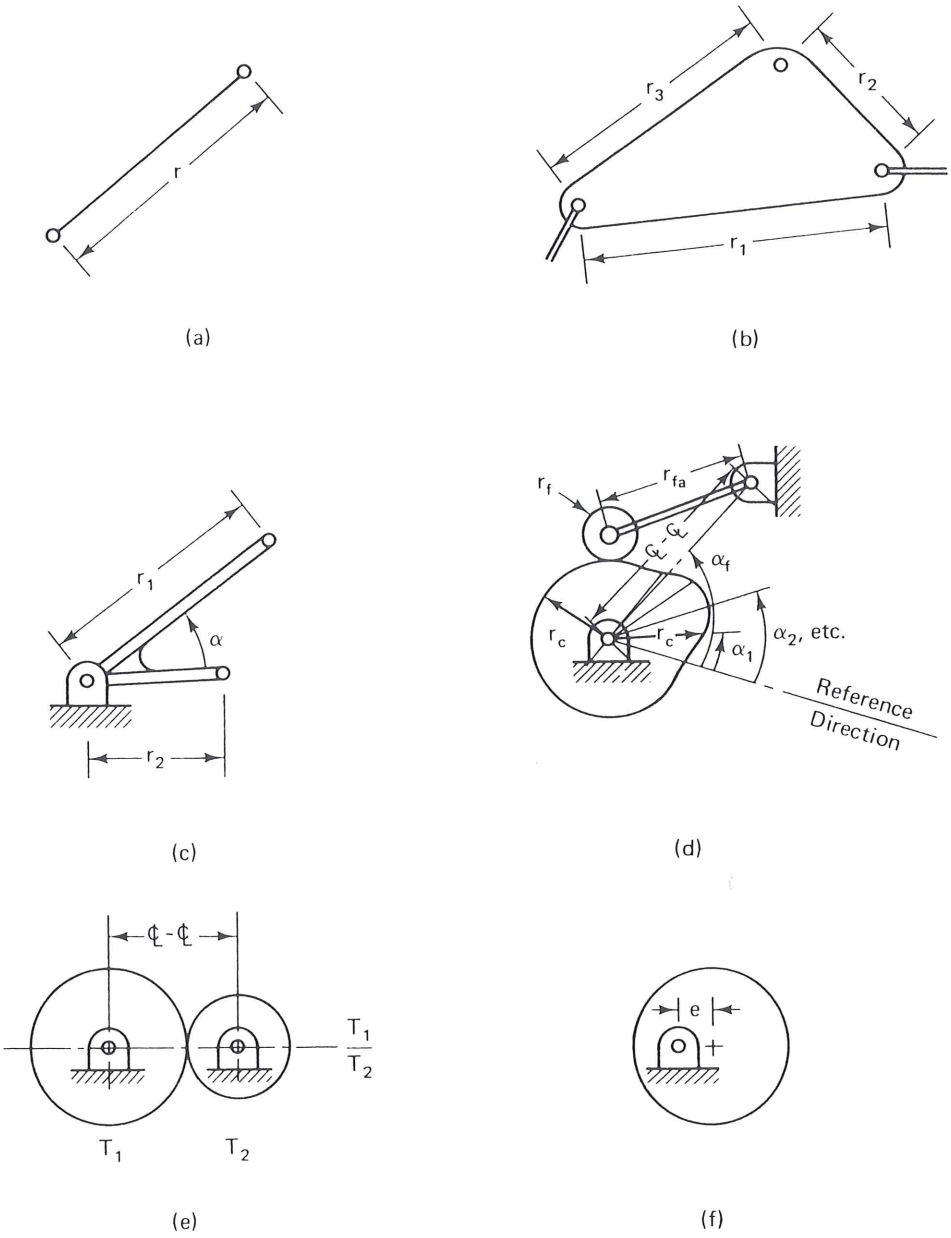

Figure 8.1 Significant dimensions; (a) binary link: has one length only; (b) ternary link: 3 lengths, 2 lengths and one angle, or 1 length and two angles; (c) bell crank: same as for ternary link; (d) cam and roller follower: center line distance, follower arm length r_{fa}, follower radius r_f, and an infinite number of radial distances to the cam surface, r_c, at angles α_1, α_2, etc., specified from a reference direction; (e) gear pair: center line distance and gear tooth ratio; (f) eccentric: eccentricity only (this is a binary link).

8.2 TASKS OF KINEMATIC SYNTHESIS

Recall from Chap. 1 that there are three customary *tasks* for kinematic synthesis: *function, path,* and *motion* generation.

In *function generation* rotation or sliding motion of input and output links must be correlated. Figure 8.4a is a graph of an arbitrary function $y = f(x)$. The kinematic synthesis task may be to design a linkage to correlate input and output such that as the input

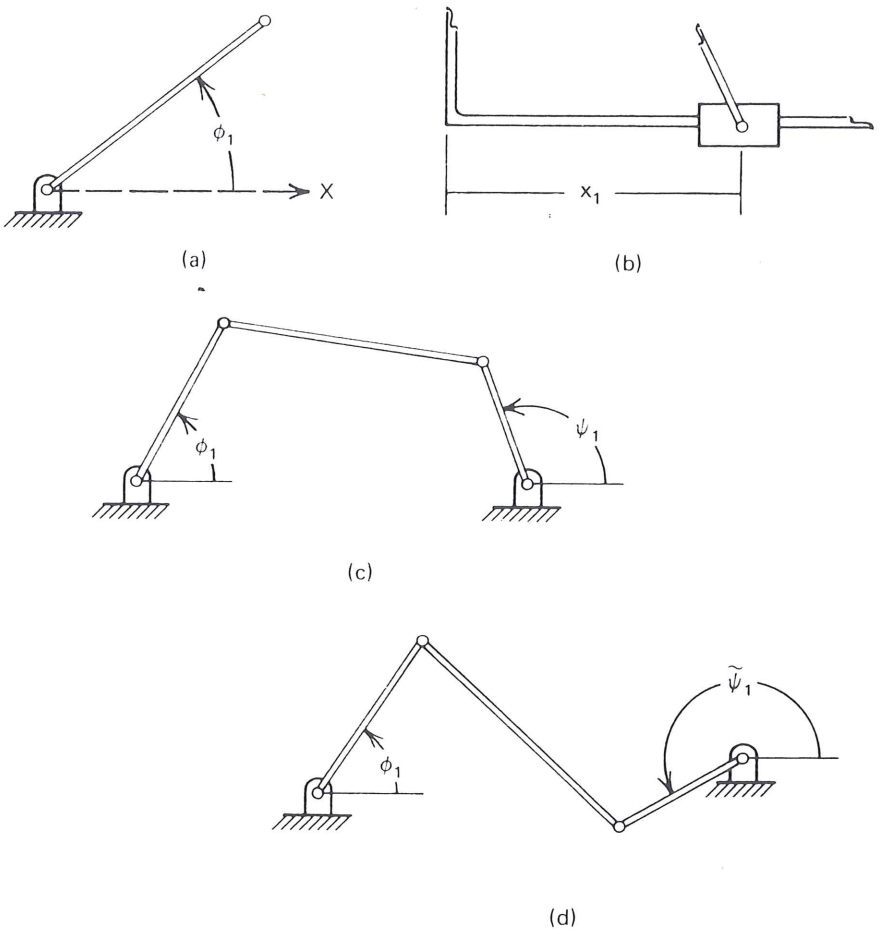

Figure 8.2 Configuration or starting position: (a) starting position of a crank; (b) starting position of a slider; (c) starting position of a four-bar linkage requires two crank angles, because one crank angle leaves two possibilities for the other crank, as shown in Fig. 8.2(d).

moves by x, the output moves by $y = f(x)$ for the range $x_0 \leq x \leq x_{n+1}$. Values of the independent parameter, $x_1, x_2, \ldots, x_n$ correspond to prescribed *precision points* $P_1, P_2, \ldots, P_n$ on the function $y = f(x)$ in a range of x between x_0 and x_{n+1}. In the case of rotary input and output, the angles of rotation ϕ and ψ (Fig. 8.5a) are the linear analogs of x and y, respectively. When the input is rotated to a value of the independent parameter x, the mechanism in the "black box" causes the output link to turn to the corresponding value of the dependent variable $y = f(x)$. This may be regarded as a simple case of a mechanical analog computer.

The subscript j indicates the jth prescribed position of the mechanism; the subscript 1 refers to the *first* or *starting* prescribed position of the mechanism, and $\Delta\phi$, Δx, $\Delta\psi$, and Δy, are the desired *ranges* of the respective variables ϕ, x, ψ, and y (e.g., $\Delta x \equiv |x_{n+1} - x_0|$, $\Delta\phi \equiv |\phi_{n+1} - \phi_0|$, etc.). Since there is a linear relationship between the angular and linear changes,

$$\frac{\phi_j - \cancel{\phi_1}^{0}}{x_j - x_1} = \frac{\Delta\phi}{\Delta x} \tag{8.1}$$

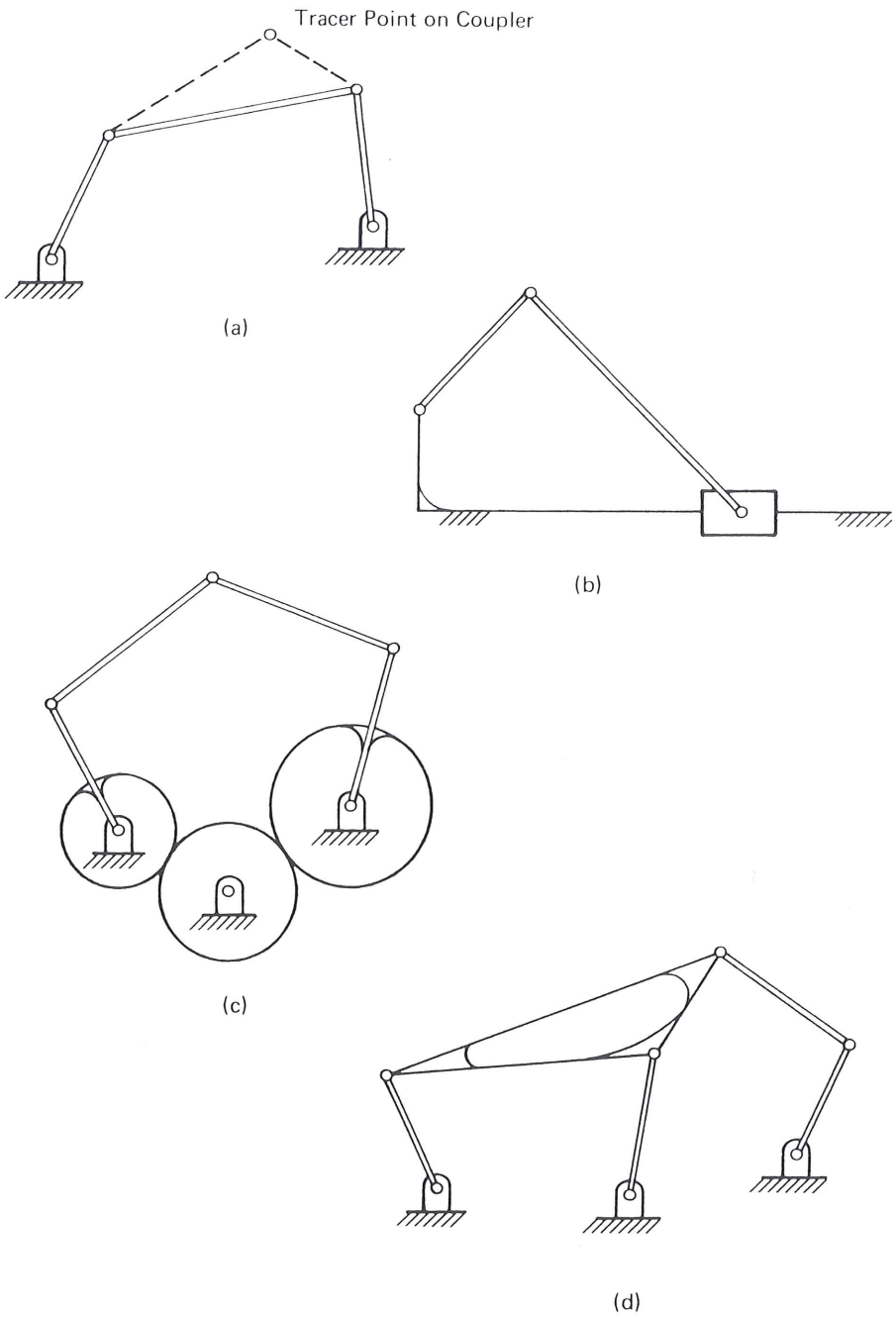

Figure 8.3 Some mechanisms of preconceived type: (a) four-bar linkage; (b) slider-crank; (c) geared five-bar linkage; (d) Stephenson III six-link mechanism.

where ϕ_1 is the datum for ϕ_j, and therefore $\phi_1 = 0$. It follows that

$$\phi_j = \frac{\Delta\phi}{\Delta x}(x_j - x_1)$$
$$\psi_j = \frac{\Delta\psi}{\Delta y}(y_j - y_1) \tag{8.2}$$

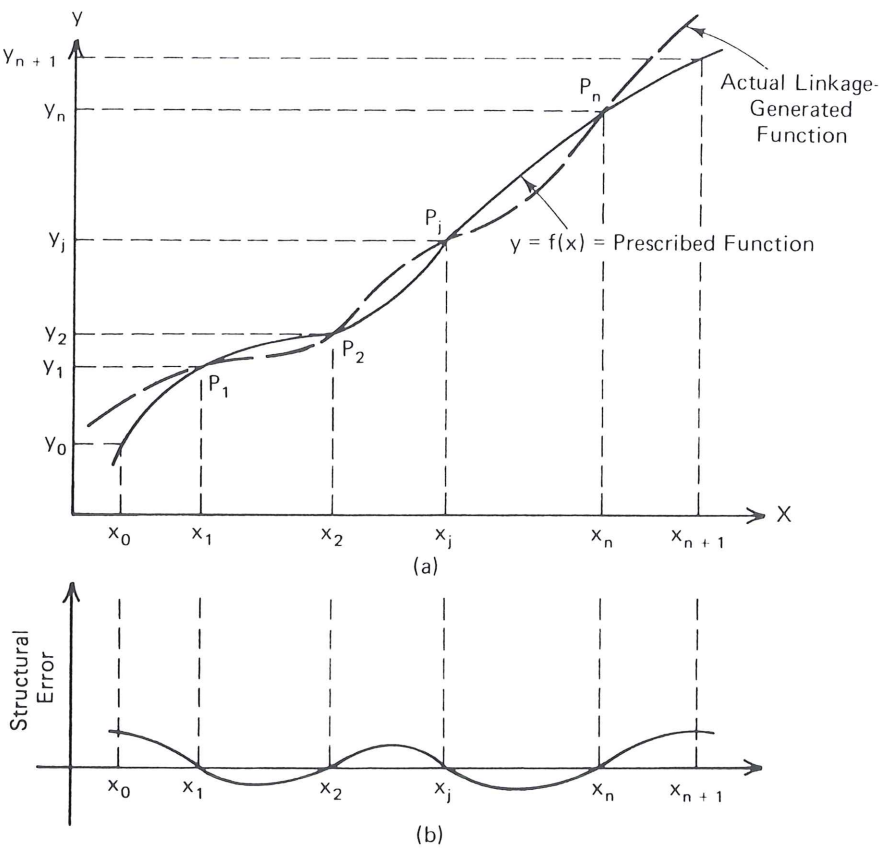

Figure 8.4 Function-generation synthesis: (a) ideal function and generated function; (b) structural error.

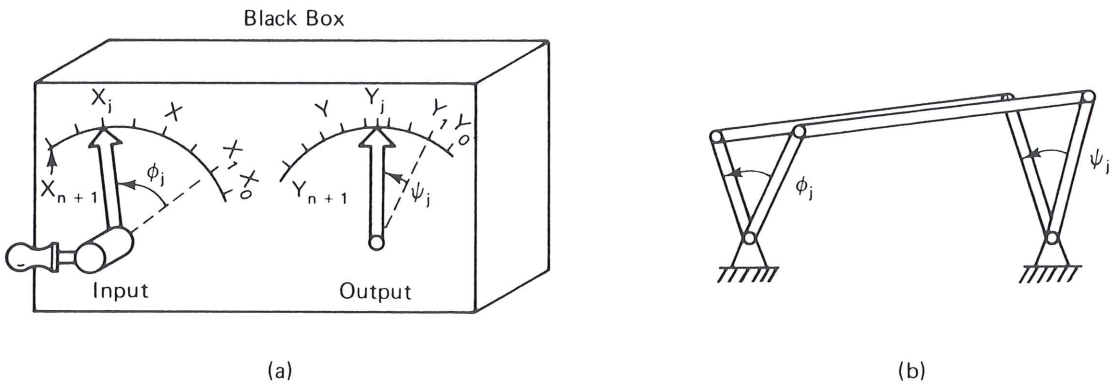

Figure 8.5 Function-generator mechanism; (a) exterior view; (b) schematic of the mechanism inside.

These relationships may also be written as

$$\phi_j = R_\phi(x_j - x_1) \tag{8.3}$$

$$\psi_j = R_\psi(y_j - y_1) \tag{8.4}$$

Where R_ϕ and R_ψ are the *scale factors* in degrees per unit variable defined by

$$R_\phi = \frac{\Delta\phi}{\Delta x} \tag{8.5}$$

$$R_\psi = \frac{\Delta\psi}{\Delta y} \tag{8.6}$$

The four-bar linkage is not capable of error-free generation of an arbitrary function and can match the function at only a limited number of precision points (see Fig. 8.4a). It is, however, widely used in industry in applications where high precision at many points is not required because the four-bar is simple to construct and maintain. The number of precision points that are used in the dimensional synthesis of the four-bar linkage varies in general between two and five.* It is often desirable to space the precision points over the range of the function in such a way as to minimize the *structural error* of the linkage. Structural error is defined as the difference between the generated function (what the linkage actually produces) and the prescribed function for a certain value of the input variable (see Fig. 8.4b).

Notice that the first precision point ($j = 1$) is not at the beginning of the range (see Fig. 8.4). The reason for this is to reduce the extreme values of the structural error. It is also evident from Eq. (8.1) that angles of rotation are measured from the first position (e.g., $\phi_1 = 0$). Section 8.10 will discuss optimal spacing of precision points for minimizing structural error.

Figure 8.6 shows a not-to-scale schematic of the input and output links of a four-bar function generator mechanism in four precision positions, illustrating the relationship between x_j and ϕ_j as well as y_j and ψ_j. The dimensional synthesis techniques described later in this chapter and Chap. 3 of Vol. 2 will show us how to use such precision-point data for the synthesis of four-bar linkages and other mechanisms for function generation.

A variety of different mechanisms could be contained within the "black box" of Fig. 8.5a. In this case, Fig. 8.5b shows a four-bar linkage function generator. A typical

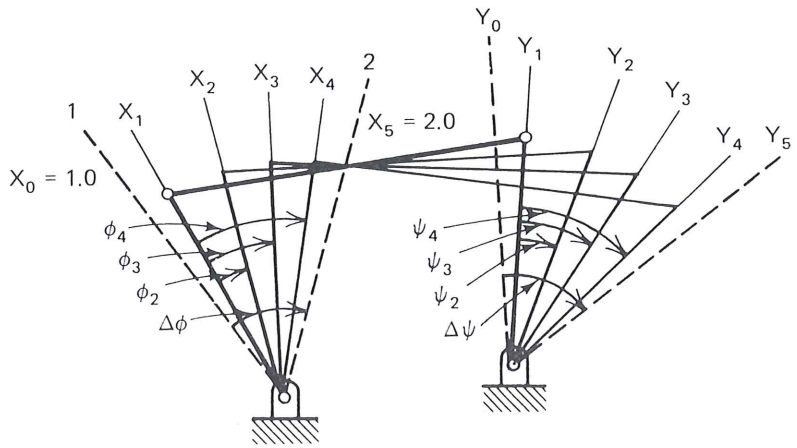

Figure 8.6 Not-to-scale schematic of a function-generator four-bar mechanism with four precision positions of the input and output links x_i and y_i, $i = 1, 2, 3, 4$, within the range $\Delta x = x_5 - x_0$ and $\Delta y = y_5 - y_0$. Input rotations ϕ and output rotations ψ are the analogs of independent and dependent variables x and y, respectively.

* Function generation synthesis up to 7 and path generation synthesis up to 9 precision points are possible, but they generally require numerical rather than the preferable closed-form methods of synthesis.

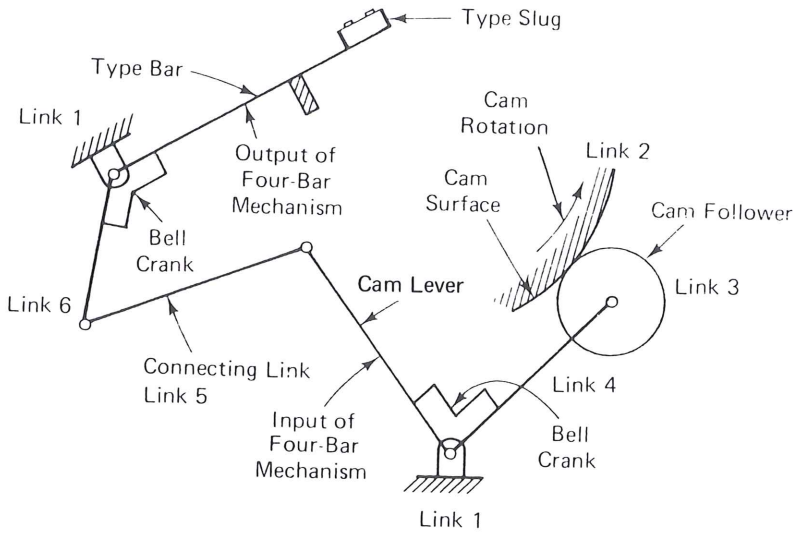

Figure 8.7 Four-bar mechanism used as the impact printing mechanism in an electric typewriter.

example of a function generator is shown schematically in Fig. 8.7. A four-bar linkage connects a cam follower, driven by the cam, to a type bar of a typewriter printing mechanism. Here the type must be moved, first by smaller then by larger angles per increment of input rotation, in order to throw the type against the platen roller with an impact. Another application of function generation would be an engine where the mixing ratios of fuel to oxidant might vary as the function $y = y(x)$. Here ϕ might control the fuel valve while ψ would control the oxidant valve. Flow characteristics of the valves and the required ratio at various fuel rates would dictate the functional relationship to be generated. Yet another example is a linkage to correlate steering positions of the front wheels of an all-terrain vehicle with the relative speed at which each individually driven wheel should rotate to avoid scuffing. Here the input crank is connected to the steering arm, while the output adjusts a potentiometer controlling the relative speed of the two drive wheels.

Mechanical function generators may also be of the type shown in Fig. 8.8 in which a *rectilinear* displacement may be the linear analog of one variable and the crank rotation may be the linear analog of another, a functionally related variable. As illustrated in Fig. 8.9, a function generator may have more degrees of freedom than one; an output variable may be a function of two or more inputs. For example, such a linkage might be used to simulate the addition, multiplication, or any other algebraic or transcendental functional correlation of several variables. Figure 8.10 shows a six-link single-degree-of-freedom function generator mechanism in which two four-link mechanisms

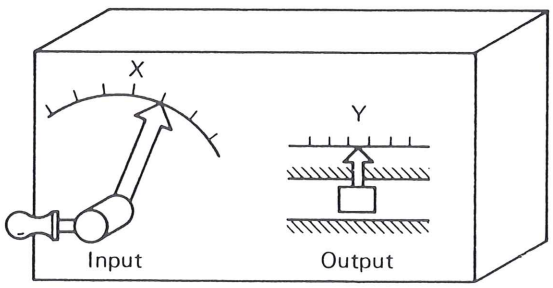

Figure 8.8 Function generator with rotary input and translational output, analogs of the independent and dependent variables of the function $y = f(x)$.

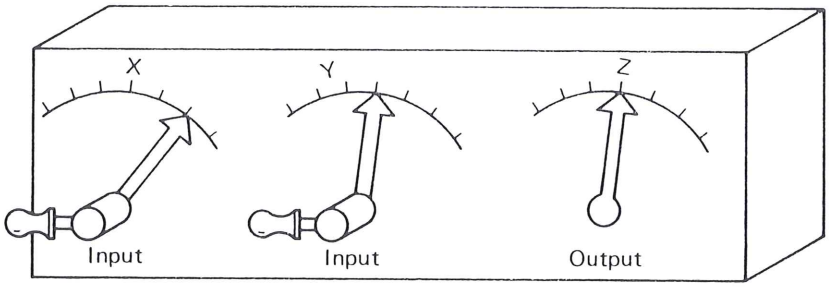

Figure 8.9 Two-degree-of-freedom function generator for generating the function $z = f(x, y)$.

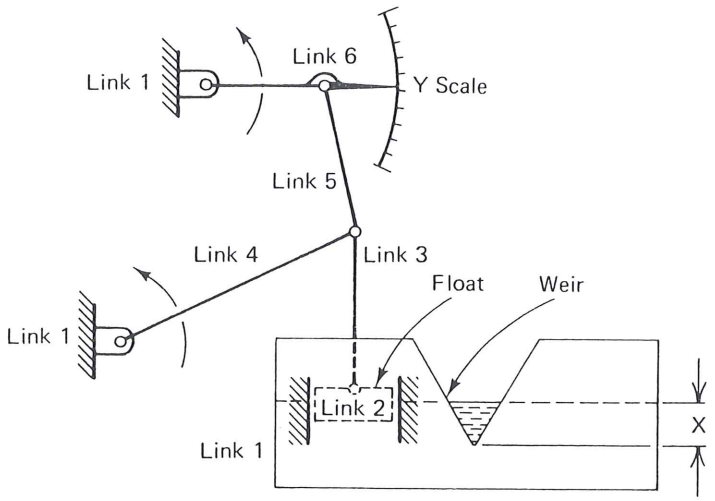

Figure 8.10 Flow-rate-indicator mechanism, $y = K_1 x K_2$, where K_1 and K_2 are constants.

are joined in a series. The objective in this linkage is to provide a measure of flow rate through the weir where the input is the vertical translation x of the water level.

In *path generation* a point on a "floating link" (not directly connected to the fixed link) is to trace a path defined with respect to the fixed frame of reference. If the path points are to be correlated with either time or input-link positions, the task is called *path generation with prescribed timing*. An example of path generation is a four-bar linkage designed to pitch a baseball or tennis ball. In this case the trajectory of point P would be such as to pick up a ball at a prescribed location and to deliver the ball along a prescribed path with prescribed timing for reaching a suitable throw-velocity and direction.

In Fig. 8.11, a linkage whose floating link will contain point P is desired such that point P will trace $y = f(x)$ as the input crank turns. Typical examples are where $y = f(x)$ is the path desired for a thread-guiding eye on a sewing machine (Fig. 8.12) or the path to advance the film in a movie camera (Fig. 8.13). Various straight-line mechanisms, such as Watt's and Robert's linkages, are examples of a special kind of path generator (see Fig. 8.14) in which geometric relationships assure the generation of straight-line segments within the cycle of the linkage's motion.

Motion-generation or *rigid-body guidance* requires that an entire body be guided through a prescribed motion sequence. The body to be guided usually is a part of a floating link. In Fig. 8.15 not only is the path of point P prescribed, but also the rotations α_j

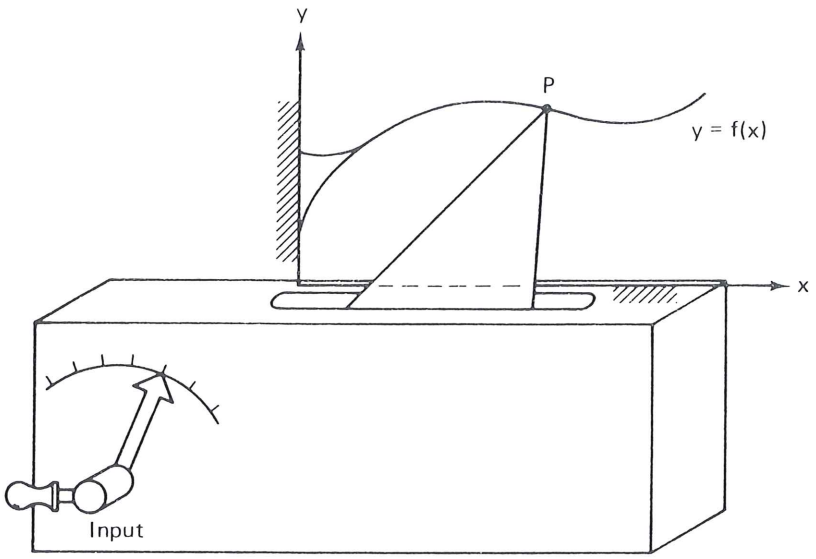

Figure 8.11 A path generator linkage.

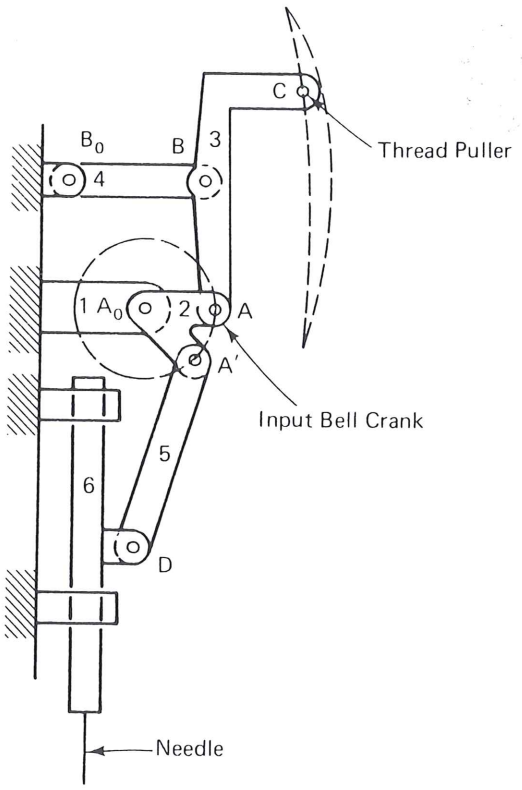

Figure 8.12 In a sewing machine, one input (bell crank 2) drives a path generator (four-bar mechanism 1, 2, 3, 4) and a function generator slider-crank (1, 2, 5, 6). The first generates the path of thread-guide *C* and the second generates the straight-line motion of the needle, whose position is a function of crank rotation.

of vector **Z** embedded in the moving body. The corresponding input rotations may or may not be prescribed. For instance, vector **Z** might represent a carrier link in automatic machinery where a point located on the carrier link (the tip of **Z**) has a prescribed path while the carrier has a prescribed angular orientation (see Fig. 8.16). Prescribing the movement of the bucket for a bucket loader is another example of motion generation.

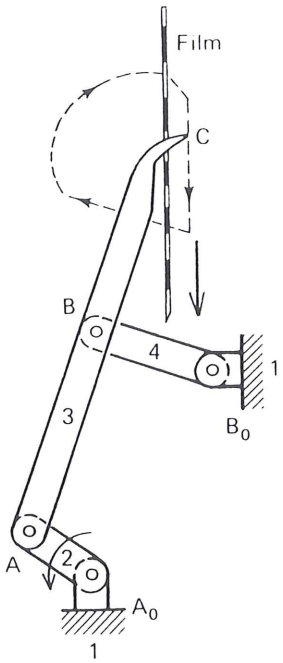

Figure 8.13 Film-advance mechanism of a movie camera or projector generates the path of point C as a function of the angle of rotation of crank 2.

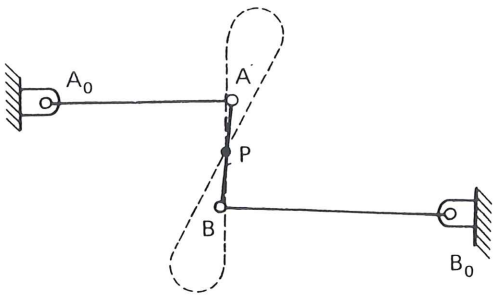

(a)

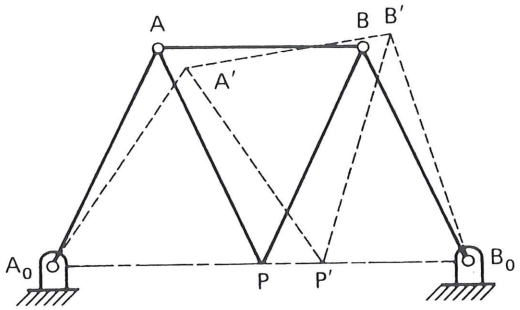

(b)

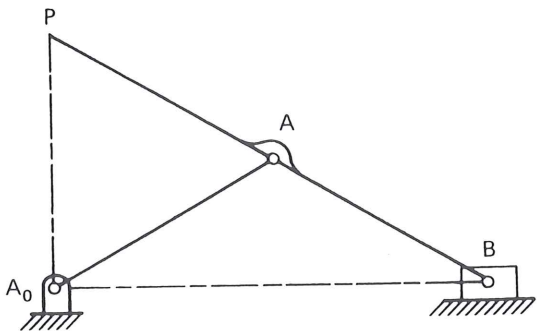

(c)

Figure 8.14 Straight-line mechanisms (a) Watt's mechanism — approximate straight-line motion traced by point P; $AP/PB = BB_0/AA_0$; (b) Robert's mechanism — approximate straight-line motion traced by point P; $A_0A = AP = PB = BB_0$, $A_0B_0 = 2AB$; (c) Scott-Russele mechanism gives exact straight-line motion traced by point P. Note the equivalence to Cardan motion (see chapt. 3, vol. 2); $A_0A = AB = AP$.

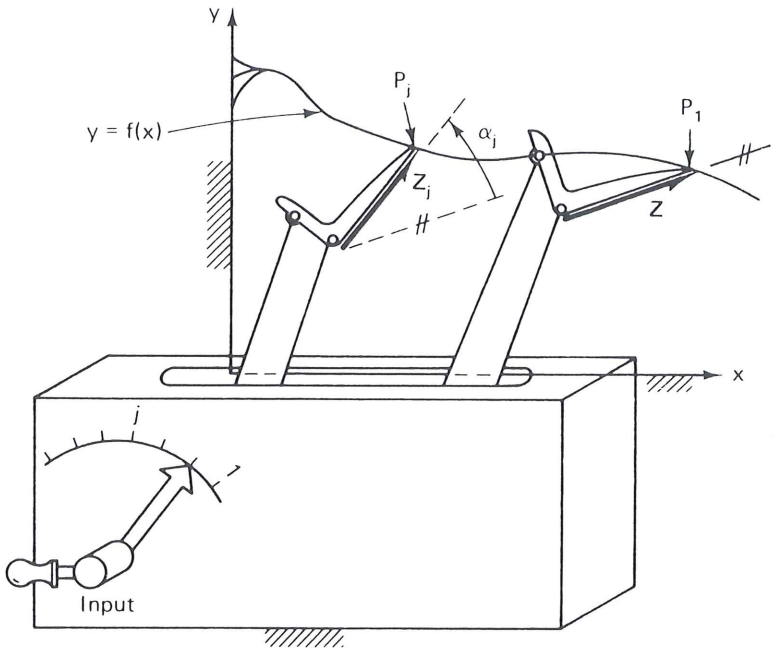

Figure 8.15 Motion-generator mechanism.

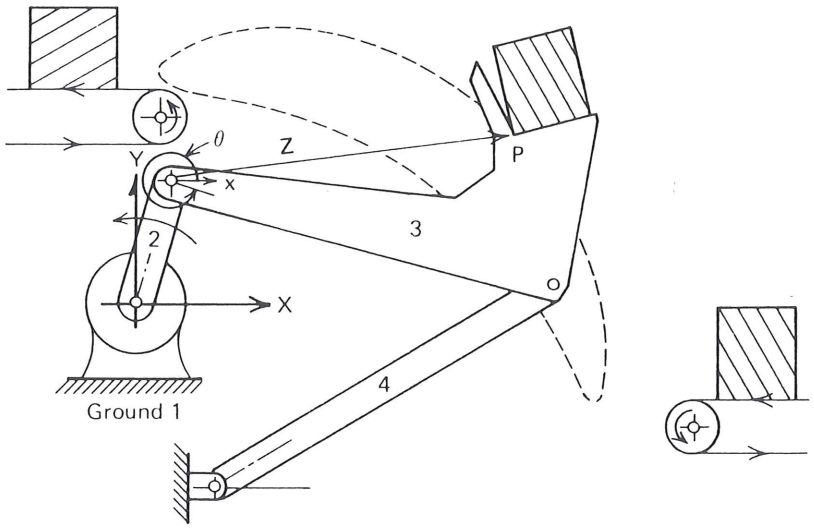

Figure 8.16 Carrier mechanism in an assembly machine.

The path of the tip of the bucket is critical since the tip must perform a scooping trajectory followed by a lifting and a dumping trajectory. The rotations of the bucket are equally important to ensure that the load is dumped from the correct position.

Since a linkage has only a finite number of significant dimensions, the designer may only prescribe a finite number of *precision conditions;* that is, we may only *prescribe* the *performance* of a linkage at a finite number of *precision points*. There are three methods of specifying the *prescribed performance* of a mechanism: *first-order* or *point approximation, higher-order approximation,* and combined *point-order approximation.**

* Approximate (rather than precise) generation of greater numbers of prescribed conditions are possible by the use of least squares or non-linear programming methods. These, however, are numerical procedures rather than closed-form solutions.

In *first-order approximation* for function and path generation, discrete points on the prescribed (or ideal) function or path are specified. Recall that Fig. 8.4a showed precision points P_1 to P_n of the ideal function. The synthesized mechanism will generate a function that will coincide with the ideal function at the precision points but will generally deviate from the ideal function between these points (Fig. 8.4b).

Structural error for path generation may be defined as the vector from the ideal to the generated path perpendicular to the ideal path or it may be defined as the vector between corresponding points on an ideal and a generated path taken at the same value of the independent variable. The latter definition is used when there is prescribed timing. In motion generation there will be both a path and an angular-structural-error curve to analyze.

In some cases a mechanism is desired to generate not only a position but also the velocity, acceleration, shock, and so on, at one or more positions (see Fig. 8.17). For example, the blade of a cutter that must slice a web of paper into sheets while the web is in motion would not only be required to match the correct position at the instant of the cut, but also several derivatives at that position in order to cut straight across and to preserve the sharpness of the blade. For *higher-order approximation,* the first derivative, dy/dx, prescribes the slope of function (or path) at that point; the second derivative, d^2y/dx^2, implies prescribing the radius of curvature; the third derivative, d^3y/dx^3, prescribes the rate of change of curvature; and so on (see Sec. 8.24).

The combination of both point and order approximations is called *point-order approximation* or approximation by *multiply separated precision points* [157]. For example, one might desire to prescribe a position and a velocity at one precision point, only a position at a second precision point, and a position and velocity at a third point.

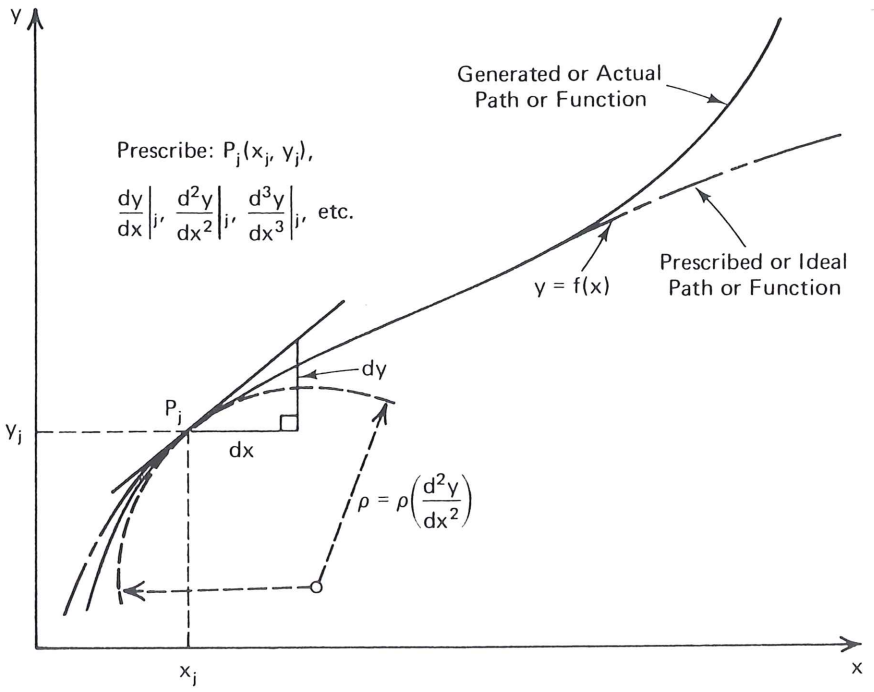

Figure 8.17 Higher-order approximation of function or path.

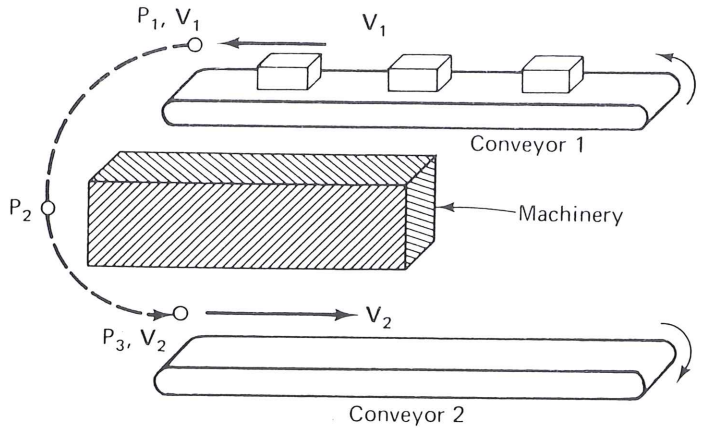

Figure 8.18 Point-order approximation for path generation. There are five prescribed conditions: three-path points and velocities at two of these, tantamount to two infinitesimally close prescribed position at P_1 and P_3.

Figure 8.18 shows such an application where a mechanism is desired to pick up an item from conveyor belt 1 traveling at velocity $\mathbf{V}_1$ and deposit it on a conveyor belt 2 traveling at $\mathbf{V}_2$, having traversed the intervening space in such a way as to avoid some machinery components. Typical application of this occurs in bookbinding, where signatures (32- or 64-page sections) of a book from conveyor 1 are to be stacked on conveyor 2 to form the complete book (see Fig. 6.34).

Kinematic synthesis has been defined here as a combination of type and dimensional synthesis. Most of the rest of this chapter and Chap. 3 of Vol. 2 are devoted to dimensional synthesis. Before moving on to dimensional synthesis, however, one of the methods to creatively discover suitable types of linkages for a prescribed task will be introduced. The method is based on structural models or associated linkages. A case study of type synthesis using another method can be found in the appendix to this chapter.

8.3 TYPE SYNTHESIS [160]

Type synthesis strives to predict which combination of linkage topology and type of joints may be best suited to solve a particular task. Frequently, a novice designer may settle for a solution which merely satisfies the requirements, since there appears to be no method to find a "best" solution. Many experienced designers perform a rudimentary form of type synthesis, sometimes without being aware they are doing so. These experts have an innate "feel" for which type of linkage will work and which will not. This ability is developed only after designing linkages for many years and is difficult to pass on to younger engineers. Many times, type synthesis is skipped due to ignorance or because the designer was not aware of the required relations between the form and function of the linkage. When this happens, a linkage may be chosen which is not capable of meeting the problem requirements. An example would be to choose a single-degree-of-freedom-linkage topology for a two-degree-of-freedom task. This is an expensive mistake, since no choice of dimensions or joint types will yield a viable solution. Besides being relatively unknown, type synthesis is difficult to apply because the principles are not as well defined as those for dimensional synthesis, and so the technique is usually not utilized to its full potential usefulness.

Type synthesis consists of many identifiable steps. For example, the questions listed below may be considered in the following order. The desired degree of freedom is known from the problem.

1. How many links and joints are required for a desired degree of freedom?
2. What are the link types and how many of each are needed for this link set?
3. How many different link sets satisfy the desired degrees of freedom?
4. How many linkage topologies can be formed from these sets of links?
5. How many unique topologies are available from which to choose?
6. How many ways can a ground link be chosen for each topology?
7. How can one predict if any topologic inversions are inherently better than all others for the task at hand?
8. How many ways can the particular types of joints, required to satisfy the task, be distributed throughout the linkage?
9. How many different links could serve as the input driver?

Type synthesis can be subdivided into topological synthesis, topological analysis, and number synthesis [117]. Questions 1 through 3 constitute number synthesis, questions 4 through 6 are topological synthesis, and questions 7 through 9 are typical of topological analysis. Figure 8.19 lists the divisions within type synthesis and shows the place of the field within kinematics.

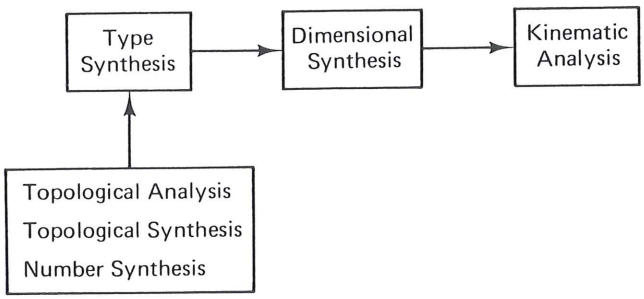

Figure 8.19 The field of type synthesis within kinematics.

The first step in type synthesis is to determine the number and type of links needed to form linkages with the correct degree of freedom. This can be done by using a modified form of the Gruebler equation (see Chap. 1) listed below as Eq. (8.7). Solution of this equation determines all the sets of *higher-order links* (those larger than binaries) which satisfy the desired degree of freedom.

$$n - (F + 3) = T + 2Q + 3P + \ldots \tag{8.7}$$

Where n = the total number of links in a mechanism

B = the number of binary links*

T = the number of ternary links

* Not included in Eq. (8.7), because links are not *higher-order links*.

Q = the number of quarternary links

P = the number of pentagonal links

F = the degree of freedom required to perform the desired task

Each higher-order link set is combined with the necessary number of binary links to total the number of links required by Gruebler's equation for the mechanism. Each set of n links is known as a *kinematic link set solution* (KLSS). There are methods to generate these solutions exhaustively and to determine a priori what the final count should be for any combination of number of links and degrees of freedom [160].

The collection of links comprising each KLSS are assembled into figures using pin joints at all link connection points. These figures define the topologic structure of the linkages formed from this set and are called *isomers*. These isomers are guaranteed to have the desired overall degree of freedom. Each isomer obtained from all kinematic link set solutions for a desired degree of freedom and number of links is called a *basic kinematic chain* (BKC). It is important to have a complete set of BKCs. The urge to accomplish this has attracted much attention over the years [32, 162–164]. Care must be taken when forming these topologic structures to exclude "bad" BKCs, those which fail the *degree-of-freedom-distribution* criterion. This criterion demands that a kinematic chain not have an imbedded zero-freedom subchain. Such a chain would be an unnecessarily complex version of a simpler one, and it should be eliminated before continuing. All KLSS, except those which describe the binary chain mechanisms, have some bad isomers. It is predictable which KLSS will yield only bad isomers, but discovering the useful isomers in the remaining KLSS can be tedious. For example, the one degree of freedom six bar chains have two kinematic link-set solutions. All isomers of one set fail the degree of freedom distribution criterion and degenerate to other linkages, while only ⅔ of the isomers from the second KLSS fail. These isomers must be individually checked.

The next step is to generate all *topologic inversions* of a given BKC. These are formed by grounding each link in a BKC, one at a time, and determining which of the resulting mechanisms are topologically unique. For example a Watt I is topologically different than a Watt II and may be capable of performing different tasks as was pointed out in Chap. 1.

Few methods exist to determine which topologic inversion is best suited for a particular task. One successful technique is called the *associated linkage concept*. It is presented below.

The final three steps determine how drivers and different types of joints can be chosen and distributed throughout the mechanism. Fig. 8.20 outlines the entire procedure described above for the case of a six-bar one-freedom linkage. At this point the topology and joint pairs for a mechanism have been determined and all that remains is to perform a dimensional synthesis.

The Associated Linkage Concept

The *associated linkage concept* was developed by R. C. Johnson and K. Towligh [91, 92] to act as a spur to creativity. An engineer armed with this technique should be able to

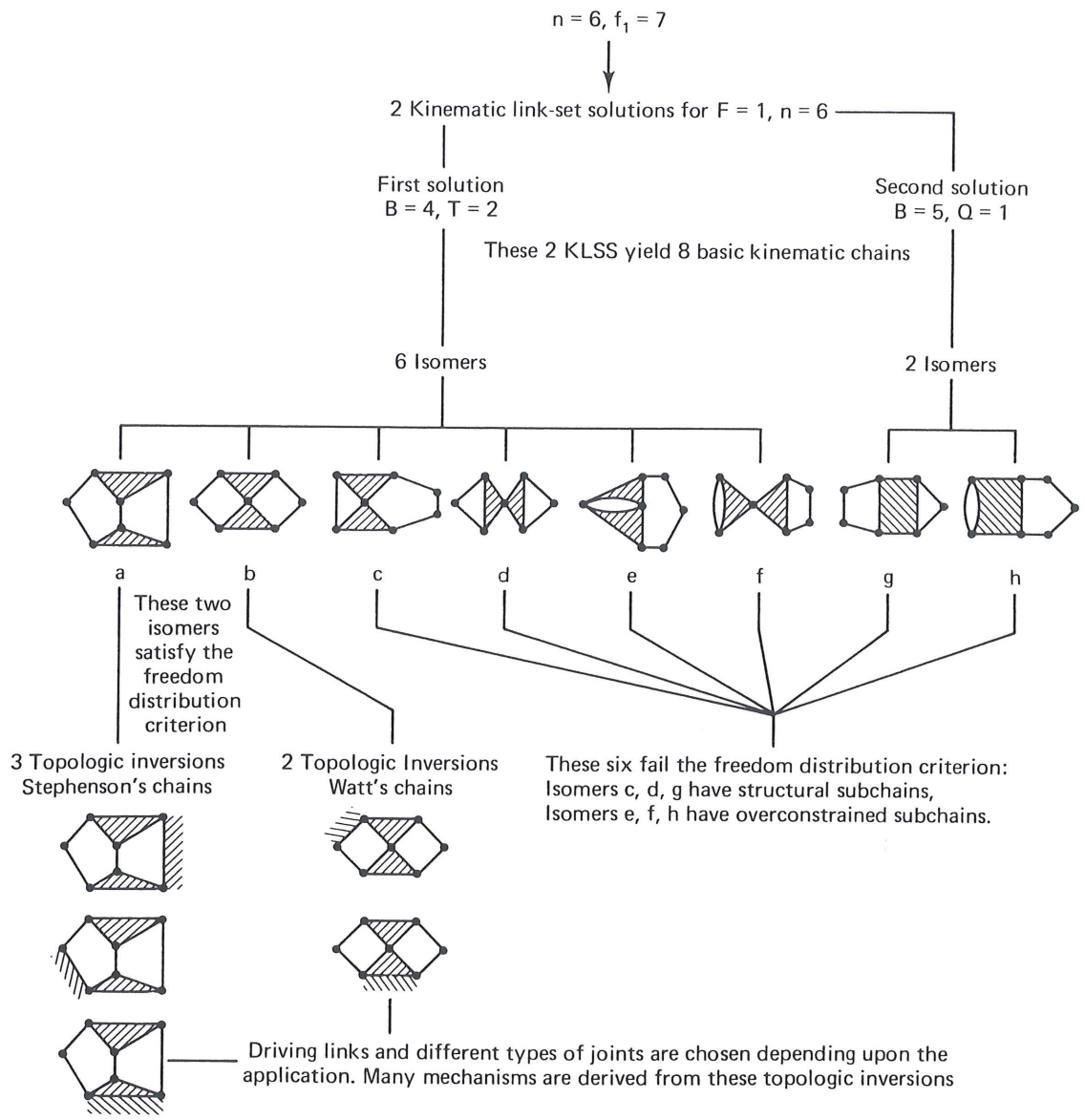

Figure 8.20 Demonstration of type synthesis for 6-bar, one-freedom chains.

generate many mechanisms for a specific task. Design rules are translated into their topologic equivalents (steps 6, 8 and 9 from above) and suitable BKCs (step 5 above) are chosen. The method consists of the following procedure:

1. The determination of rules that must be satisfied for the selection of a suitable "associated linkage." These rules are derived by observing the specific design application.
2. The application of suitable asociated linkages to the synthesis of different types of devices. (See Table 1.2 for equivalent lower-pair joints for velocity matching of higher-pair connections.)

This technique of applying number synthesis to the creative design of practical devices will be illustrated by several examples.

Synthesis of Some Slider Mechanisms

Suppose that it is desired to derive types of mechanisms for driving a slider with rectilinear translation along a fixed path in a machine. Assume that the drive shaft will be fixed against translation and that it must rotate with unidirectional rotation. Also, assume that the slider must move with a reciprocating motion.

A basic rule for this example is that a suitable associated linkage must have a single degree of freedom ($F = +1$) when one link is fixed. Let us start with the least complicated associated linkage chain (which is the four-bar) since simplicity is an obvious design objective (Fig. 8.21a). The four-bar associated linkage has four revolute joints. If one of the revolutes (joint *c-d*) is replaced by a slider, the slider-crank mechanism is derived as shown in Fig. 8.21b.

Increasing the degree of complexity, a Stephenson six-bar chain (in which ternary links are not directly connected) is considered next as a suitable associated linkage (Fig. 8.22a). By varying the location of the slider one creates the slider mechanisms of Fig. 8.22b–f, different from the slider-crank of Fig. 8.21. Finally, in Fig. 8.23, from a Watt six-bar chain (in which the ternary links are direct connected) we derive only one new mechanism (Fig. 8.23b), which is of the same degree of complexity as those in Fig. 8.22; Fig. 8.23c, d, and e are merely slider-cranks, with an added passive dyad. Thus five different six-link mechanisms, each having only a single slider joint, can be derived for this problem.

This general procedure could be extended to other suitable linkages of greater complexity, including those containing *higher pairs*.* Thus cams and sliding pivots may be incorporated in the derivations of different types of mechanisms, such as those illustrated in Fig. 8.24, derived from the four-bar chain as the associated linkage.

Synthesis of Some Gear-Cam Mechanisms

A typical meshing gear set is shown in Fig. 8.25 with two typical teeth in contact. At the instant of observation the meshing gear set is equivalent to a hypothetical quadric

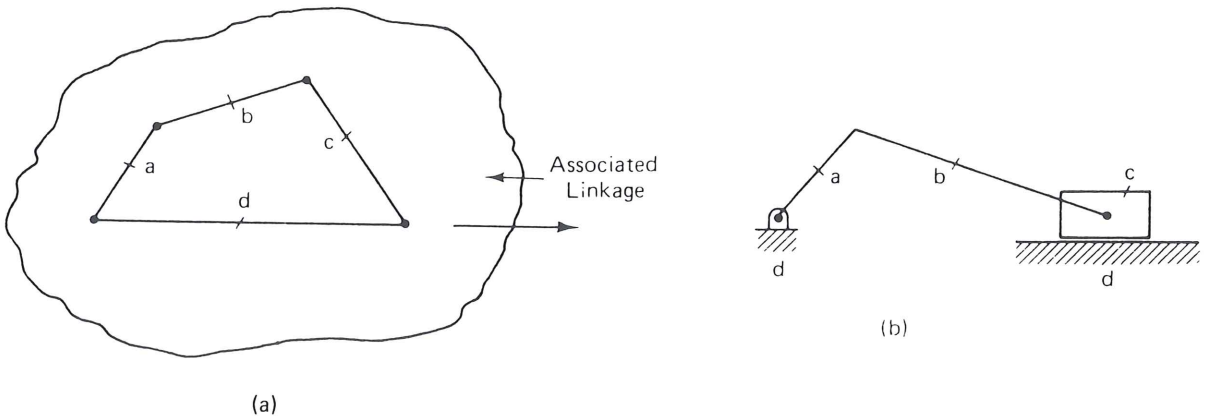

Figure 8.21 Slider-crank mechanism and its associated linkage; (a) four-bar chain; (b) slider-crank mechanism.

* Sec. 6.10 describes this technique applied to cam-modulated linkages.

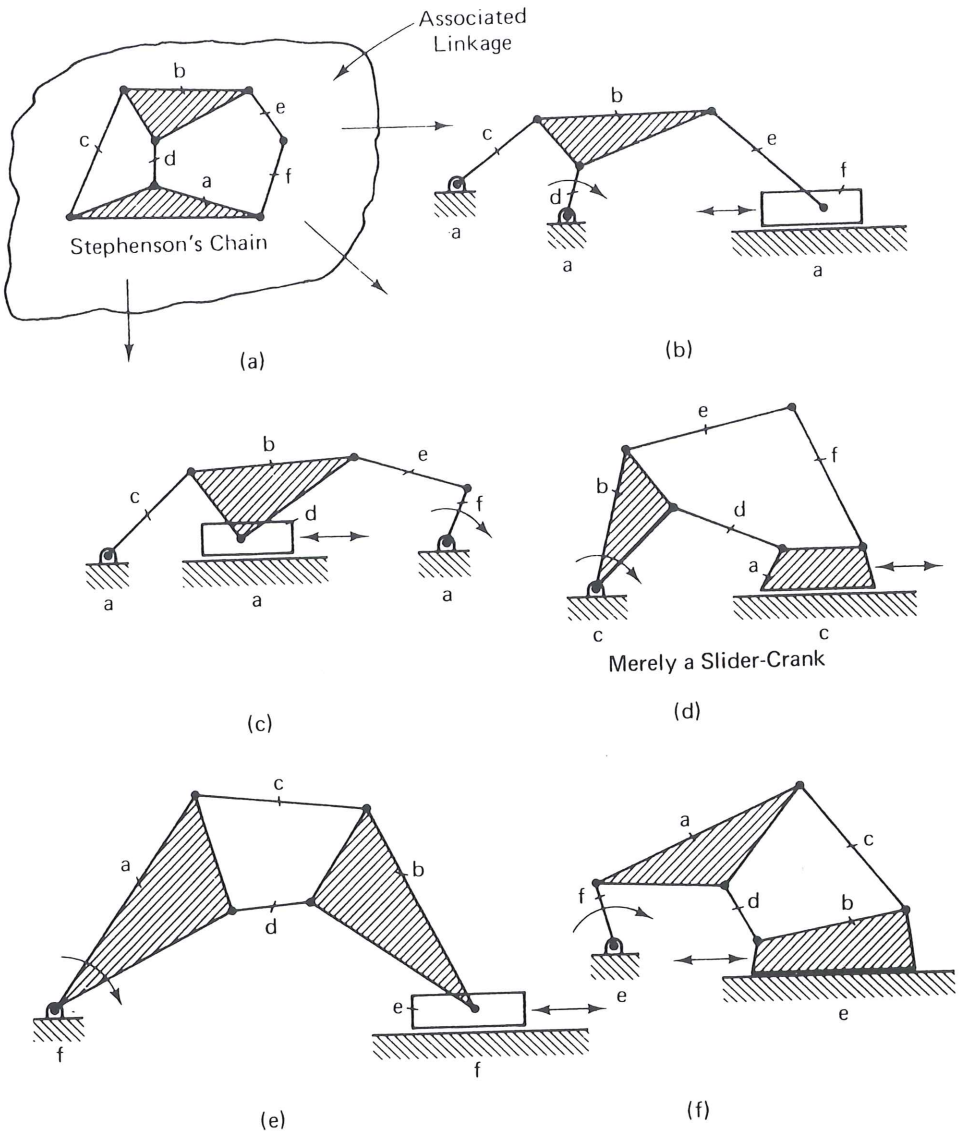

Figure 8.22 Slider mechanisms derived from Stephenson's six-bar chain as the associated linkage. Note that (d) shows merely a slider crank with redundant (superfluous) links, the passive dyad consisting of links e and f.

chain (see Table 1.2). Hence, as shown in Fig. 8.25, a meshing gear set has a four-bar chain as an associated linkage. The basic rules for a suitable associated linkage involved in the synthesis of a mechanism containing a meshing gear set are as follows:

1. The number of degrees of freedom with one link fixed must be $F = +1$.
2. The linkage must contain at least one four-sided closed loop. This is true since the meshing gear set corresponds to a four-sided closed loop containing two centers of rotation, $R_{p/f}$ and $R_{g/f}$, and two base points, B_p and B_g, which are the instantaneous centers between gear p and the fictitious coupler C and between gear g and C, respectively. In the gear set, coupler C is replaced by the higher-pair contact between the tooth profiles. Hence B_p and B_g coincide with the cen-

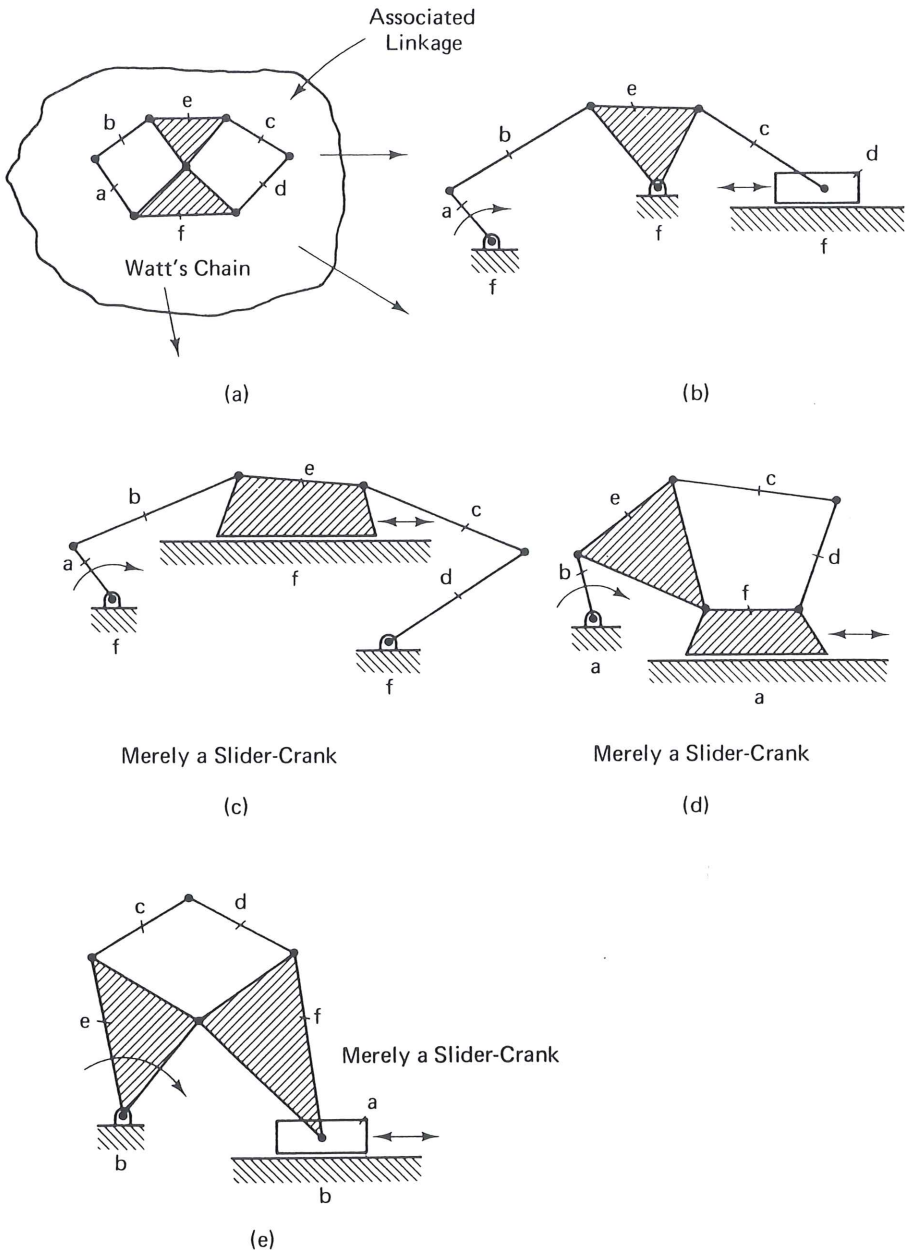

Figure 8.23 Slider mechanisms derived from Watt's chain six-bar as the associated linkage.

ters of curvature of the respective involute tooth profiles at their point of contact. In traversing this four-sided closed loop, the two centers of rotation must be encountered in succession, such as *RRBB* rather than *RBRB*.

3. The four-sided closed loop must contain at least one binary link. This is true because in the four-sided closed loop the link connecting the two base points must be a binary link. This is evident since the base points on the meshing gears are instantaneous and they are joined by a hypothetical connecting rod in the equivalent quadric chain.

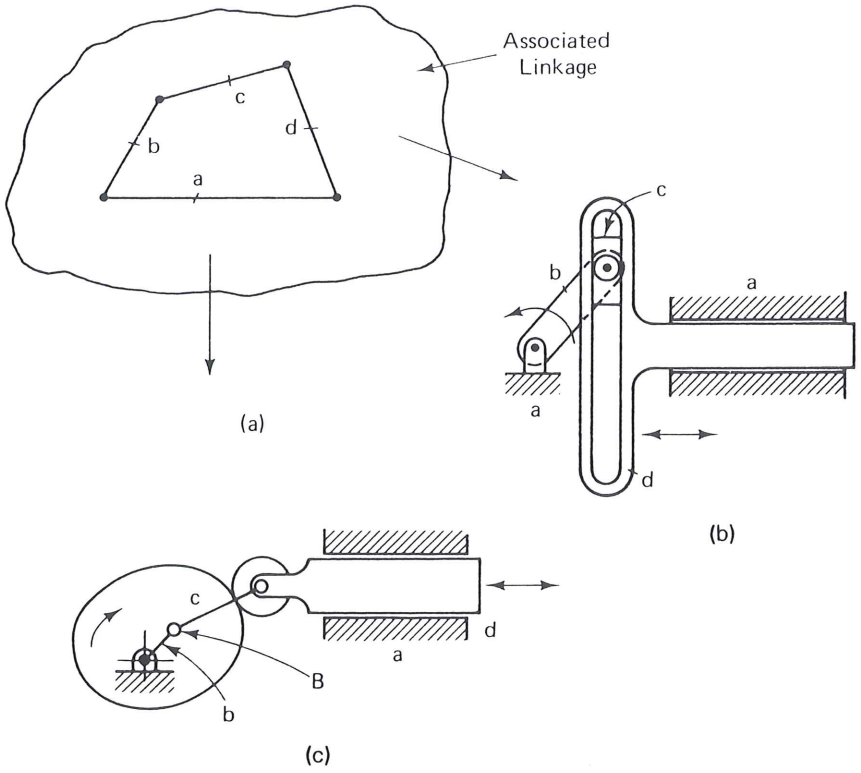

Figure 8.24 Derivation of some slider mechanisms containing cams and sliding pivots from the four-bar chain as the associated linkage. Notice that point *B* is the center of curvature of the cam contour at the point of contact of the cam; (a) four-bar chain; (b) Scotch yoke; (c) disk cam with translating follower.

Suppose that it is required to design a gear mechanism for driving a slider with arbitrary motion along fixed ways in a machine. Assume that the driving shaft must have unidirectional rotation and the slider must have a reciprocating motion. One possible design would be the mechanism shown in Fig. 8.26, where the driving cam provides arbitrary motion and a gear and rack drive the slider. In Fig. 8.27 an equivalent linkage for this mechanism is shown together with its associated linkage. Incidentally, a gear and rack is a special gear type with one base point and one center of rotation at infinity.

Simplicity in design is a practical goal worth striving for. Suppose that we wish to explore different, simpler mechanism types for the basic problem described in the preceding paragraph (assuming that a cam, follower, gear, and rack are to be employed for driving the slider). The simplest suitable associated linkage for this application would be either Watt's chain or Stephenson's chain. From these chains three different mechanism types are derived (Figs. 8.28 and 8.29), where Fig. 8.29c would require a flexible shaft for driving the cam.

Synthesis of Some Internal-Force-Exerting Devices

Kurt Hain [83] has applied number synthesis to the design of differential brakes and differential clamping mechanisms by recognizing the analogy with preloaded structures. This analogy shows that, for the synthesis of internal-force-exerting devices in general,

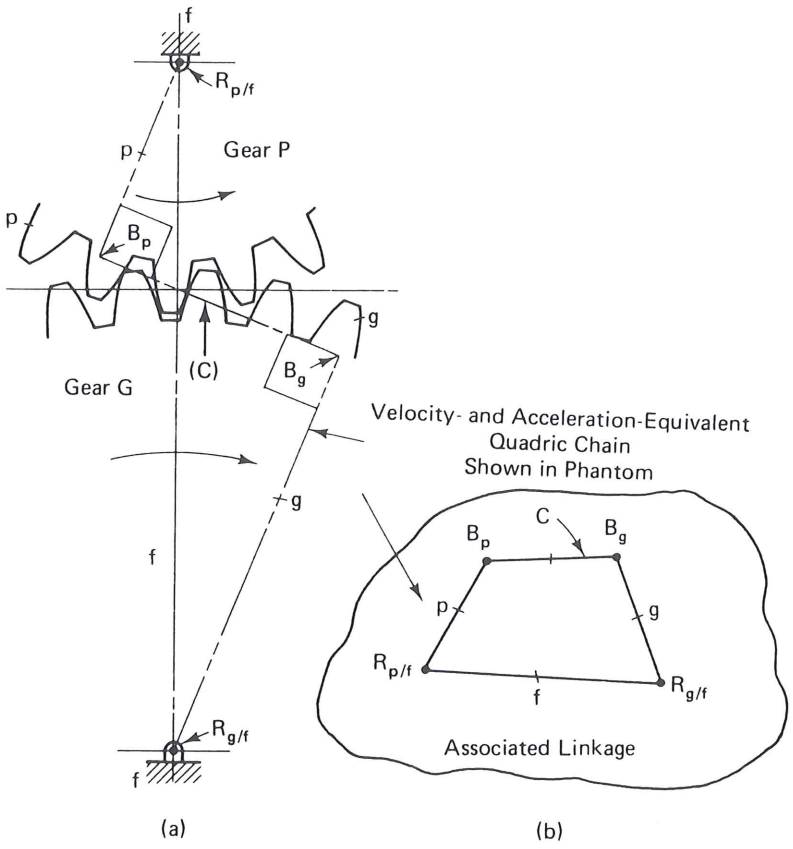

Figure 8.25 Meshing gear set with its associated linkage. B_g and B_p are the centers of curvature of the involutes at the contact point of gear G and gear P, respectively; (a) gear pair; (b) associated linkage.

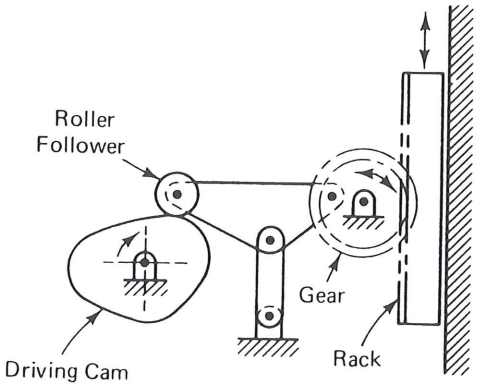

Figure 8.26 Slider mechanism with cam and gear.

a suitable associated linkage must have $F = -1$ for the number of degrees of freedom with one link fixed. Also, *forces* exerted by the device on the work piece correspond to *binary links* in the associated linkage, recognizing that a binary link is a two-force member. Let us apply this technique to the synthesis of two practical devices. First, different types of compound-lever snips are explored, followed by several types of yoke riveters.

Synthesis of Compound-lever Snips. Simply constructed compound-lever snips are to be designed for cutting through tough materials with a relatively small amount of effort. The actuating force is designated by P and the resisting force by F_r. We will assume that the compound-lever snips should be hand-operated and mobile.

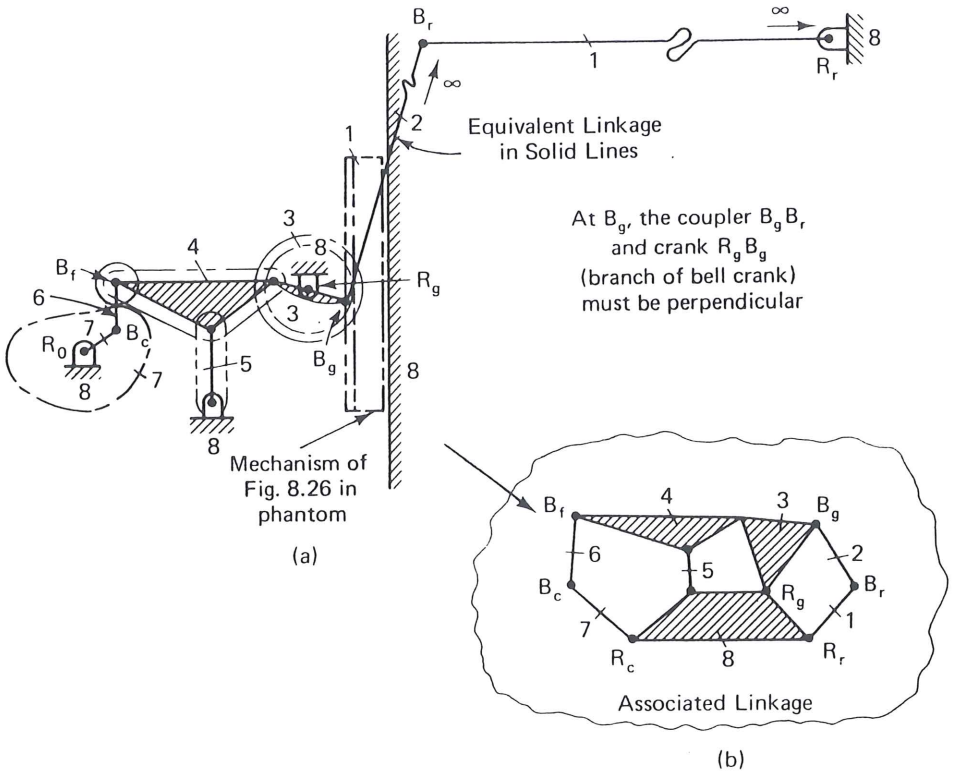

Figure 8.27 Slider mechanism of Fig. 8.26 with equivalent linkage (a) and associated linkage (b) from which it was derived.

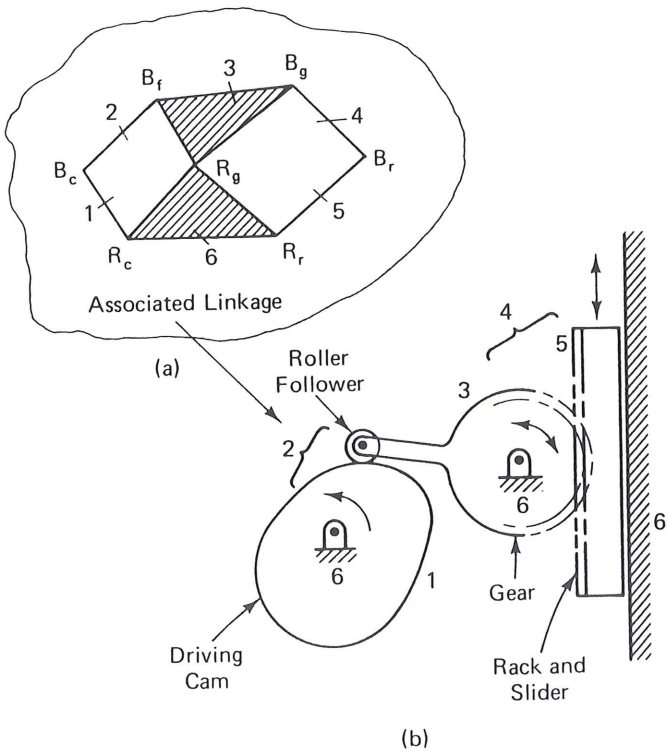

Figure 8.28 Cam-gear-slider mechanism derived from Watt's chain.

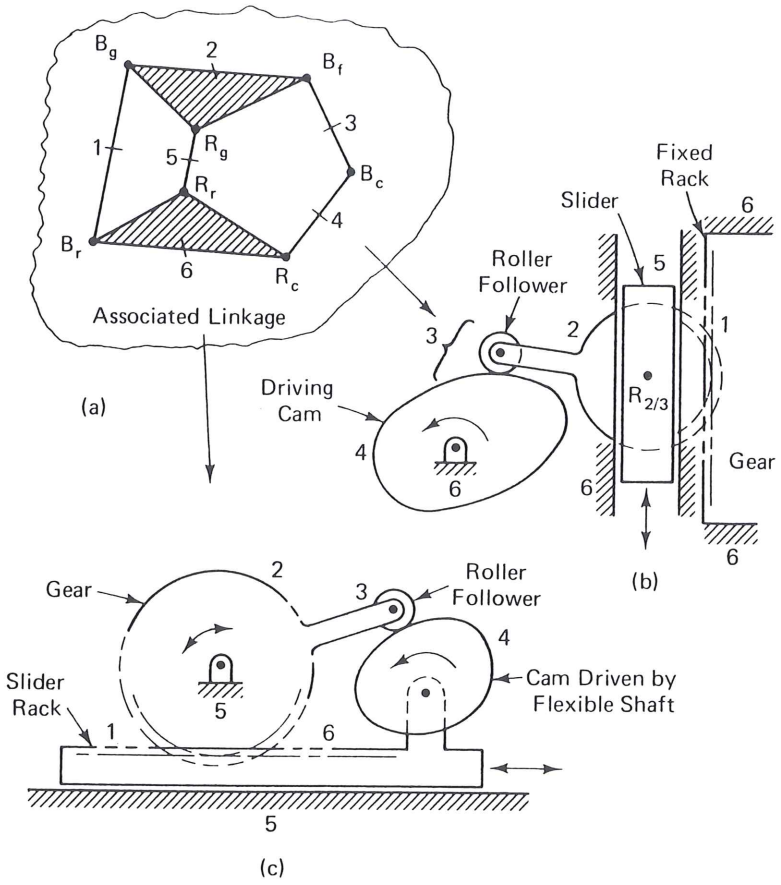

Figure 8.29 Cam-gear-slider mechanisms derived from Stephenson's chain.

Hence there will be no ground link in the construction. However, a high amplification of force is required in the device. Therefore, in the associated linkage, binary links P and F_r must not be connected by a single link; otherwise, a simple lever type of construction will result in relatively low force amplification.

In summary, for application to the synthesis of compound-lever snips, the rules or requirements for a suitable associated linkage are as follows:

1. $F = -1$.
2. There must be at least two binary links because of the two forces P and F_r.
3. Two binary links P and F_r must not connect the same link, because in that case the snips will be simple instead of compound.

The associated linkages in Figs. 8.30, 8.31, and 8.32 satisfy the requirements. Each suitable associated linkage yields a different mechanism for compound-lever snips.

Synthesis of yoke riveters. The configuration for an existing yoke-riveter design [91] is shown in Fig. 8.33. Let us apply number synthesis in the creation of other types of yoke-riveter designs.

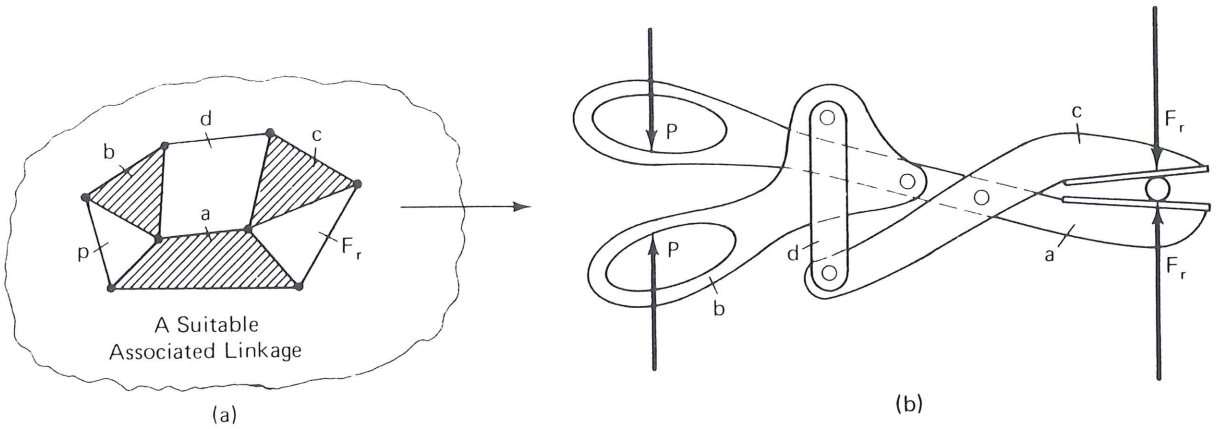

Figure 8.30 Synthesis of compound lever snips from a suitable associated linkage.

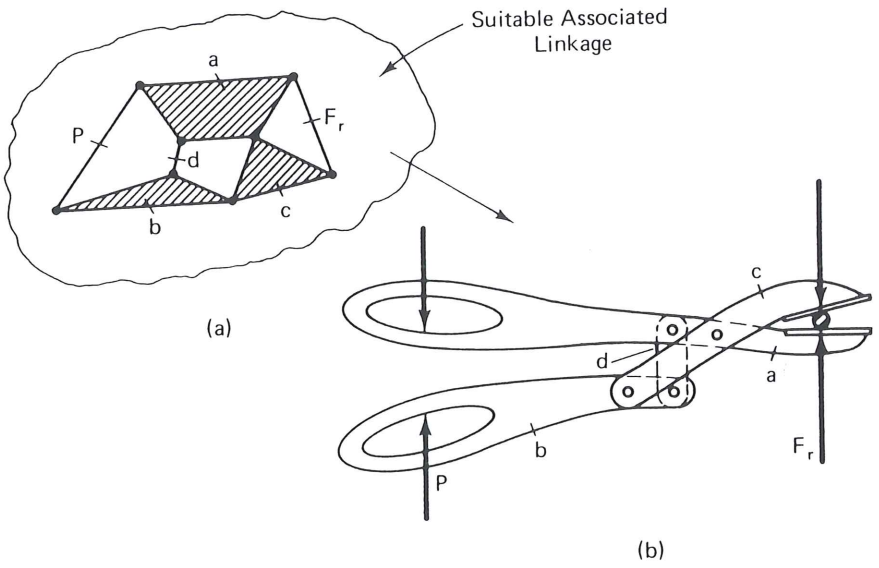

Figure 8.31 Synthesis of compound-lever snips from a suitable associated linkage.

The following characteristics are assumed to be requirements for a suitable yoke riveter in our particular application:

1. Simple features of construction.
2. Self-contained, portable unit.
3. High force amplification between power piston and rivet die.
4. One part of the two-part rivet die and the relatively large pneumatic power cylinder are fixed to the frame link.
5. Another part of the rivet die and the power piston are to slide relative to the frame link.

From Fig. 8.33 of the existing yoke-riveter design the associated plane linkage with single pin joints is derived as shown in Fig. 8.34. Applying Gruebler's equation (Chap. 1) to the linkage in Fig. 8.34, we obtain $F = -1$, which is expected, since this

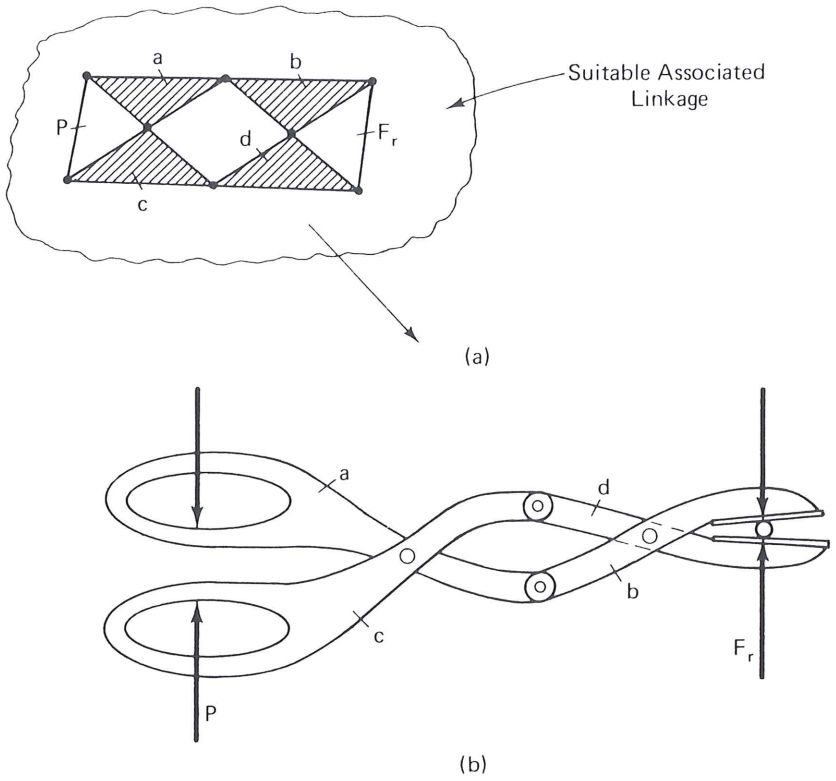

Figure 8.32 Different design derived from another suitable associated linkage for compound-lever snips.

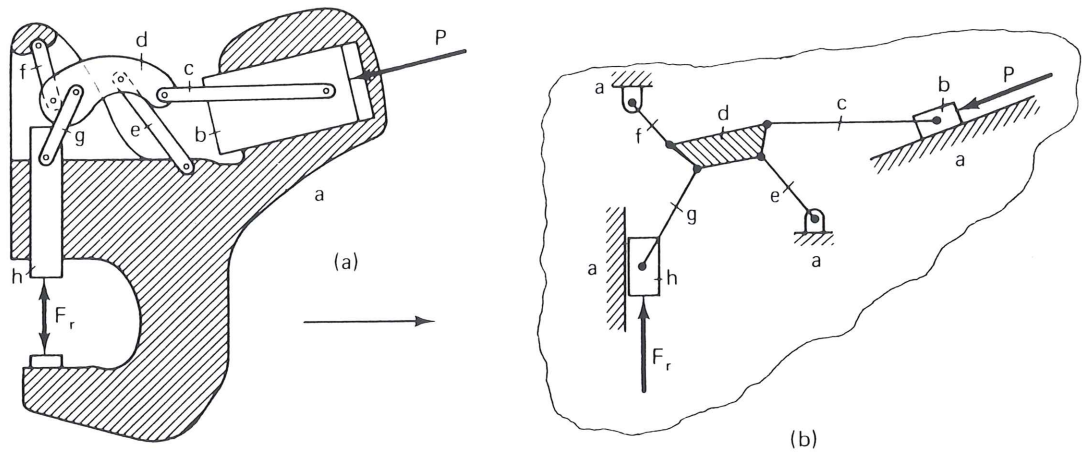

Figure 8.33 Existing yoke riveter (a) and the equivalent toggle linkage in inset (b).

value of F is characteristic of the associated linkage for any internal-force-exerting device: $F = 3(n - 1) - 2f_1$. Note that $n = 10$, including the binary links representing P and F_r, connecting a with b and a with h, respectively. Note also that the number of pin joints, f_1, is 14. Therefore,

$$F = 3(10 - 1) - 2(14) = -1$$

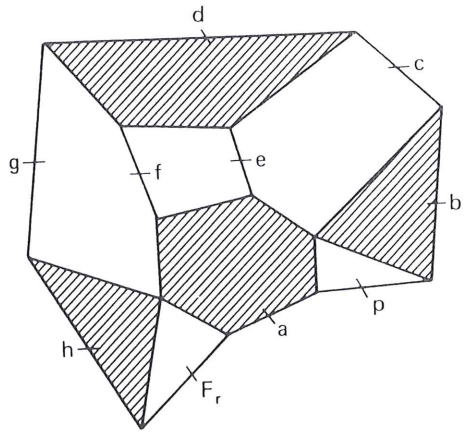

Figure 8.34 Associated linkage for the existing yoke riveter of Fig. 8.33.

In the synthesis of new configurations of yoke riveters, it will be necessary to reverse the procedure just illustrated in going from Fig. 8.33 to Fig. 8.34. Thus first it will be necessary to select a suitable associated linkage for a new yoke-riveter design. From a careful study of Figs. 8.33 and 8.34, and from a consideration of the desired features of a suitable yoke riveter listed previously, the following rules or requirements for a suitable associated linkage are obtained.

1. $F = -1$.
2. There must be at least two binary links (for P and F_r).
3. The binary links corresponding to P and F_r must be connected to the same link at one end, which is the frame link, and to different *ternary* links at their other end. This assures simple construction of the linkage with high force amplification between the rivet die set and the power piston.
4. The frame link must be at least a quaternary link for P, F_r, and two lower-pair sliding joints for the rivet die and power piston.
5. The different *ternary* links mentioned in requirement 3 must be connected to the frame link, since the power piston and rivet die are to have a lower-pair sliding connection with the frame link.

Since simplicity of construction is a feature of practical importance, the simpler associated linkage in the inset of Fig. 8.35a is a suitable choice. From this associated linkage the simple toggle-type riveter is derived.

The associated linkage method for type synthesis is one of the useful techniques used for synthesizing mechanism *types*. Similar methods of analysis are sometimes employed in patent cases in determining whether a device is of the same or different type than others. Another type-synthesis method is described in the appendix of this chapter by way of a case study.

Observe that nothing yet has been said regarding actual dimensions of these type-synthesized mechanisms. The specific dimensions will control the relative motions and the force transmission characteristics of the examples given above.

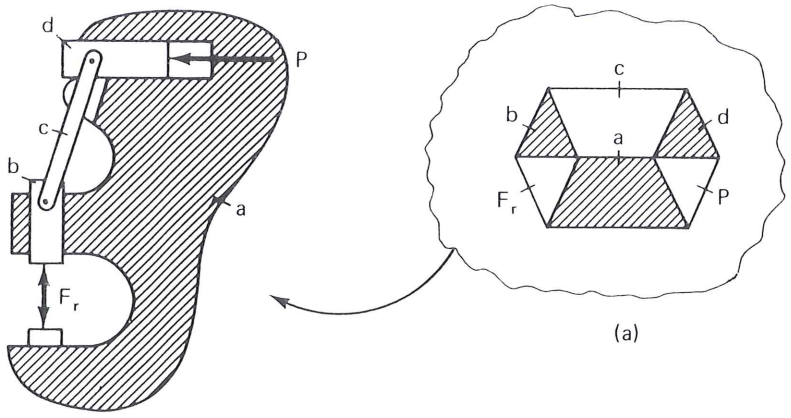

Figure 8.35 Simple toggle-type riveter; (a) associated linkage; (b) the mechanism derived from (a).

8.4 TOOLS OF DIMENSIONAL SYNTHESIS

The two basic tools of dimensional synthesis are geometric contruction and analytical (mathematical) calculation.

Geometric or graphical methods of synthesis provide the designer with a fairly quick, straightforward method of design. Graphical techniques do have limitations of accuracy due to drawing error, which can be very critical and because of complexity of solution to achieve suitable results, the geometric construction may have to be repeated many times.

Analytical methods of synthesis are suitable for automatic computation and have the advantages of accuracy and repeatability. Once a mechanism is modeled mathematically and coded for a computer, mechanism parameters are easily manipulated to create new solutions without further programming. Although this text emphasizes analytical synthesis, it is important to have experience in graphical techniques for use in the initial phases of kinematic synthesis. The next several sections present a review of useful geometric approaches before moving on to analytical synthesis.

8.5 GRAPHICAL SYNTHESIS—MOTION GENERATION: TWO PRESCRIBED POSITIONS [139]

Suppose that we wish to guide a link in a mechanism in such a way that it will assume several arbitrarily prescribed distinct (finitely separated) positions. For two positions of motion generation, this can be accomplished by a simple rotation (Fig. 8.36) about a suitable center of rotation. This *pole* (see Sec. 4.2 of Vol. 2), P_{12}, is found graphically by way of the *midnormals* a_{12} and b_{12} to the connecting line segments of two *corresponding* positions each of points A and B, namely A_1, A_2 and B_1, B_2.

If pole P_{12} happens to fall off the frame of the machine, we may use a four-bar linkage to guide link AB from position 1 to position 2 (Fig. 8.37). Two fixed pivots, one each anywhere along the two midnormals, will accomplish this task. The construction is as follows.

8.12 ANALYTICAL SYNTHESIS TECHNIQUES

Figures 8.37 to 8.39 show that the geometric construction of four-bar motion generators for two and three prescribed positions is a fairly simple task. Suppose, however, that we wish to find an "optimal" four-bar motion generator for a specific application—perhaps a case that has constraints on ground and moving pivot locations, transmission angle, link-length ratio, and/or mechanical advantage. The construction of Fig. 8.39, although simple, may be too time consuming to repeat until a suitable solution is obtained. A graphical search through two infinities of solutions is inconceivable. What other alternatives are available? By choosing the position of the circle point A_1 in Fig. 8.39, we have arbitrarily picked two free choices—those free choices in turn specify the corresponding center point A_0. These two free choices for the three-precision-point motion-generation synthesis of one side of the four-bar linkage can be picked with different strategies in mind toward various design objectives.

In order to obtain a handle on the design variables and free choices, an analytical model of the linkage must be developed. Several mathematical techniques for modeling linkages have been utilized for planar synthesis objectives. These include algebraic methods, matrix methods, and complex numbers. For planar linkages, the complex numbers technique is the simplest, yet the most versatile method. In this text we therefore concentrate on the latter method. Before exploring the question of free choices versus synthesis options, the complex-number technique will be reviewed,* especially as it relates to modeling linkages for synthesis.

8.13 COMPLEX-NUMBER MODELING IN KINEMATIC SYNTHESIS

Any planar mechanism can be represented by a general chain, consisting of one or more loops of successive bar-slider members (Fig. 8.55). For example, the offset slider-crank

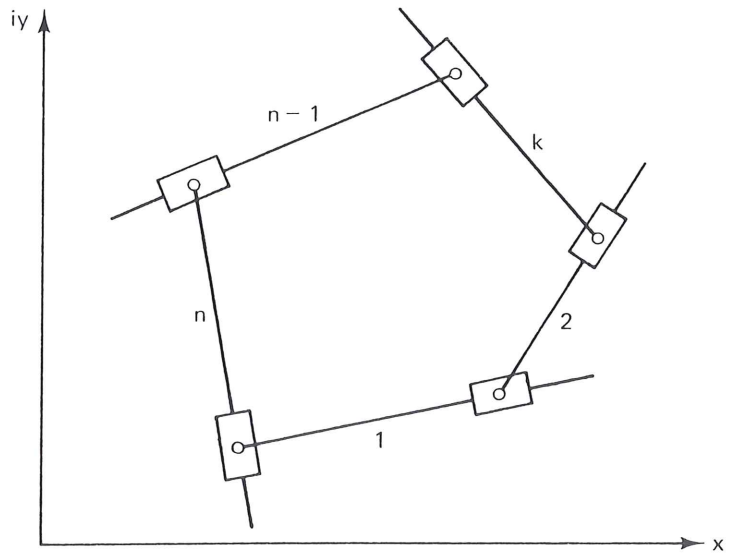

Figure 8.55 General planar chain.

* A more complete review of complex numbers is given in the appendix to Chap. 3.

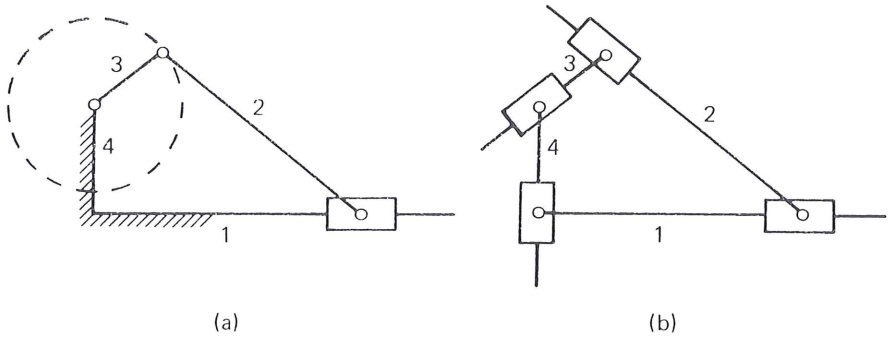

Figure 8.56 (a) offset slider-crank mechanism; (b) its equivalent general chain.

mechanism of Fig. 8.56a may be derived from the general chain (Fig. 8.56b) by fixing the sliders to their respective bars between members 1 and 4, 4 and 3, and 3 and 2 as well as fixing bars 1 and 4 to ground.

Complex numbers readily lend themselves as an ideal tool for modeling linkage members as parts of planar chains. For each bar-slider member of Fig. 8.55, the position of the pivot on the slider with respect to the pivot of the bar can be defined by the relative position vector $\mathbf{Z}_k$ (Fig. 8.57a) expressible as a complex number. The first or starting position of the kth bar can be written as

$$\mathbf{Z}_k = Z_k e^{i\theta_1} = Z_k(\cos\theta_1 + i\sin\theta_1) \tag{8.9}$$

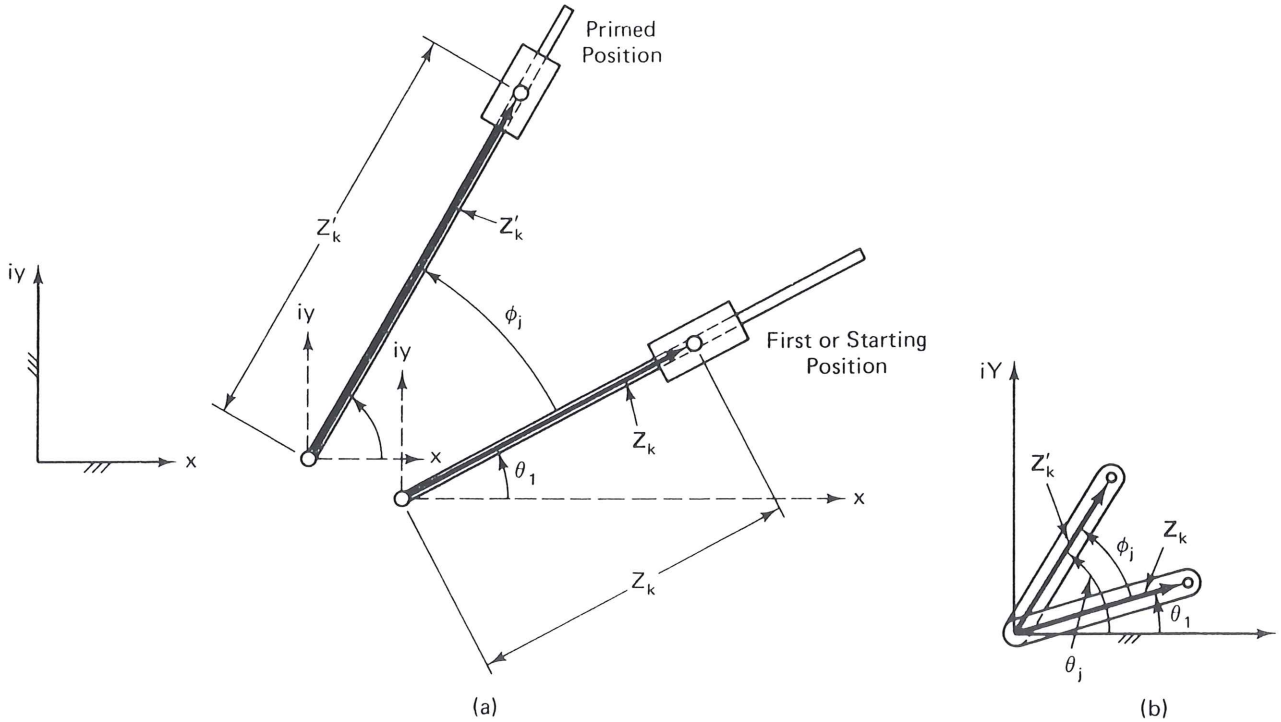

Figure 8.57 Complex-vector representation of a bar-slider pair; (a) stretch rotation; (b) pure rotation.

where $i \equiv \sqrt{-1}$

k = kth bar of the chain

$Z_k = |\mathbf{Z}_k|$ = length between the pivot of the bar and the pivot on the slider in the first position

$\theta_1 = \arg \mathbf{Z}_k$ = angle measured to vector $\mathbf{Z}_k$ from the real axis of a fixedly oriented rectangular coordinate system translating with the pivot of the bar (angles measured counterclockwise are positive)

If there is no change in the length of the kth bar in the chain from the first to the primed (jth) position as shown in Fig. 8.57b, $\mathbf{Z}'_k$ is expressible as

$$\mathbf{Z}'_k = Z_k e^{i(\theta_1 + \phi_j)} = Z_k e^{i\theta_1} e^{i\phi_j} \tag{8.10}$$

where

$$\phi_j = \theta_j - \theta_1 \tag{8.11}$$

Notice that as a link moves in the plane, a coordinate system is pinned to the base of the link (Fig. 8.57a). This coordinate system remains parallel to a fixed set of coordinates so that θ_j and θ_1 are arguments of $\mathbf{Z}$ in the jth and first positions respectively while ϕ_j is the angle of rotation from position 1 to j. Using Eq. (8.9) yields

$$\mathbf{Z}'_k = \mathbf{Z}_k e^{i\phi_j} \tag{8.12}$$

If there is a change in length of the kth bar, and if this change is defined by

$$\rho_j \equiv \frac{Z'_k}{Z_k} \tag{8.13}$$

then

$$\mathbf{Z}'_k = \mathbf{Z}_k \rho_j e^{i\phi_j} \tag{8.14}$$

$e^{i\phi_j}$ in Eqs. (8.12) and (8.14) is termed the *rotational operator* [138, 140] and will rotate a vector from its initial position by the angle ϕ_j without changing the length of the vector. The factor ρ_j is the *stretch ratio,** while $\rho_j e^{i\phi_j}$ is called the *stretch rotation operator* [138]. We may now model any bar-slider member in a planar mechanism by a vector and express its motion with respect to any reference in terms of an initial position, a stretch, and a rotation. How can we collect the links of the mechanism into one model and develop some equations to work with?

8.14 THE DYAD OR STANDARD FORM

The great majority of planar linkages may be thought of as combinations of vector pairs called *dyads* [145]. For example, the four-bar linkage in Fig. 8.58 can be perceived as two dyads: the left side of the linkage represented as a vector pair (W and Z) shown in

* See, for example, the slider-crank of Fig. 8.82 and Eq. (8.83).

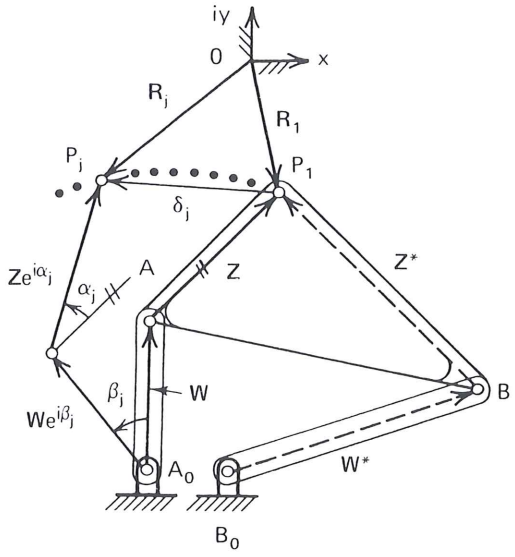

Figure 8.58 Notation associated with a dyad shown as it would model the left half of a four-bar linkage. The dyad (**W** and **Z**) is drawn in its first and jth positions.

solid lines, and the right side represented by the dashed dyad (**W*** and **Z***). The vectors that represent the coupler $\overrightarrow{AB}$ and the ground link $\overrightarrow{A_0B_0}$ are easily determined by vector addition when these dyads are synthesized [see Eqs. (8.25) and (8.26)]. The path point of the coupler link moves along a path from position P_1 to P_j defined in an arbitrary complex coordinate system by $\mathbf{R}_1$ and $\mathbf{R}_j$.

All vector rotations are measured from the starting position, positive counterclockwise (Figs. 8.58 and 8.59). Angle β_2 is the rotation of vector **W** from the first to the second position, while β_3 is the rotation from the first to the third position. Similarly, angles α_j are rotations of the vector **Z** from its first to its jth position (see Fig. 8.59).

Suppose that we specify two positions for an unknown dyad by prescribing the values of $\mathbf{R}_1$, $\mathbf{R}_j$, α_j, and β_j (Fig. 8.58). To find the unknown starting position vectors of the dyad, **W** and **Z**, a loop closure equation may be derived by summing the vectors clockwise around the loop containing $\mathbf{W}e^{i\beta_j}$, $\mathbf{Z}e^{i\alpha_j}$, $\mathbf{R}_j$, $\mathbf{R}_1$, **Z**, and **W**:

$$\mathbf{W}e^{i\beta_j} + \mathbf{Z}e^{i\alpha_j} - \mathbf{R}_j + \mathbf{R}_1 - \mathbf{Z} - \mathbf{W} = 0 \tag{8.15}$$

or

$$\boxed{\mathbf{W}(e^{i\beta_j} - 1) + \mathbf{Z}(e^{i\alpha_j} - 1) = \boldsymbol{\delta}_j} \tag{8.16}$$

where the displacement vector along the prescribed trajectory from P_1 to P_j is

$$\boldsymbol{\delta}_j \equiv \mathbf{R}_j - \mathbf{R}_1 \tag{8.17}$$

Equation (8.16) is the *standard-form* equation. This equation is simply the vector sum around the loop containing the first and jth positions of the dyad forming the left side of the four-bar linkage. As we will see, Eq. (8.16) is called the standard form if $\boldsymbol{\delta}_j$

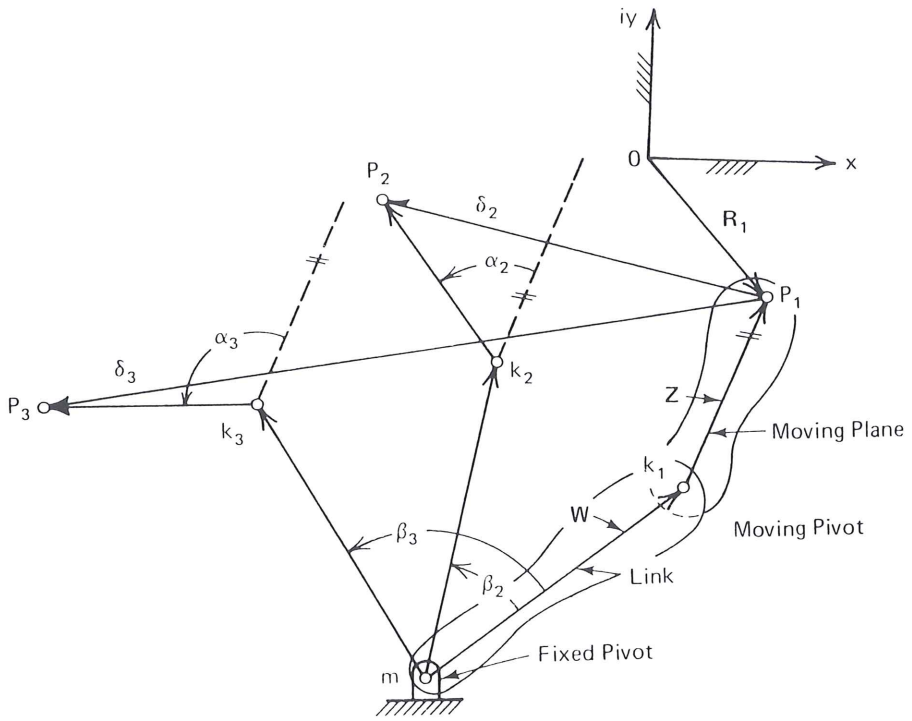

Figure 8.59 Schematic of the **W**, **Z** dyad shown in three positions. The precision points P_1, P_2, P_3 are located by $\mathbf{R}_1$, $\mathbf{R}_2$, $\mathbf{R}_3$, while all rotations are expressed from the first dyad position.

and either α_j or β_j are prescribed or known. This requirement is consistent with the definitions of the usual tasks of kinematic synthesis: motion generation, path generation with prescribed timing, and function generation.

8.15 NUMBER OF PRESCRIBED POSITIONS VERSUS NUMBER OF FREE CHOICES

For how many positions can we synthesize a four-bar linkage for motion, path, or function generation? A finite number of parameters (the two components of each vector) completely describe this linkage in its starting position. Therefore, there are only a finite number of prescribable parameters which can be imposed in a synthesis effort. The four-bar motion generator will be used to determine how many positions may actually be prescribed. In Fig. 8.58, the path displacement vectors $\boldsymbol{\delta}_j$ and coupler rotations α_j will be prescribed in a *motion-generation task*.

Table 8.1 illustrates how to determine the maximum number of prescribable positions for the synthesis of a four-bar motion generator. Although Table 8.1 is based on the left side of the linkage of Fig. 8.58 [Eq. (8.16)], the right side of the linkage will yield the same results [see Eq. (8.24)]. The table shows that, for two positions there are two independent scalar equations contained in the vector equation Eq. (8.16): the summation of x components and the summation of the y components of the vectors. These are called the *real* and *imaginary* parts of the equation, each a scalar equation in itself. This system of two scalar equations contains five scalar unknowns: two coordinates each

TABLE 8.1 MAXIMUM NUMBER OF SOLUTIONS FOR THE UNKNOWN DYAD **W, Z** WHEN δ_j AND α_j ARE PRESCRIBED IN THE EQUATION:

$$\mathbf{W}(e^{i\beta_j} - 1) + \mathbf{Z}(e^{i\alpha_j} - 1) = \delta_j \tag{8.16}$$

Number of positions (n): $j = 2, 3, \ldots, n$	Number of scalar equations	Number of scalar unknowns	Number of free choices (scalars)	Number of solutions
2	2	5(**W**, **Z**, β_2)	3	$O(\infty^3)$
3	4	6(above + β_3)	2	$O(\infty^2)$
4	6	7(above + β_4)	1	$O(\infty^1)$
5	8	8(above + β_5)	0	Finite

of the vectors **W** and **Z** (W_x, W_y, Z_x, and Z_y) and the input rotation β_2. If three of the five unknowns are chosen arbitrarily, the equations can be solved for the remaining two unknowns. Since in general there is an infinite number of choices for each of the three free choices, the number of possible solutions for the two-position synthesis problem is on the order of *infinity cubed,* symbolized by $O(\infty^3)$.

In the case of three-prescribed positions of the moving plane, specified by three precision points P_1, P_2 and P_3 and two angles of rotation, α_2 and α_3, there are two more real equations but only one more scalar unknown (β_3). Thus two free choices can be made and $O(\infty)^2$ solutions are available. Each additional prescribed position in Table 8.1 adds two scalar equations and one scalar unknown. Thus, for four positions, there is one free choice and a single infinity of solutions. For five prescribed positions there are no free choices available, and at best a finite number of solutions will exist (see Chap. 3 of Vol. 2). Five prescribed positions is therefore the maximum number of precision points possible for the standard-form solutions for the motion-generation dyad of Fig. 8.58.

Table 8.1 correlates the number of prescribed positions, the number of free choices, and the number of closed-form solutions expected for the standard form. However, Table 8.1 does not say anything directly about the difficulty in solving the sets of standard-form equations in closed form. An important question is this: can a linear equation-solver technique be applied for two, three, four, and five prescribed positions?

The answer lies in the form of the respective sets of equations of synthesis: are they linear or nonlinear in the unknown reals? A nonlinearity test will be applied to Eq. (8.16) for each row of Table 8.1.

Two positions. There are three free choices to be made in Eq. (8.16). For example, if $\boldsymbol{\delta}_2$ and α_2 were prescribed, **Z** and β_2 could be chosen arbitrarily, yielding a simple linear solution for the remaining unknown, **W**:

$$\mathbf{W} = \frac{\boldsymbol{\delta}_2 - \mathbf{Z}(e^{i\alpha_2} - 1)}{e^{i\beta_2} - 1} \tag{8.18}$$

This case of motion generation for two positions for a dyad is analogous to the graphical technique described in Sec. 8.5. *In both cases there are three infinities of solutions.* Design methods can be developed for two prescribed positions with the ability to optimize other indices of performance *a priori*, such as the transmission angle.

Three positions. Here, according to Table 8.1, two free choices must be made, so one may expect *two infinities of solutions,* as in the graphical method (Sec. 8.6). The system of equations for three positions is

$$\begin{aligned} \mathbf{W}(e^{i\beta_2} - 1) + \mathbf{Z}(e^{i\alpha_2} - 1) &= \boldsymbol{\delta}_2 \\ \mathbf{W}(e^{i\beta_3} - 1) + \mathbf{Z}(e^{i\alpha_3} - 1) &= \boldsymbol{\delta}_3 \end{aligned} \tag{8.19}$$

If $\boldsymbol{\delta}_2$, $\boldsymbol{\delta}_3$, α_2, and α_3 are prescribed, β_2 and β_3 can be picked arbitrarily. Thus system (8.19) is a set of complex equations, *linear* in the complex unknowns $\mathbf{W}$ and $\mathbf{Z}$ (the vectors representing the dyad in its first position) with known coefficients. The system can be solved by Cramer's rule:

$$\mathbf{W} = \frac{\begin{vmatrix} \boldsymbol{\delta}_2 & e^{i\alpha_2} - 1 \\ \boldsymbol{\delta}_3 & e^{i\alpha_3} - 1 \end{vmatrix}}{\begin{vmatrix} e^{i\beta_2} - 1 & e^{i\alpha_2} - 1 \\ e^{i\beta_3} - 1 & e^{i\alpha_3} - 1 \end{vmatrix}} \tag{8.20}$$

$$\mathbf{Z} = \frac{\begin{vmatrix} e^{i\beta_2} - 1 & \boldsymbol{\delta}_2 \\ e^{i\beta_3} - 1 & \boldsymbol{\delta}_3 \end{vmatrix}}{\begin{vmatrix} e^{i\beta_2} - 1 & e^{i\alpha_2} - 1 \\ e^{i\beta_3} - 1 & e^{i\alpha_3} - 1 \end{vmatrix}} \tag{8.21}$$

Equations (8.20) and (8.21) are readily programmed on a hand calculator or microcomputer.

The three-position motion-synthesis case yields a linear solution if β_2 and β_3 are free choices. The two free choices in Eq. system (8.16) may be made with different strategies (as will be explored in Sec. 8.19 and 8.20), but will always involve two infinities of solutions [43, 44, 58, 61, 64, 108, 124, 125].

Four positions. The system of equations for four prescribed positions of the moving plane is as follows:

$$\begin{aligned} \mathbf{W}(e^{i\beta_2} - 1) + \mathbf{Z}(e^{i\alpha_2} - 1) &= \boldsymbol{\delta}_2 \\ \mathbf{W}(e^{i\beta_3} - 1) + \mathbf{Z}(e^{i\alpha_3} - 1) &= \boldsymbol{\delta}_3 \\ \mathbf{W}(e^{i\beta_4} - 1) + \mathbf{Z}(e^{i\alpha_4} - 1) &= \boldsymbol{\delta}_4 \end{aligned} \tag{8.22}$$

Table 8.1 allows only one free choice from among the seven real unknowns: coordinates of $\mathbf{W}$, $\mathbf{Z}$ and angles β_2, β_3, and β_4. Recall that $\boldsymbol{\delta}_j$ and α_j, $j = 2, 3, 4$, are prescribed. Thus only one of the rotations or one coordinate of a link vector can be picked arbitrarily. System (8.22) contains three unknown angles β_j in transcendental expressions. Even if we pick one β_j as a free choice, Eq. system (8.22) requires a nonlinear equation-solving technique. Thus three precision points comprise the maximum number which may be prescribed and yet obtain a linear solution. For the four-position problem, Chap. 3 of Vol. 2 presents a closed-form nonlinear solution for Eq. (8.22), yielding up to an infinity of solutions. The LINCAGES and KINSYN software packages are built around

the three and four prescribed position cases [6, 50, 51, 57, 60, 62, 93, 114, 124, 125, 136, 171]. Refer to color inserts in this book for LINCAGES example output.

Five positions. The system of equations for five positions, which adds one equation added to Eq. system (8.22) with $j = 5$, is also nonlinear in the unknowns β_j, and there are no free choices available. This case is also solved in closed form in Chap. 3 of Vol. 2.

8.16 THREE PRESCRIBED POSITIONS FOR MOTION, PATH, AND FUNCTION GENERATION

This chapter concentrates on kinematic synthesis objectives that yield linear solutions—those easily solved graphically, on a hand calculator, or by a simple computer program. In the preceding section we discovered that, for motion generation of a dyad, three positions were the limit for a linear solution. Table 8.1 shows that there are two free choices to be made amongst the variables $\mathbf{W}$, $\mathbf{Z}$, β_2 and β_3. Although there is good logic in choosing β_2 and β_3, as was done in Eqs. (8.20) and (8.21), other free choices may be made to satisfy strategies other than one that has a simple equation set. This and the next section will continue with the standard form solution procedure, followed by other design strategies for three prescribed positions in subsequent sections.

Notice that the balancing of the number of equations and the number of unknowns in Table 8.1 was based on motion synthesis. Equation (8.16) has been termed the *standard form* with the understanding that both δ_j and α_j or β_j were prescribed. The numbers in Table 8.1 will be the same if β_j were prescribed instead of α_j, which, as we know from Sec. 8.2, is the case for path generation with prescribed timing.

We will look at the four-bar mechanism of Fig. 8.60, as well as a six-bar linkage in Sec. 8.20, and attempt to express the synthesis of these linkages in the standard form for motion, path, and function generation. If this can be accomplished, only one computer program will be needed to synthesize these linkages for either of these tasks. (This generality of the standard form also extends to the nonlinear solutions of Chap. 3 of Vol. 2.)

Synthesis of a Four-Bar Motion Generator for Three Precision Points

The four-bar linkage of Fig. 8.60 is to be synthesized for motion generation. As suggested in Sec. 8.14, there are two independent dyads in the four-bar linkage, which will be called the *left-hand side* and the *right-hand side*. Each dyad connects a ground pivot (a center point) to the path point on the coupler by way of joint A or B of the coupler (the circle point). The equations describing the displacements of the left-hand side have already been derived, but in the notation of Fig. 8.60 the standard form is

$$\mathbf{Z}_2(e^{i\phi_j} - 1) + \mathbf{Z}_5(e^{i\gamma_j} - 1) = \delta_j, \qquad j = 2, 3 \tag{8.23}$$

where δ_j and γ_j are prescribed.

the three and four prescribed position cases [6, 50, 51, 57, 60, 62, 93, 114, 124, 125, 136, 171]. Refer to color inserts in this book for LINCAGES example output.

Five positions. The system of equations for five positions, which adds one equation added to Eq. system (8.22) with $j = 5$, is also nonlinear in the unknowns β_j, and there are no free choices available. This case is also solved in closed form in Chap. 3 of Vol. 2.

8.16 THREE PRESCRIBED POSITIONS FOR MOTION, PATH, AND FUNCTION GENERATION

This chapter concentrates on kinematic synthesis objectives that yield linear solutions—those easily solved graphically, on a hand calculator, or by a simple computer program. In the preceding section we discovered that, for motion generation of a dyad, three positions were the limit for a linear solution. Table 8.1 shows that there are two free choices to be made amongst the variables W, Z, β_2 and β_3. Although there is good logic in choosing β_2 and β_3, as was done in Eqs. (8.20) and (8.21), other free choices may be made to satisfy strategies other than one that has a simple equation set. This and the next section will continue with the standard form solution procedure, followed by other design strategies for three prescribed positions in subsequent sections.

Notice that the balancing of the number of equations and the number of unknowns in Table 8.1 was based on motion synthesis. Equation (8.16) has been termed the *standard form* with the understanding that both δ_j and α_j or β_j were prescribed. The numbers in Table 8.1 will be the same if β_j were prescribed instead of α_j, which, as we know from Sec. 8.2, is the case for path generation with prescribed timing.

We will look at the four-bar mechanism of Fig. 8.60, as well as a six-bar linkage in Sec. 8.20, and attempt to express the synthesis of these linkages in the standard form for motion, path, and function generation. If this can be accomplished, only one computer program will be needed to synthesize these linkages for either of these tasks. (This generality of the standard form also extends to the nonlinear solutions of Chap. 3 of Vol. 2.)

Synthesis of a Four-Bar Motion Generator for Three Precision Points

The four-bar linkage of Fig. 8.60 is to be synthesized for motion generation. As suggested in Sec. 8.14, there are two independent dyads in the four-bar linkage, which will be called the *left-hand side* and the *right-hand side*. Each dyad connects a ground pivot (a center point) to the path point on the coupler by way of joint A or B of the coupler (the circle point). The equations describing the displacements of the left-hand side have already been derived, but in the notation of Fig. 8.60 the standard form is

$$\mathbf{Z}_2(e^{i\phi_j} - 1) + \mathbf{Z}_5(e^{i\gamma_j} - 1) = \delta_j, \qquad j = 2, 3 \tag{8.23}$$

where δ_j and γ_j are prescribed.

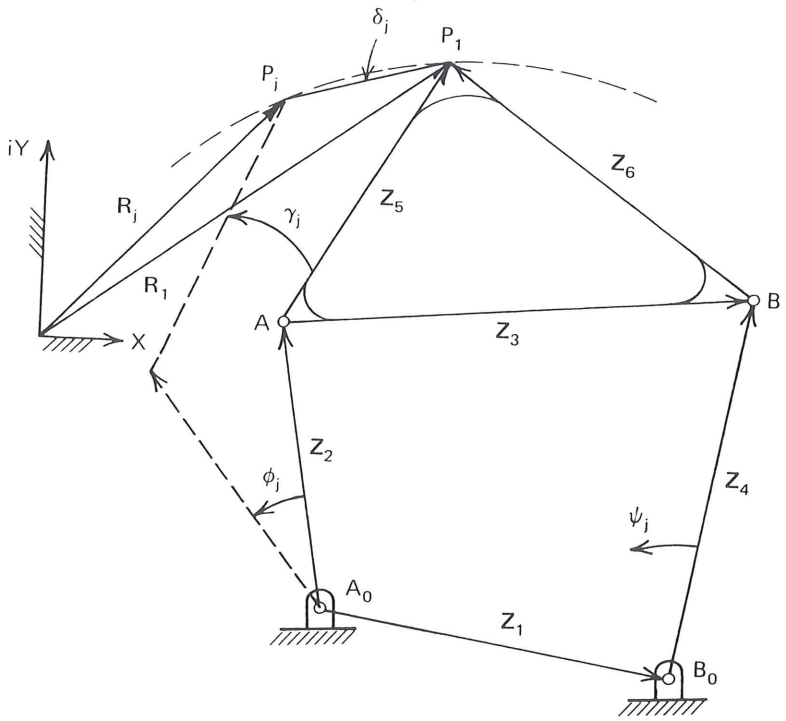

Figure 8.60 Four-bar motion- and path-generator mechanism.

The displacement equations for the right-hand side of the linkage may be written as

$$\mathbf{Z}_4(e^{i\psi_j} - 1) + \mathbf{Z}_6(e^{i\gamma_j} - 1) = \boldsymbol{\delta}_j, \qquad j = 2, 3 \tag{8.24}$$

where $\boldsymbol{\delta}_j$ and γ_j are prescribed.

If we assume ϕ_j and ψ_j arbitrarily, Eqs. (8.23) and (8.24) can be solved by Cramer's rule for $\mathbf{Z}_2$, $\mathbf{Z}_5$, $\mathbf{Z}_4$, and $\mathbf{Z}_6$. See the form of solution in Eqs. (8.20) and (8.21). The other two linkage vectors are simply

$$\mathbf{Z}_3 = \mathbf{Z}_5 - \mathbf{Z}_6 \tag{8.25}$$

and

$$\mathbf{Z}_1 = \mathbf{Z}_2 + \mathbf{Z}_3 - \mathbf{Z}_4 \tag{8.26}$$

Example 8.3

This example* will help demonstrate the correlation between the graphical and complex number methods for three-precision-point standard-form motion synthesis. The graphical solution will be demonstrated first. Figure 8.61a shows a rigid body in three desired positions. The angular orientation and precision positions of the body in three positions are known. Suppose points A and B are chosen as proposed circle-point locations. Choosing these locations constitutes making four free choices, the x and y coordinates of both points. These choices dictate the location of the ground pivots A_0 and B_0 shown in Fig. 8.61b, found by the intersection of the perpendicular bisectors as described in Sec. 8.6 (refer to Fig. 8.39). The resulting starting positions of the input and output dyads, $\mathbf{W}_A\mathbf{Z}_A$ and $\mathbf{W}_B\mathbf{Z}_B$, and the arguments of the input and output links at the three precision positions are:

* Contributed by Ray Giese and John Titus.

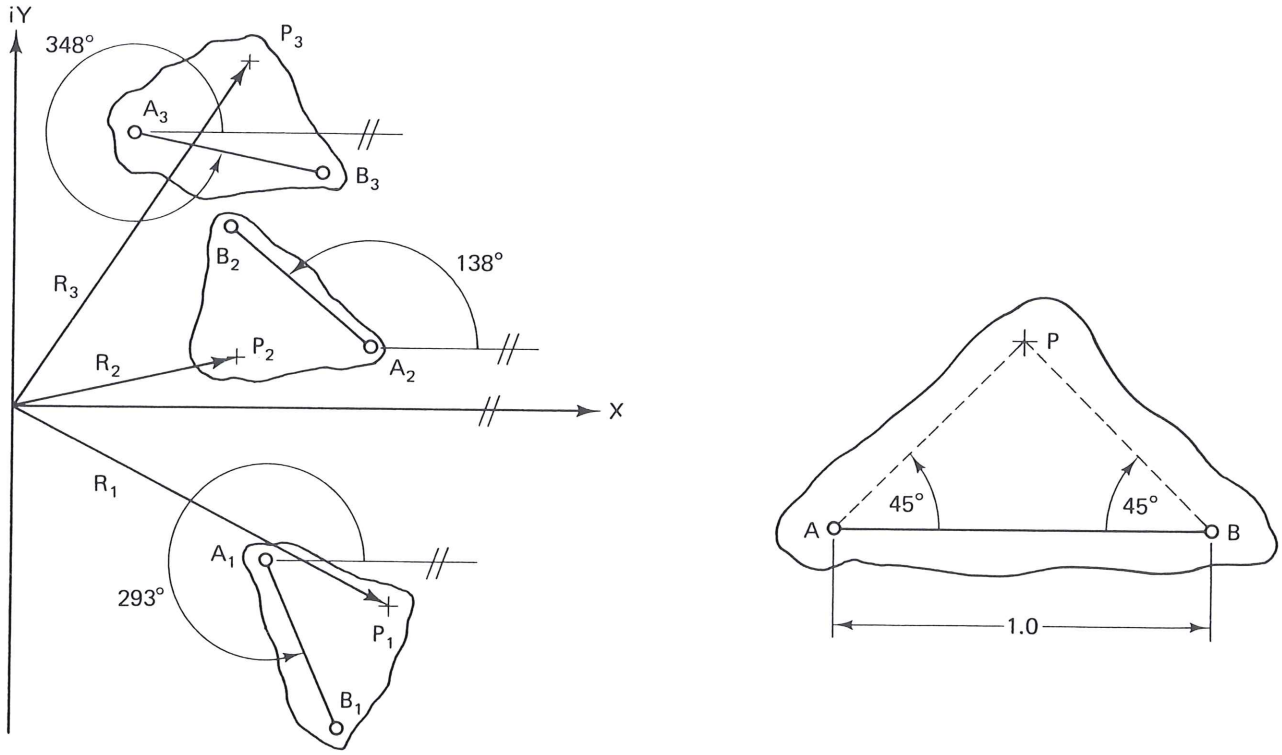

(a)

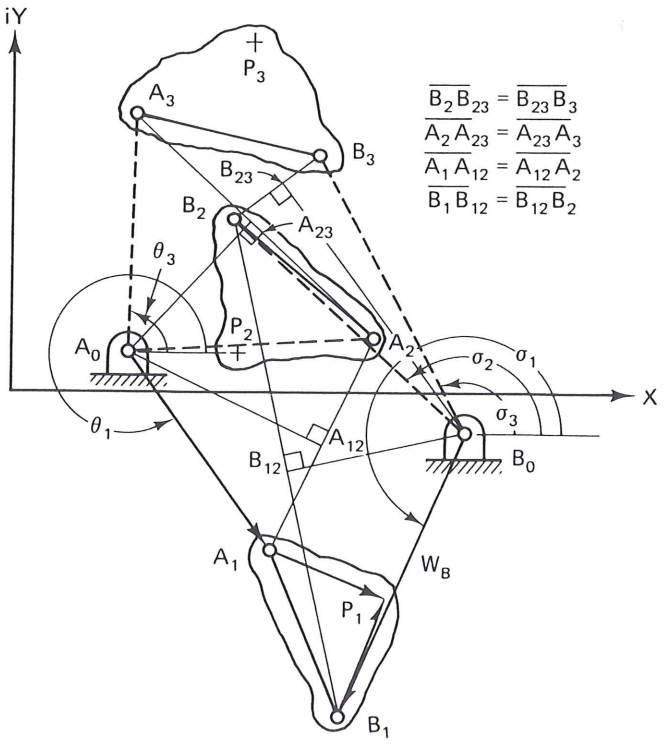

(b)

Figure 8.61 Three position motion synthesis of a four-bar linkage: (a) coupler link AB shown in three prescribed coplanar positions as a rigid body; (b) graphical construction for locating A_0 and B_0.

$$\mathbf{W}_A = .72 - 1.06i \qquad \mathbf{W}_B = -.66 - 1.55i$$

$$\theta_1 = 304.2°, \qquad \sigma_1 = 247.1°$$

$$\theta_2 = 2.6°, \qquad \sigma_2 = 136.7°$$

$$\theta_3 = 88.4°, \qquad \sigma_3 = 116.6°$$

$$\mathbf{Z}_A = .656 - .265i \qquad \mathbf{Z}_B = .265 + .656i$$

($\mathbf{Z}_A$ and $\mathbf{Z}_B$ are known from the choices for points A and B)

Now we shall try to match the graphically generated solution with the standard-form method. Solving for the input side first, using path tracer point P, we compute from Fig. 8.61.

$$\boldsymbol{\delta}_2 = \mathbf{R}_2 - \mathbf{R}_1 = (1.2 + .25i) - (2.0 - 1.1i) = -.8 + 1.35i$$

$$\boldsymbol{\delta}_3 = \mathbf{R}_3 - \mathbf{R}_1 = (1.25 + 1.9i) - (2.0 - 1.1i) = -.75 + 3.0i$$

$$\alpha_2 = 138° - 293° = -155° = 205°$$

$$\alpha_3 = 348° - 293° = 55°$$

The input link rotation angles are free choices in the motion generation solution. We choose the same angles as found in the graphical solution to demonstrate the correlation between the two solutions:

$$\beta_2 = \theta_2 - \theta_1 = 2.6° - 304.2° = -301.6° = 58.4°$$

$$\beta_3 = \theta_3 - \theta_1 = 88.4° - 304.2° = -215.8° = 144.2°$$

The input link solution as given by Eq. (8.20) is

$$\mathbf{W}_A = \frac{\boldsymbol{\delta}_2(e^{i\alpha_3} - 1) - \boldsymbol{\delta}_3(e^{i\alpha_2} - 1)}{(e^{i\beta_2} - 1)(e^{i\alpha_3} - 1) - (e^{i\beta_3} - 1)(e^{i\alpha_2} - 1)}$$

$$\mathbf{W}_A = \frac{\boldsymbol{\delta}_2 e^{i\alpha_3} - \boldsymbol{\delta}_3 e^{i\alpha_2} + \boldsymbol{\delta}_3 - \boldsymbol{\delta}_2}{e^{i(\beta_2+\alpha_3)} - e^{i(\beta_3+\alpha_2)} - e^{i\beta_2} - e^{i\alpha_3} + e^{i\beta_3} + e^{i\alpha_2}}$$

Using Euler's equation ($e^{i\theta} = \cos\theta + i \sin\theta$) and substituting the values for the variables, we obtain

$$\mathbf{W}_A = \frac{-3.462 + 4.171i}{-4.194 - .403i}$$

$$\mathbf{W}_A = .723 - 1.064i = 1.287 \measuredangle 304.21°$$

which, when compared to the graphical solution, shows less than 1% difference. This is well within graphical accuracy. Vector $\mathbf{Z}_A$ is calculated from Eq. (8.21).

$$\mathbf{Z}_A = \frac{\boldsymbol{\delta}_3(e^{i\beta_2} - 1) - \boldsymbol{\delta}_2(e^{i\beta_3} - 1)}{(e^{i\beta_2} - 1)(e^{i\alpha_3} - 1) - (e^{i\beta_3} - 1)(e^{i\alpha_2} - 1)}$$

$$\mathbf{Z}_A = \frac{\boldsymbol{\delta}_3 e^{i\beta_2} - \boldsymbol{\delta}_2 e^{i\beta_3} - \boldsymbol{\delta}_3 + \boldsymbol{\delta}_2}{e^{i(\beta_2+\alpha_3)} - e^{i(\beta_3+\alpha_2)} - e^{i\beta_2} - e^{i\alpha_3} + e^{i\beta_3} + e^{i\alpha_2}}$$

$$\mathbf{Z}_A = \frac{-2.856 + .847i}{-4.1941 - .4025i}$$

$$\mathbf{Z}_A = .656 - .265i = .707 \measuredangle 338°$$

This is exactly the value that was chosen for $\mathbf{Z}_A$ in the graphical solution. The output side dyad is synthesized using the same values for δ_2, δ_3, α_2 and α_3 but requires two free choices for the output link rotation angles. Again, we choose the values determined in the graphical synthesis.

$$\beta_2 = \sigma_2 - \sigma_1 = 136.7° - 247.1° = -110.4° = 249.6°$$

$$\beta_3 = \sigma_3 - \sigma_1 = 116.6° - 247.1° = -130.5° = 229.5°$$

The same procedure is followed for the output side as for the input side, resulting in

$$\mathbf{W}_B = \frac{-3.462 + 4.171i}{-1.481 - 2.852i}$$

$$\mathbf{W}_B = -.655 - 1.554i = 1.686 \measuredangle 247.15°$$

This is exactly the graphical solution for this link. Finally, the output coupler side is found to be:

$$\mathbf{Z}_B = \frac{-1.477 - 1.727i}{-1.481 - 2.852i}$$

$$\mathbf{Z}_B = .265 + .656i = .707 \measuredangle 68°$$

Again, this is the same as that found in the graphical solution.

Synthesis of a Four-Bar Path Generator with Prescribed Timing

Suppose that the four-bar linkage of Fig. 8.60 is to be synthesized for path generation with prescribed timing. The very same equations as derived for motion generation, Eqs. (8.23) to (8.26) will apply in this case, but the prescribed angles will be different. Instead of γ_j in Eq. (8.32), ϕ_j will be prescribed and γ_j, $j = 2, 3$, are free choices. Thus Eq. (8.23) will still be in the standard form. As for Eq. (8.24), in order to connect the right-hand side with the left side, vector $\mathbf{Z}_6$ must rotate by the same rotations (γ_j) as $\mathbf{Z}_5$. Thus the same γ_j, $j = 2, 3$, that were picked as free choices for Eq. (8.23), are prescribed in Eq. (8.24). Therefore, the four-bar path generator with prescribed timing has the same solution procedure as the four-bar motion generator.

Synthesis of a Four-Bar Function Generator

The standard form for a four-bar function generator can be derived from Fig. 8.60 as follows. Recall that in function generation we wish to correlate the prescribed rotations of the input link (ϕ_j) and the output link (ψ_j). Therefore, the upper portion of the coupler link ($\mathbf{Z}_5$ and $\mathbf{Z}_6$) is of no concern for this task. Figure 8.62 shows the basic four-bar of Fig. 8.60 in the first and jth position. The vector loop containing $\mathbf{Z}_2$, $\mathbf{Z}_3$, and $\mathbf{Z}_4$ is

$$\mathbf{Z}_2(e^{i\phi_j} - 1) + \mathbf{Z}_3(e^{i\gamma_j} - 1) - \mathbf{Z}_4(e^{i\psi_j} - 1) = 0 \qquad (8.27)$$

Since this vector equation is not in the standard form, Table 8.2 is formulated to help correlate the number of free choices and the number of prescribed positions. The

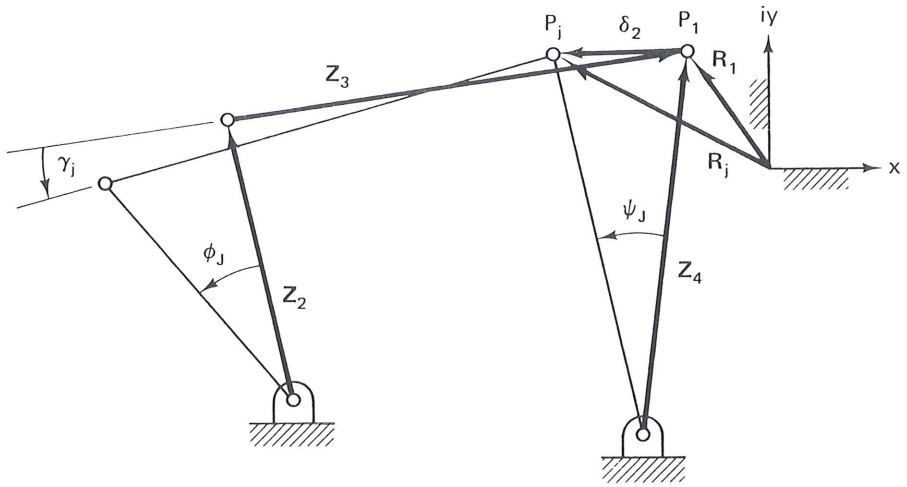

Figure 8.62 Four-bar function-generator mechanism.

TABLE 8.2 NUMBER OF AVAILABLE SOLUTIONS IN THE SYNTHESIS OF FOUR-BAR FUNCTION GENERATORS (FIG. 8.62) ACCORDING TO THE EQUATION

$$\mathbf{Z}_2(e^{i\phi_j} - 1) + \mathbf{Z}_3(e^{i\gamma_j} - 1) - \mathbf{Z}_4(e^{i\psi_j} - 1) = 0 \qquad (8.27)$$

Number of positions (n): $j = 2, 3, \ldots, n$	Number of scalar equations	Number of scalar unknowns	Number of free choices (scalars)	Number of solutions
2	2	7($\mathbf{Z}_2$, $\mathbf{Z}_3$, $\mathbf{Z}_4$, γ_2)	5	$O(\infty)^5$
3	4	8(above + γ_3)	4	$O(\infty)^4$
4	6	9(above + γ_4)	3	$O(\infty)^3$
5	8	10(above + γ_5)	2	$O(\infty)^2$
6	10	11(above + γ_6)	1	$O(\infty)^1$
7	12	12(above + γ_7)	0	Finite

same development as that done in connection with Table 8.1 is repeated here. Notice that the maximum number of prescribed positions is seven when a triad (three links) is used and when two of the three rotations are prescribed, as they must be for function generation.

Picking $\mathbf{Z}_4$ as an arbitrary choice ($\mathbf{Z}_2$ could be picked instead) will convert Eq. (8.27) to the standard form:

$$\mathbf{Z}_2(e^{i\phi_j} - 1) + \mathbf{Z}_3(e^{i\gamma_j} - 1) = \boldsymbol{\delta}_j = \mathbf{Z}_4(e^{i\psi_j} - 1) \qquad (8.28)$$

The justification for picking $\mathbf{Z}_4$ is twofold: first, by comparing Tables 8.1 and 8.2, the latter becomes equivalent to the first if two of the original seven real unknowns of Table 8.2 are picked arbitrarily; second, by choosing $\mathbf{Z}_4$, we are actually specifying the scale and orientation of the function generator. In fact, once a four-bar is synthesized for function generation, the entire linkage may be scaled up or down and oriented in any direction without changing the functional relationship between input and output link rota-

tions [$\psi_j = f(\phi_j)$]. Therefore, new function-generation solutions do not result from allowing $\mathbf{Z}_4$ to be an unknown. (Path and motion generators *do change* their prescribed path with a change in scale; therefore, only in function generation synthesis of four-bar linkages do we pick one of the link vectors arbitrarily).

Equation (8.28) is now in the standard form. In fact, function generation can be thought of as a special case of path generation with prescribed timing, the path of $\mathbf{Z}_4$ being along a circular arc. Note also that the only dyad that needs to be synthesized for function generation is that of Eq. (8.28) for $j = 2, 3$.

Sections 8.21 and 8.22 show other techniques for generating design equations for function generation: Freudenstein's equation and the loop-closure-equation technique. The number of free choices here does coincide with the latter method. These other techniques do not necessarily yield the standard form, although they can also be so formulated (see Chap. 3 of Vol. 2).

8.17 THREE-PRECISION-POINT SYNTHESIS PROGRAM FOR FOUR-BAR LINKAGES*

A program can be written to synthesize a four-bar motion, path, or function generator mechanism for three finitely separated precision points utilizing the notation of Fig. 8.60 (Fig. 8.63 is a flowchart for this program). The system of equations, Eq. (8.23), $j = 2,3$ for the left side of the four-bar and the equations for the right side, Eq. (8.24), $j = 2,3$ are solved by Cramer's rule as suggested in Eqs. (8.20) and (8.21). The input data required are the rotations of the input, output, and coupler links: PHI2, PHI3, GAM2, GAM3, PSI2, PSI3, (ϕ_2, ϕ_3, γ_2, γ_3, ψ_2, ψ_3) and the path displacements: XDEL2, YDEL2, XDEL3, YDEL3 (the x and y coordinates of $\boldsymbol{\delta}_2$ and $\boldsymbol{\delta}_3$). As can be seen by the examples below, the output of the program can include a repeat of the input data, link vectors in the starting position of the synthesized linkage in both Cartesian and polar form, as well as the coordinates of the coupler points: A, B, and P with respect to A_0. Figures 8.64, 8.65, and 8.66 show linkages that have been synthesized for motion, path, and function generation, respectively.

Notice that arbitrary choices must be made for all three examples according to Table 8.1. Thus for motion generation, ϕ_2, ϕ_3, ψ_2, and ψ_3 are free choices. For path generation with prescribed timing γ_2, γ_3, ψ_2, and ψ_3 are free choices. The procedure of Sec. 8.16 is not used here in the function-generation case. Rather than expanding the program of Fig. 8.63, the function generator is synthesized by prescribing ϕ_2, ϕ_3, ψ_2, ψ_3. With this method $\boldsymbol{\delta}_2$, $\boldsymbol{\delta}_3$, and γ_2, γ_3 are free choices. The only portion of the output of interest would be $\mathbf{Z}_2$, $\mathbf{Z}_3$, $\mathbf{Z}_4$, and $\mathbf{Z}_1$ (see Fig. 8.60 and the example of Fig. 8.66).

Example 8.4: Motion Generation

Completion of an assembly line requires the synthesis of a motion generator linkage to transfer boxes from one conveyor belt to another as depicted in Fig. 8.64a. A pickup and release position plus an intermediate location are specified. For simplicity, a four-bar link-

* The computer disc which accompanies this text includes a three position synthesis program that parallels this section.

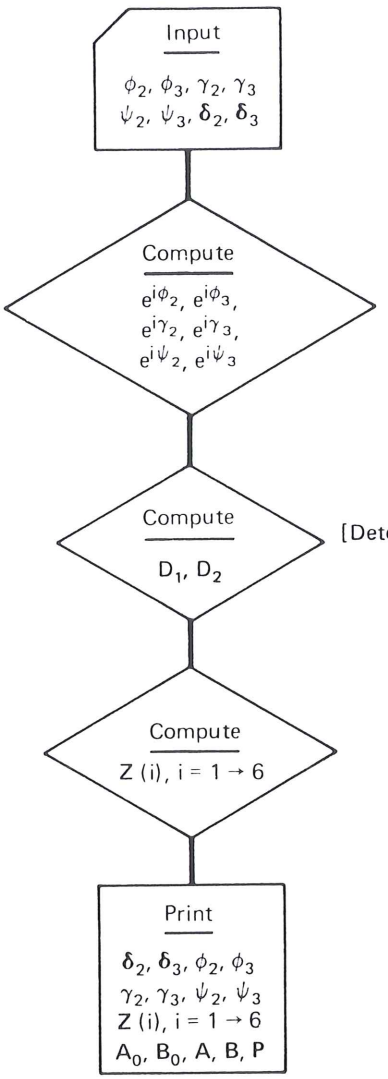

Figure 8.63 Flowchart of three-precision-point four-bar synthesis program (see Fig. 8.60).

age (Fig. 8.60) is the type chosen for the task. From Fig. 8.64a, prescribed quantities for the motion generation are

$$\delta_2 = -6 + 11i, \qquad \gamma_2 = 22°$$
$$\delta_3 = -17 + 13i, \qquad \gamma_3 = 68°$$

The free choices are arbitrarily set* as

$$\phi_2 = 90°, \qquad \psi_2 = 40°$$
$$\phi_3 = 198°, \qquad \psi_3 = 73°$$

Table 8.3 shows a copy of the computer printout for this example, while Fig. 8.64b shows the solution drawn in three positions.

---

* By specifying input rotations about twice as large as output rotations, these choices are meant to bring about a crank-rocker type of four-bar solution. The ability to bring this about is a valuable attribute of the three-position standard-form method.

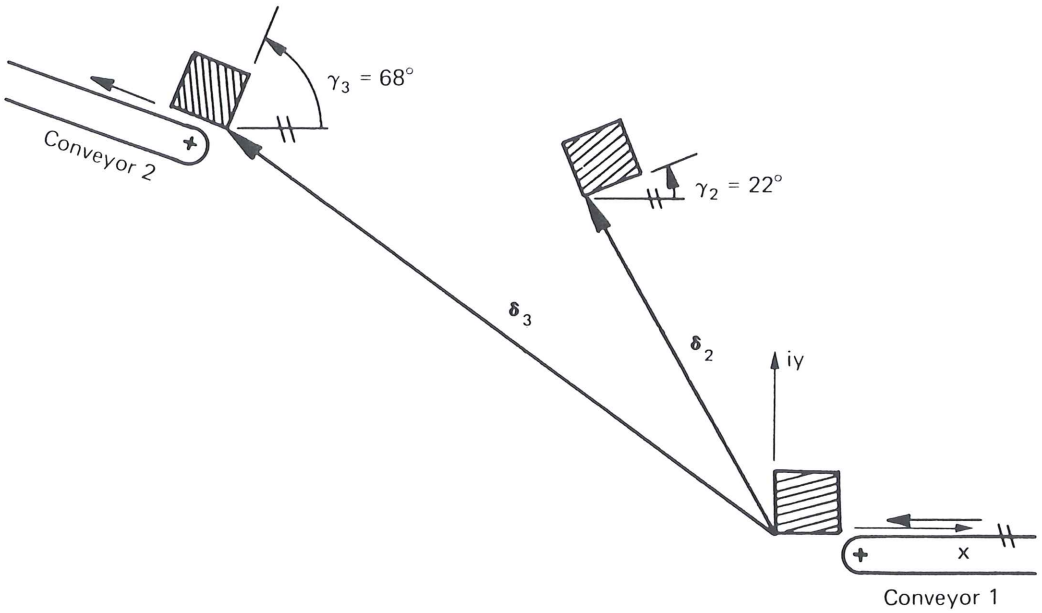

(a)

First Position ————————
Second Position - - - - - - - -
Third Position —— - - —— - -

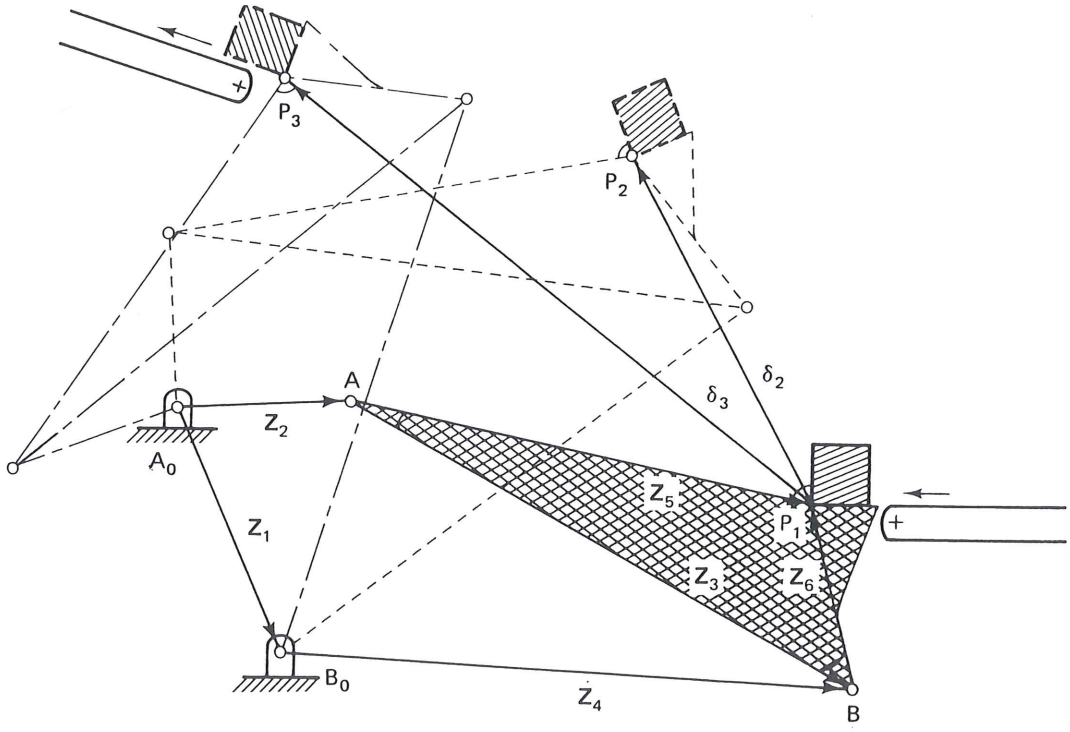

(b)

Figure 8.64 (a) three prescribed positions for four-bar motion synthesis; (b) synthesized conveyor linkage of Example 8.4 using the program of Fig. 8.63.

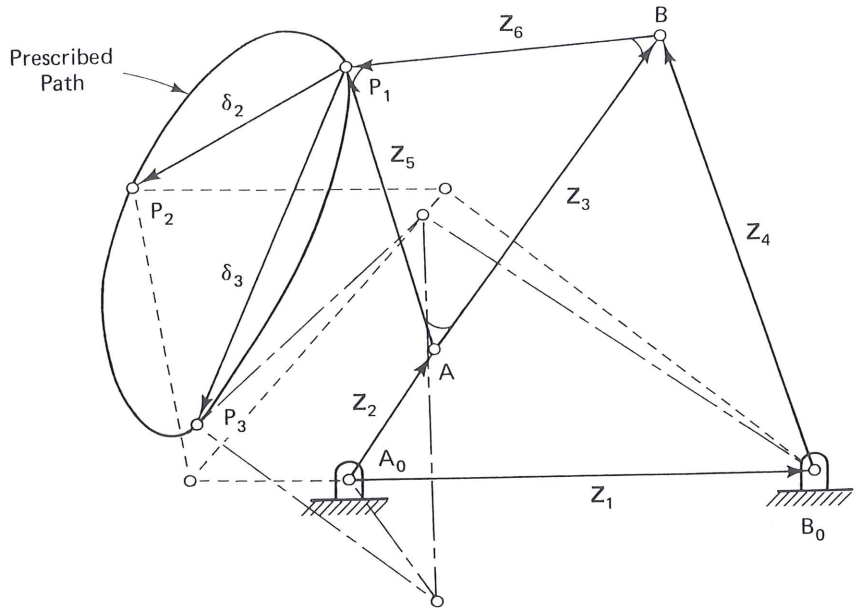

Figure 8.65 Four-bar path generator with three prescribed path points.

TABLE 8.3 COMPUTER PRINTOUT OF 3-POSITION MOTION-GENERATOR SYNTHESIS OF FOUR-BAR LINKAGE

INPUT DATA

	X COMPONENT	Y COMPONENT	
DELTA 2 =	−6.0000	11.0000	
DELTA 3 =	−17.0000	13.0000	
PHI 2 = 90.000	GAMMA 2 = 22.000		PSI 2 = 40.000
PHI 3 = 198.000	GAMMA 3 = 68.000		PSI 3 = 73.000

COMPUTED VECTORS

	X COMPONENT	Y COMPONENT	LENGTH	DIRECTION (DEG)
Z(2) =	5.7550	.4809	5.7751	4.777
Z(5) =	14.6106	−3.4698	15.0169	−13.359
Z(4) =	18.3746	−.6611	18.3864	−2.061
Z(6) =	−1.4207	5.9518	6.1190	103.426
Z(3) =	16.0313	−9.4215	18.5948	−30.443
Z(1) =	3.4118	−8.2796	8.9550	−67.605

LINKAGE PIVOT AND COUPLER LOCATIONS

	X COMPONENT	Y COMPONENT
A_0 =	0	0
B_0 =	3.4118	−8.2796
A =	5.7550	.4809
B =	21.7863	−8.9407
P =	20.3656	−2.9889

Example 8.5: Path Generation with Prescribed Timing (Fig. 8.65)

A stirring operation requires the generation of an elliptical path. A four-bar linkage is picked for this task. Since a crank rocker is required, the input rotations are also to be prescribed. Specified quantities are

$$\delta_2 = -1.4 - 0.76i, \qquad \phi_2 = 126°$$

$$\delta_3 = -1.0 - 2.3i, \qquad \phi_3 = 252°$$

TABLE 8.4 COMPUTER PRINTOUT OF PATH GENERATION EXAMPLE

INPUT DATA

	X COMPONENT	Y COMPONENT
DELTA 2 =	−1.4000	−.7600
DELTA 3 =	−1.0000	−2.3000

PHI 2 = 126.000 GAMMA 2 = −6.000 PSI 2 = 33.000
PHI 3 = 252.000 GAMMA 3 = 37.000 PSI 3 = 37.000

COMPUTED VECTORS

	X COMPONENT	Y COMPONENT	LENGTH	DIRECTION (DEG)
Z(2) =	.5919	.8081	1.0017	53.777
Z(5) =	−.5182	1.8246	1.8967	105.856
Z(4) =	−.9412	2.8331	2.9854	108.376
Z(6) =	−1.9958	−.1888	2.0047	−174.596
Z(3) =	1.4776	2.0134	2.4974	53.725
Z(1) =	3.0107	−.0117	3.0107	−.223

LINKAGE PIVOT AND COUPLER LOCATIONS

	X COMPONENT	Y COMPONENT
A_0 =	0	0
B_0 =	3.0107	−.0117
A =	.5919	.8081
B =	2.0695	2.8214
P =	.0737	2.6326

Arbitrarily chosen variables are

$$\gamma_2 = -6^\circ, \qquad \psi_2 = 33^\circ$$
$$\gamma_3 = 37^\circ, \qquad \psi_3 = 37^\circ$$

Table 8.4 is a copy of the computer-generated output for this example. Figure 8.65 illustrates the computer-generated linkage solution in its three prescribed positions.

Example 8.6: Function Generation

Figure 8.66a shows a barber's chair in which a single control arm is to actuate both the foot rest and the head rest. Notice the nonlinear relationship between the angles of rotation of the three members in the three specified positions. The type of linkage chosen for this task is a Watt II six-bar, which is simply two four-bars in series (usually connected through a bell crank). Specified quantities for the *first four-bar* function generator (between the head rest and the control arm) are

$$\phi_2 = 50^\circ, \qquad \psi_2 = 22.5^\circ$$
$$\phi_3 = 75^\circ, \qquad \psi_3 = 45^\circ$$

Arbitrarily chosen are

$$\delta_2 = -0.07 + 0.4i, \qquad \gamma_2 = 7^\circ$$
$$\delta_3 = -0.3 + 0.7i, \qquad \gamma_3 = 12^\circ$$

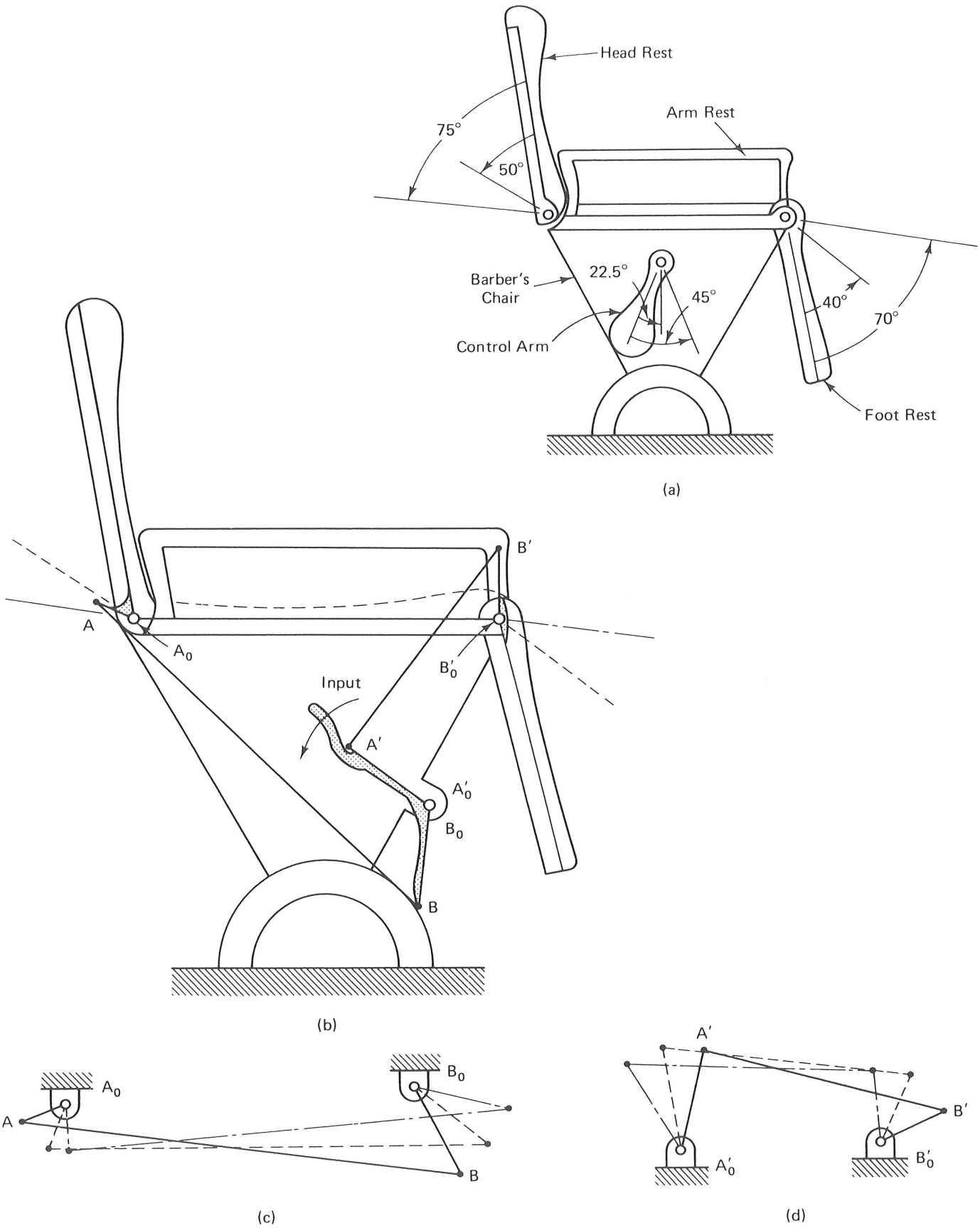

Figure 8.66 Four-bar function-generator linkages in reclining chair mechanism; (a) prescribed corresponding angular positions of foot rest, back rest, and control arm; (b) schematic of the completed mechanism; (c) head rest linkage; (d) foot rest linkage. The two four-bars in series constitute the Watt II six-bar.

The *second four-bar* function generator (between the control arm and the foot rest) has specified variables of

$$\phi_2 = 22.5°, \qquad \psi_2 = 40°$$
$$\phi_3 = 45°, \qquad \psi_3 = 70°$$

Arbitrarily chosen are

$$\delta_2 = -0.07 + 0.4i, \qquad \gamma_2 = 8°$$
$$\delta_3 = -0.3 + 0.7i, \qquad \gamma_3 = 13°$$

Table 8.5 is a printout for both sides of the six-bar linkage. Figure 8.66b illustrates how both these solutions are put together by appropriate rescaling and reorientation as one of the numerous possible Watt's II six-bar solutions to this problem, while Fig. 8.66c and d show the two four-bar halves in their three design positions.

TABLE 8.5 COMPUTER OUTPUT OF FOUR-BAR SYNTHESES OF RECLINER MECHANISM

HEAD REST LINKAGE

INPUT DATA

	X COMPONENT	Y COMPONENT		
DELTA 2 =	−.0700	.4000		
DELTA 3 =	−.3000	.7000		
PHI 2 = 50.000	GAMMA 2 = 7.000		PSI 2 = 22.500	
PHI 3 = 75.000	GAMMA 3 = 12.000		PSI 3 = 45.000	

COMPUTED VECTORS

	X COMPONENT	Y COMPONENT	LENGTH	DIRECTION (DEG)
Z(2) =	.0404	−.4640	.4657	−85.022
Z(5) =	1.8676	3.2580	3.7554	60.178
Z(4) =	1.0009	.2777	1.0388	15.506
Z(6) =	.2552	−.9384	.9725	−74.788
Z(3) =	1.6124	4.1965	4.4956	68.982
Z(1) =	.6518	3.4548	3.5158	79.315

LINKAGE PIVOT AND COUPLER LOCATIONS

	X COMPONENT	Y COMPONENT
A_0 =	0	0
B_0 =	.6518	3.4548
A =	.0404	−.4640
B =	1.6528	3.7325
P =	1.9080	2.7941

FOOT REST LINKAGE

INPUT DATA

	X COMPONENT	Y COMPONENT		
DELTA 2 =	−.0700	.4000		
DELTA 3 =	−.3000	.7000		
PHI 2 = 22.500	GAMMA 2 = 8.000		PSI 2 = 40.000	
PHI 3 = 45.000	GAMMA 3 = 13.000		PSI 3 = 70.000	

TABLE 8.5 (CONT.)

COMPUTED VECTORS

	X COMPONENT	Y COMPONENT	LENGTH	DIRECTION (DEG)
Z(2) =	.9642	.2270	.9906	13.247
Z(5) =	.3001	−.6696	.7338	−65.859
Z(4) =	.5189	−.4332	.6759	−39.857
Z(6) =	−.1359	1.6410	1.6466	94.733
Z(3) =	.4360	−2.3105	2.3513	−79.315
Z(1) =	.8813	−1.6503	1.8709	−61.897

LINKAGE PIVOT AND COUPLER LOCATIONS

	X COMPONENT	Y COMPONENT
A_0 =	0	0
B_0 =	.8813	−1.6503
A =	.9642	.2270
B =	1.4002	−2.0835
P =	1.2643	−.4426

8.18 CIRCLE-POINT AND CENTER-POINT CIRCLES

This section describes an alternative approach to choosing the two free choices indicated in Table 8.1. The angular unknowns will be considered as candidates for parameters on which the locations of the fixed and moving pivots of the solution dyads will depend. Loerch [108] discovered that, if an arbitrary value is chosen for one unprescribed angular parameter while the other angular parameter is allowed to assume all possible values, the resulting loci of corresponding fixed pivots m and moving pivots k_1 are found to be pairs of circles. For example, in Fig. 8.59, if δ_2, δ_3, α_2, β_2, and β_3 are chosen to have fixed values, the points m and k_1 trace circular loci as α_3 ranges between 0 and 2π. These will be referred to as M and K_1 circles, respectively. A complex-number formulation will be used to generate these circles analytically.

Dyad Equations

The vectors of the dyad m, k_1, P_1, are defined in Fig. 8.67. The loop-closure equations for the dyad in three finitely separated positions are

First position:

$$\mathbf{R} + \mathbf{W} + \mathbf{Z} = 0 \tag{8.29}$$

Second position:

$$\mathbf{R} + \mathbf{W}e^{i\beta_2} + \mathbf{Z}e^{i\alpha_2} = \delta_2 \tag{8.30}$$

Third position:

$$\mathbf{R} + \mathbf{W}e^{i\beta_3} + \mathbf{Z}e^{i\alpha_3} = \delta_3 \tag{8.31}$$

The unknown location of the moving pivot k_1 is defined by the vector $-\mathbf{Z}$ with respect to P_1, the origin of the fixed-coordinate system (as shown in Fig. 8.67), which coincides with the given initial position P_1 of the tracer point of the moving plane. The yet

Using Eqs. (8.96) and (8.97), we have

$$\mathbf{D} = +6.75 + 0.0i$$

$$\mathbf{Z}_2 = 3.89 - 0.59i, \qquad \mathbf{Z}_3 = -4.44 + 1.19i, \qquad \mathbf{Z}_4 = -1.56 + 0.59i$$

8.24 THREE-PRECISION-POINT SYNTHESIS: ANALYTICAL VERSUS GRAPHICAL

Thus far, both graphical and analytical approaches have been presented for three finitely separated positions of motion-, path with timing-, and function-generation synthesis of a four-bar linkage. Both techniques are straightforward. Which is better? The answer: both are equally important. Graphical techniques are extremely useful in the initial stages of synthesis. If a graphical construction does not yield an "optimal" solution in a reasonable amount of time or if the error sensitivity is high (e.g., the need to locate the intersection of lines that form an acute angle), then the analytical standard-form method is very attractive. In such cases the preliminary graphical solution will yield reasonable values for arbitrarily assumed (free-choice) quantities, which will help obtain workable computer solutions. The Cramer's rule solution described above is easily programmed for digital computation (the flowchart of a three-precision-point program is shown in Fig. 8.63) and numerous accurate solutions can be obtained in a fraction of the time required for a graphical construction. (Section 8.18 shows an alternative computer graphics technique for three precision points, which is a combined graphical and analytical method.)

A notable correlation between the graphical and analytical methods should be emphasized at this point. In both techniques, for the three-position synthesis of each dyad, there are two infinities of solutions for motion-, path-generation with prescribed timing, and function generation. As pointed out above, a function-generator four-bar linkage actually appears to require two additional scalars as free choices: the two components of the starting position vector of one of the links. However, picking that link specifies only the scale and orientation of the linkage. No new function generators are obtained by varying this link, because the functional relationship of the input and output rotations is not affected by this choice.

A very useful reference for linkage design is an atlas of four-bar coupler curves by *Hrones and Nelson* [89]. Approximately 7300 coupler curves of crank-rocker four-bar linkages are displayed (e.g., see Fig. 8.83). The black dots represent coupler points whose coupler curves are plotted. These can be used as "tracer points" in a path or motion generator linkage. Each dash on the coupler curves represents 10° of input crank rotation to provide an indication of coupler point velocity. The crank always has length 1 while the lengths of the coupler A, follower B and the fixed link C vary from page to page, yielding a variety of families of coupler curves. This atlas is extremely useful in the initial stages of a path- or in some cases motion-generation synthesis effort. A designer may be able to find several coupler curve forms that nearly accomplish the task at hand and then use these linkages to come up with proper "free-choices" (see Sec. 8.15) to help find a more nearly optimal linkage in a shorter time. Also, it may turn out that

there are no crank-rocker four-bars that satisfy the design requirements and the *type* synthesis step may have to be reconsidered.

APPENDIX: CASE STUDY—TYPE SYNTHESIS OF CASEMENT WINDOW MECHANISMS [54]

A powerful alternative method of type synthesis to the associated linkage approach presented in this chapter is applied here in an industrial application.

Structure Phase of Type Synthesis

Freudenstein and Maki [76] suggest separation of *structure* and *function* in the conceptual phase of mechanism synthesis. They point out that the degree of freedom of a mechanism imposes constraint on the structure of the mechanism. Rather than using Gruebler's equation (see Chap. 1) and Eq. (8.7) for degrees of freedom of mechanisms, they suggest the following forms:

$$F = \lambda(l - j - 1) + \sum_{i=1}^{j} f_i \tag{8.98}$$

and

$$L_{\text{IND}} = j - l + 1 \tag{8.99}$$

where F = number of degrees of freedom of mechanism

l = number of links of mechanism (including the fixed link; all links are considered as rigid bodies having at least two joints)

j = number of joints of mechanism; each joint is assumed as binary (i.e., connecting two links); if a joint connects more than two links, the number of joints $j = N - 1$, where N = the number of links at the common joint

f_i = degree of freedom of ith joint; this is the freedom of the relative motion between the connected links

λ = degree of freedom of the space within which the mechanism operates; for plane motion and motion on a surface $\lambda = 3$ and for spatial motions $\lambda = 6$

L_{IND} = number of independent circuits or closed loops in the mechanism

Combining Eqs. (8.98) and (8.99), we obtain

$$\sum f_i = F + \lambda L_{\text{IND}} \tag{8.100}$$

Since we are dealing with planar motion and a single degree of freedom,

$$F = 1, \qquad \lambda = 3$$

SISTEMI ARTICOLATI - ESERCIZIO 1 – Generazione di movimenti (3 posizioni)

Progettare un q.a. per trasferire scatole dal nastro convogliatore 1 al nastro 2
DATI:

$\delta_2 = -6 + 11i$ $\alpha_2 = 22°$

$\delta_3 = -17 + 13i$ $\alpha_3 = 68°$

Scelti ad arbitrio:

$\beta_2 = 90°$ $\beta_2^* = 40°$

$\beta_3 = 198°$ $\beta_3^* = 73°$

Si calcoli il modulo e la fase di **W,Z,W*,Z*.** Si disegni inoltre il quadrilatero articolato nelle tre posizioni desiderate

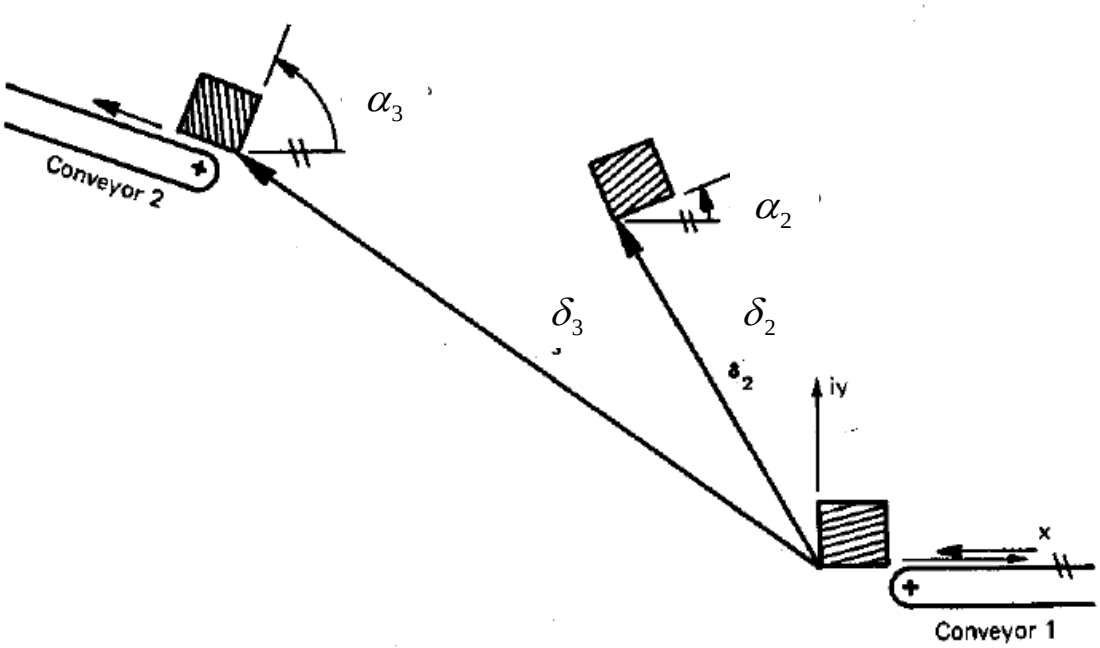

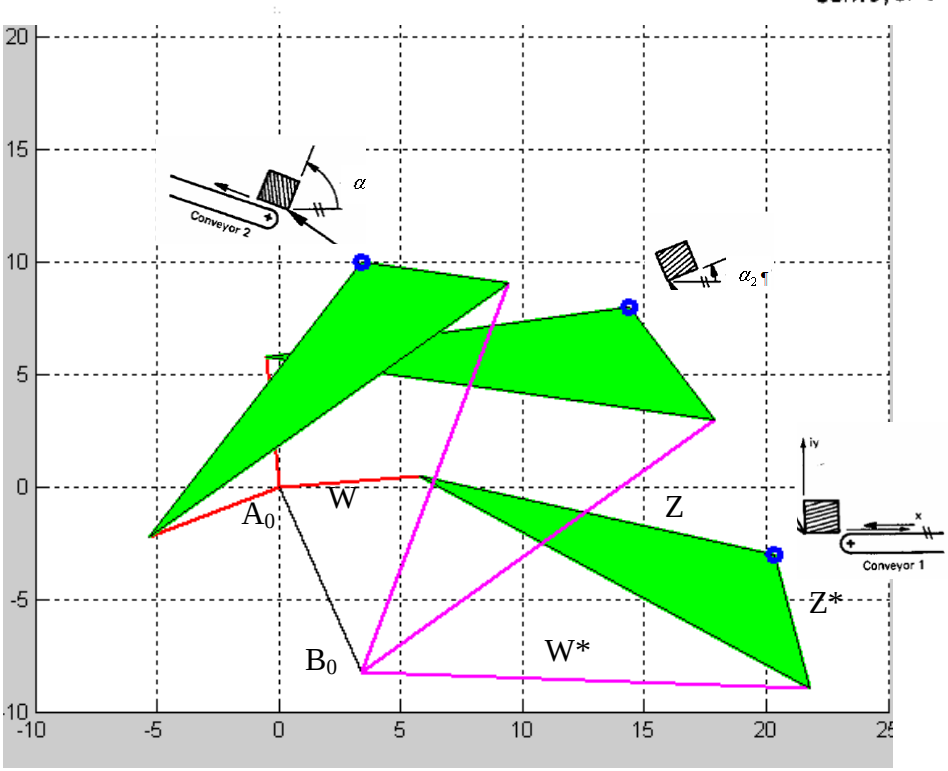

TRACCIA DI SOLUZIONE - Suggerimenti per programma in Matlab:

1) inizializzare le variabili:

```
g_2_r=pi/180;  %traforma gradi in radianti
alfa(2)=22*g_2_r;
alfa(3)=68*g_2_r;
delta(2)=
...
```

2) definire la matrice A_SX
3) definire la matrice B

risolvere il sistema lineare: `X_SX=A_SX\B;`

4) calcolare il modulo di W e Z (usa il comando *abs*)
5) calcolare la fase di W e Z (usa il comando *angle* e poi trasforma in gradi)

usa *fprintf* per mostrare a video i risultati di modulo e fase – `fprintf('modulo di W:  %0.3f \n',abs(X_SX(1)));`

6) ripeti i punti 1-5 per il lato dx
7) Disegnare il quadrilatero articolato ottenuto nelle tre posizioni

```
%%%PLOT DEI RISULTATI%%%%%%%%%%%%%%%%%
figure('position',[100 100 600 600])
hold on
for j=1:3
    W=X_SX(1)*exp(i*beta(j)); %da notare che quando k=1 beta(1)=0
    Wstar=X_DX(1)*exp(i*betastar(j));
    Z=X_SX(2)*exp(i*alfa(j));
    Zstar=X_DX(2)*exp(i*alfa(j));
    AB=Z-Zstar; %è il segmento di biella
    A0B0=W+AB-Wstar;  %è il telaio
    %disegno per punti il quandrilatero
    A0x=0;
    A0y=0;
    B0x=real(A0B0);
    B0y=imag(A0B0);
    Ajx=real(W);
    Ajy=imag(W);
    Pjx=real(W+Z);
    Pjy=imag(W+Z);
    Bjx=real(A0B0+Wstar);
    Bjy=imag(A0B0+Wstar);

    plot([A0x,B0x],[A0y,B0y],'k','linewidth',[2]);
    plot([A0x,Ajx],[A0y,Ajy],'r','linewidth',[2]);
    plot([Ajx,Pjx],[Ajy,Pjy],'g','linewidth',[2]);
    plot([Ajx,Bjx],[Ajy,Bjy],'g','linewidth',[2]);
    plot([B0x,Bjx],[B0y,Bjy],'m','linewidth',[2]);
    plot([Bjx,Pjx],[Bjy,Pjy],'g','linewidth',[2]);
    patch([Ajx,Bjx,Pjx],[Ajy,Bjy,Pjy],'g')
    plot(Pjx,Pjy,'o','linewidth',[3]);
    grid on
    axis([-10 25 -10 25])
end
hold off
```

SISTEMI ARTICOLATI - ESERCIZIO 3 – Generazione di traiettorie per 3 punti di precisione

Progettare un q.a. in cui un punto di biella descriva una traiettoria ellittica passante per 3 punti di precisione.

DATI

$\delta_2 = -1.4 - 0.76i \qquad \beta_2 = 126° \qquad \beta_2{}^* = 33°$

$\delta_3 = -1 - 2.3i \qquad \beta_3 = 252° \qquad \beta_3{}^* = 37°$;

Scelti ad arbitrio:

$\alpha_2 = -6°$

$\alpha_3 = 37°$

Si calcoli, il modulo e la fase di **W, Z**, **W*, Z***. Si disegni inoltre il quadrilatero articolato nelle tre posizioni desiderate.

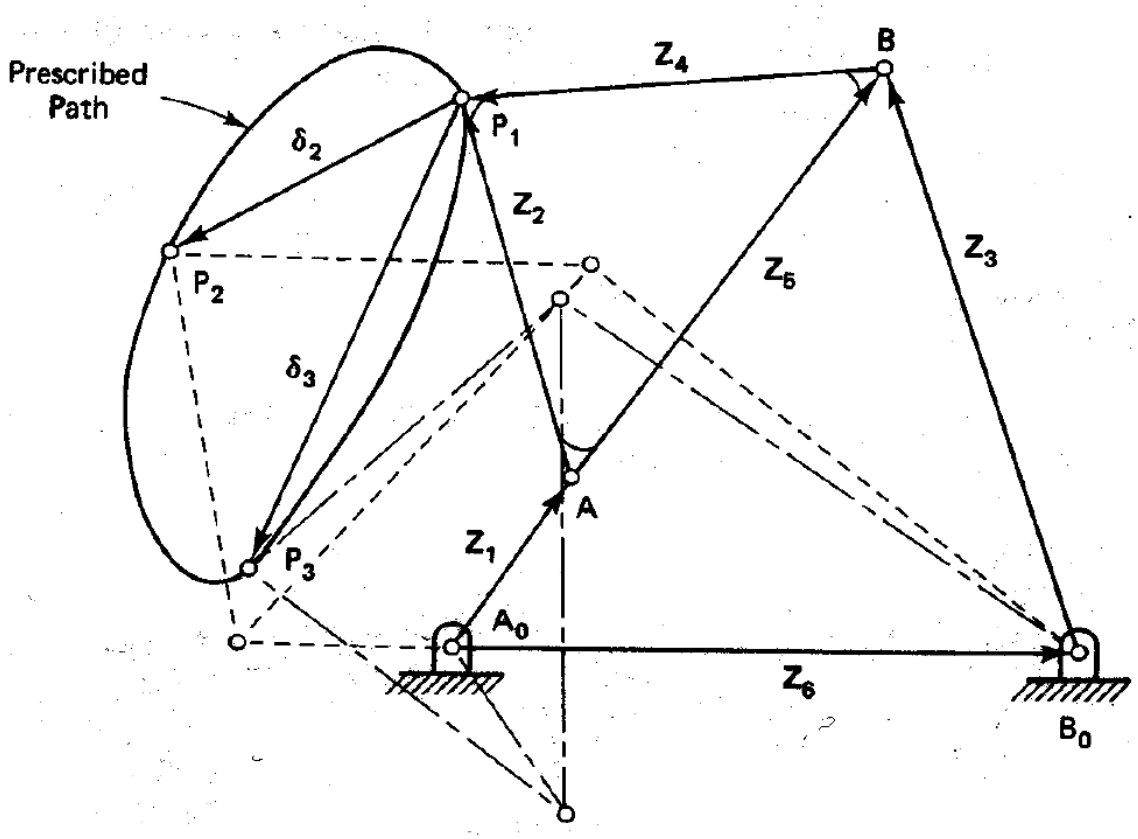

La traccia di soluzione non viene fornita poiché analoga all'esercizio di guida di corpo rigido.

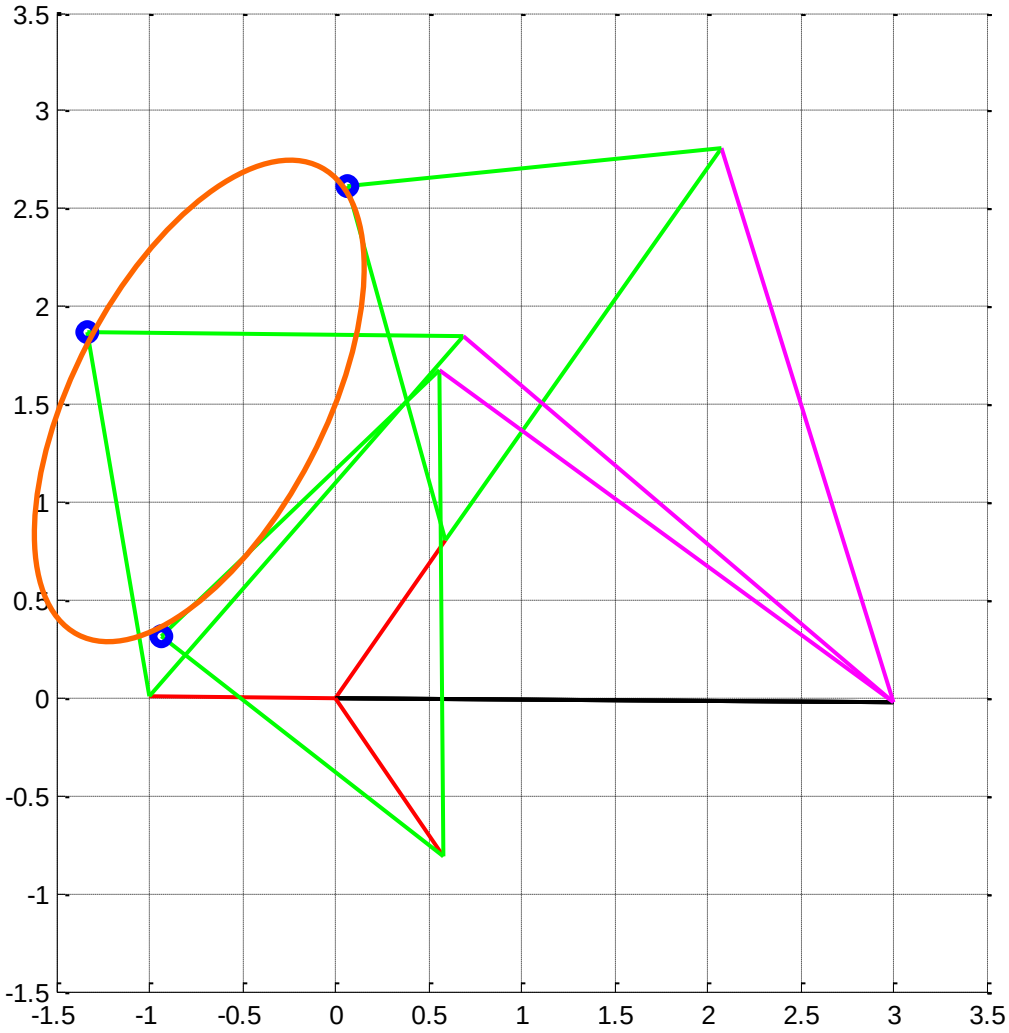
3.5
3
2.5
2
1.5
1
0.5
0
-0.5
-1
-1.5
-1.5
-1
-0.5
0
0.5
1
1.5
2
2.5
3
3.5

SISTEMI ARTICOLATI - ESERCIZIO 2 – Generazione di funzioni (3 posizioni)

Progettare un meccanismo per movimentare schienale e poggiapiedi della poltrona in figura.

DATI del primo quadrilatero

$\beta_2 = 50°$ $\qquad$ $\beta_2^* = 22.5°$

$\beta_3 = 75°$ $\qquad$ $\beta_3^* = 45°$

Scelti ad arbitrio:

$\alpha_2 = 7°$
$\alpha_3 = 12°$; $\qquad$ $W^* = 0 - i$;

DATI del secondo quadrilatero

$\beta_2 = 22.5°$ $\qquad$ $\beta_2^* = 40°$

$\beta_3 = 45°$ $\qquad$ $\beta_3^* = 70°$

Scelti ad arbitrio:

$\alpha_2 = 8°$
$\alpha_3 = 13°$; $\qquad$ $W^* = 0 + i$;

Si calcoli, per ognuno dei due q.a. il modulo e la fase di **W e AB**(segmento di biella). Si disegnino inoltre i quadrilateri articolati nelle tre posizioni desiderate.

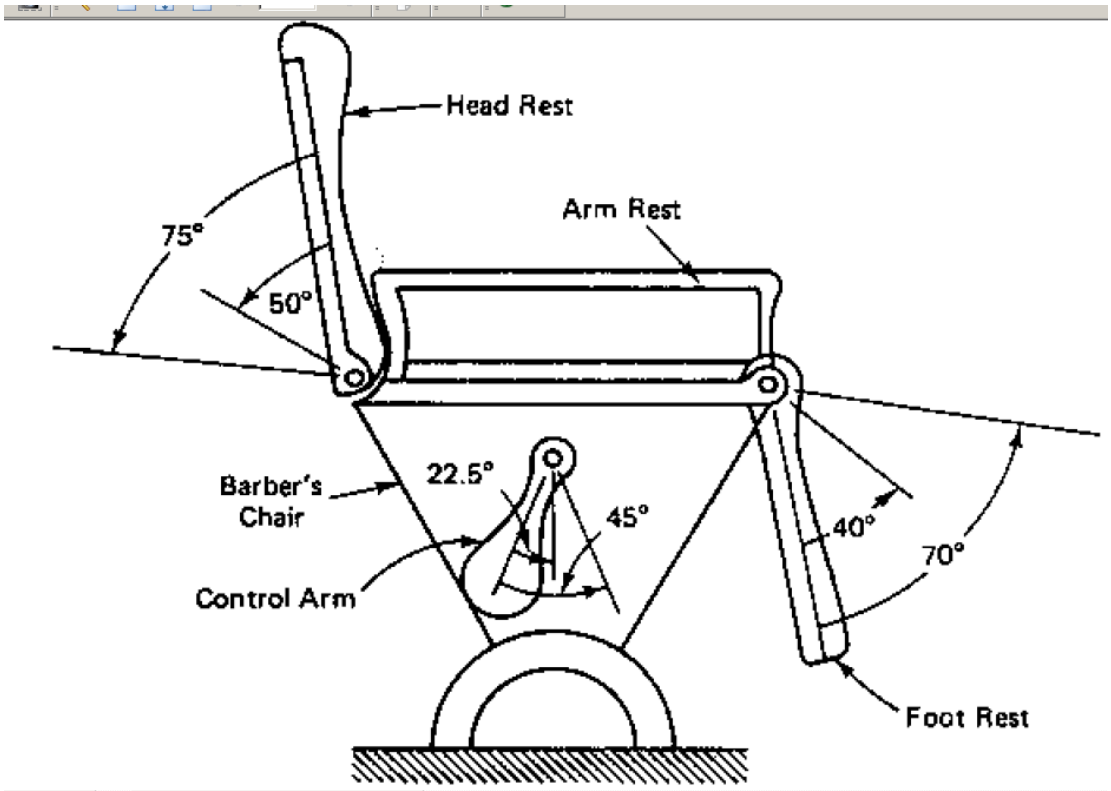

Occorre che il primo quadrilatero(regolatore dello schienale) per una rotazione di 22.5° e 45° del "control arm" sposti lo schienale di 50° e 75° rispettivamente.
Occorre che il secondo quadrilatero(regolatore del poggiapiedi) per una rotazione di 22.5° e 45° del "control arm" sposti il poggiapiedi di 40° e 70°.

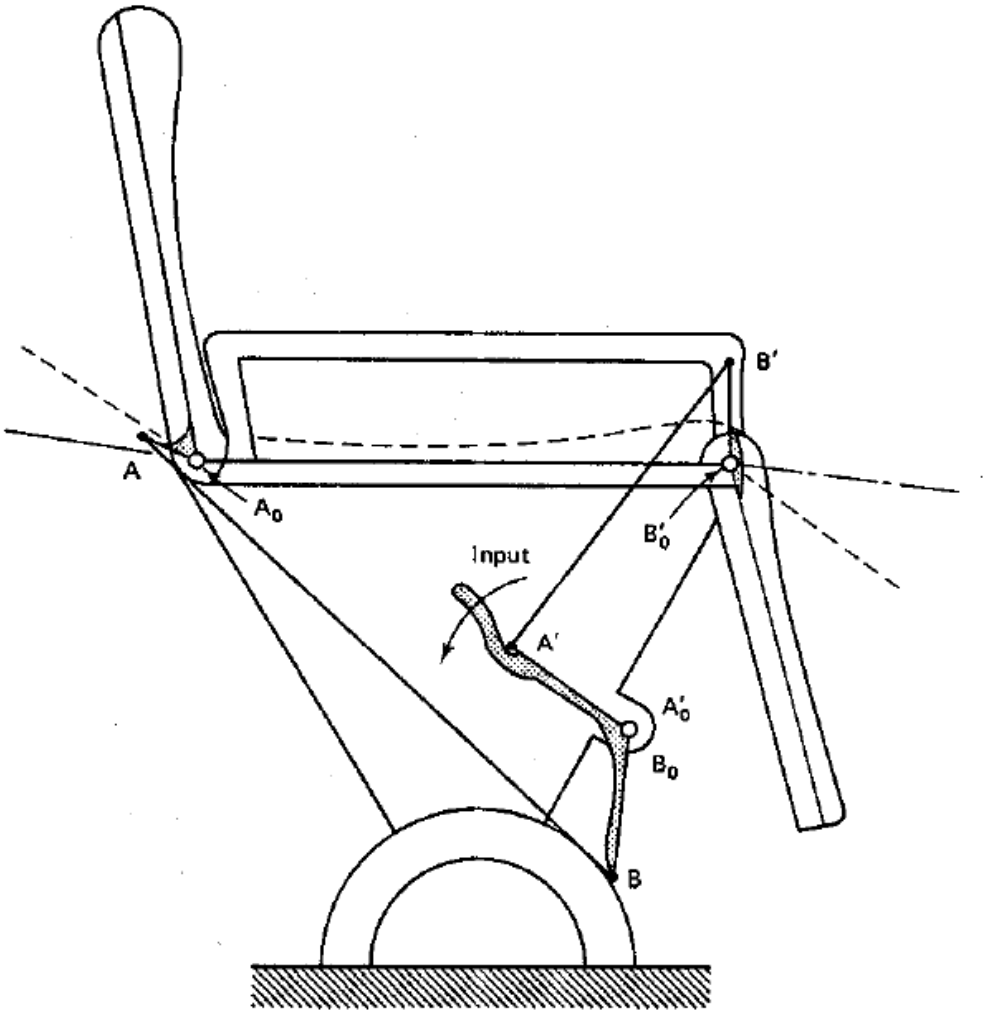
B'
A
A_0
B'_0
Input
A'
A'_0
B_0
B

TRACCIA DI SOLUZIONE per il quadrilatero 1- Suggerimenti per programma in Matlab:

1) inizializzare le variabili:

```
g_2_r=pi/180;  %traforma gradi in radianti
beta(2)=
betastar(2)=
…
alfa(2)
Wstar_scelto=-i;
delta(2)=Wstar_scelto*(exp(i*betastar(2))-1);
...
```

2) definire la matrice A (mediante i coefficienti a,b,c,d,
3) definire la matrice B

risolvere il sistema lineare: `X=A\B;`

4) calcolare il modulo di W e AB (usa il comando *abs*)
5) calcolare la fase di W e AB (usa il comando *angle* e poi trasforma in gradi)

usa *fprintf* per mostrare a video i risultati di modulo e fase – `fprintf('modulo di AB:     %0.3f \n',abs(X(2)));`

6) Disegnare il quadrilatero articolato ottenuto nelle tre posizioni

```
%%%PLOT DEI RISULTATI%%%%%%%%%%%%%%%%%
```

```
figure('position',[100 100 600 600])
hold on
for j=1:3
    W=X(1)*exp(i*beta(j)); %da notare che quando k=1 beta(1)=0
    Wstar=Wstar_scelto*exp(i*betastar(j));
    AB=X(2)*exp(i*alfa(j));
    A0B0=W+AB-Wstar;  %è il telaio
    %disegno per punti il quandrilatero
    A0x=0;
    A0y=0;
    B0x=real(A0B0);
    B0y=imag(A0B0);
    Ajx=real(W);
    Ajy=imag(W);
    Bjx=real(W+AB);
    Bjy=imag(W+AB);


    plot([A0x,B0x],[A0y,B0y],'k','linewidth',[2]);
    plot([A0x,Ajx],[A0y,Ajy],'r','linewidth',[2]);
    plot([Ajx,Bjx],[Ajy,Bjy],'g','linewidth',[2]);
    plot([B0x,Bjx],[B0y,Bjy],'m','linewidth',[2]);

    grid on
%     axis([-0.5 4 -3.5 1])
end
hold off
```

7) Ripeti per il secondo quadrilatero

Cosa accade ai quadrilateri articolati se la scelta arbitraria di W* si riduce del 50% in modulo?

Esempio di RISULTATI

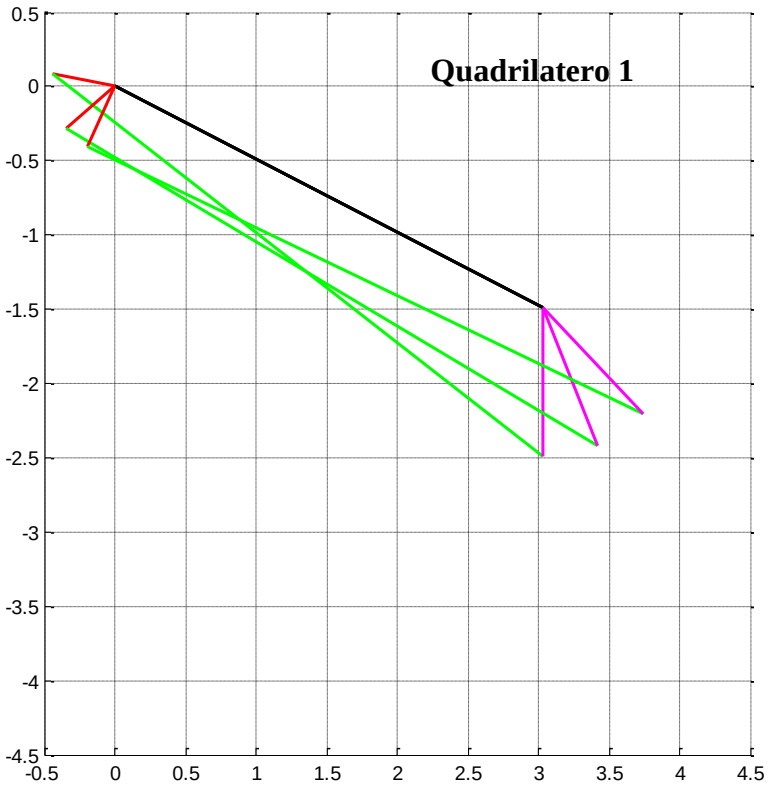

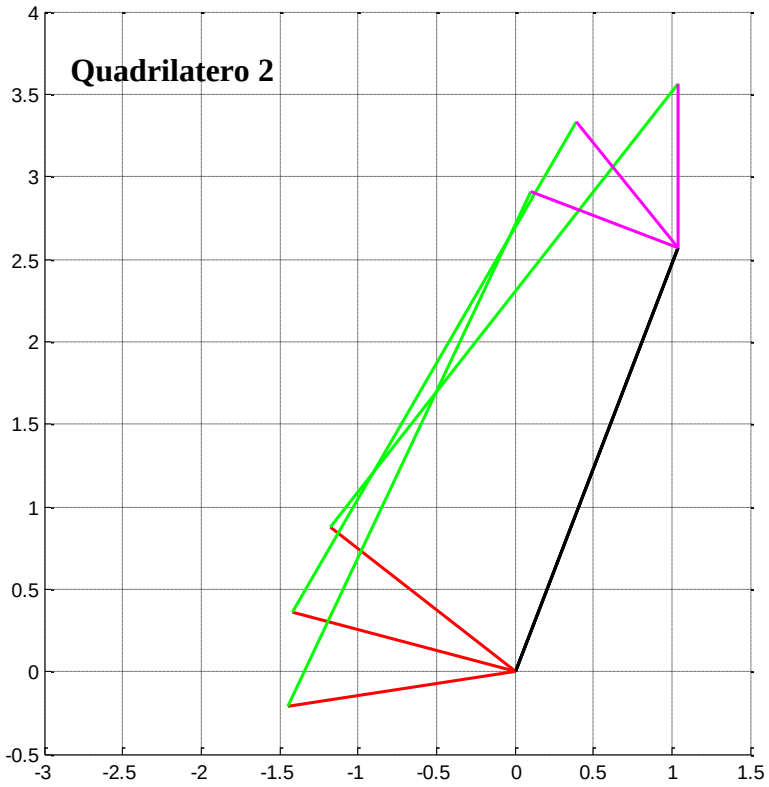

SINTESI DI
SISTEMI ARTICOLATI
CON ATLANTI
DI TRAIETTORIE

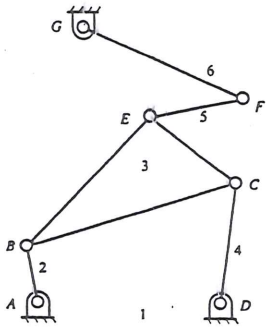

Figure 4.51 Six-link mechanism that can be designed using coupler curves.

4.5.1 Design of Six-Bar Linkages Using Coupler Curves

Coupler curves from four-bar linkages and slider-crank mechanisms are used in two main ways. The first is to use the motion of the coupler in the area of the curve to perform some function. A common use for such points is in packaging and conveying equipment. Figure 4.49 shows a coupler mechanism design for packing hay in a round bale.[17] Figure 4.50 shows a mechanism which has been used to feed film in a motion picture projector.[18]

A second use for coupler curves is to facilitate the design of six-link mechanisms where the output link is to have a prescribed motion relative to the input link. Such a mechanism is represented schematically in Fig. 4.51, where link 2 is the input and link 6 is the output. The output dyad (links 5 and 6) is driven by the coupler point (E) of the four-bar linkage. By properly selecting the coupler curve, different functional relationships between ϕ and θ can be achieved. This is illustrated in the following two examples.

EXAMPLE 4.4 *(Design of a Six-Link Dwell Mechanism Using Coupler Curve)*

PROBLEM

A mechanism of the type shown in Fig. 4.51 is to be designed such that link 6 is an oscillating lever and link 2 rotates a full 360°. The output link is to oscillate through a range of 30° during the first 120° of crank rotation. Link 6 is then to dwell for 90° of crank rotation and return during the remaining 150° of crank rotation.

SOLUTION

To solve this problem, it is necessary to have access to an atlas of coupler curves or to use a program that can generate the coupler curves. Regardless of the procedure used, we must be able to determine the geometry of the curve and the travel distance along the curve as a function of input rotation. In the Hrones and Nelson atlas and in the programs *hr_crankrocker.m* and *hr_slidercrank.m* provided on the disk with this book, a dashed line is used for each 5° of crank rotation. We will use the four-bar program *hr_crankrocker.m* to generate candidate coupler curves. The first step is to visualize the shape of coupler curve that can be used to drive links 5 and 6. Several different geometries might be used, but the simplest is a curve of roughly elliptical shape. The coupler curves used are displayed in Figs. 4.52 and 4.53, and the design procedure is shown in Fig. 4.54. The procedure is described in the following:

1. Test different coupler curves to determine whether a portion of the curve in the vicinity of the minor axis is roughly circular in shape for the desired dwell period (90°). Figure 4.52

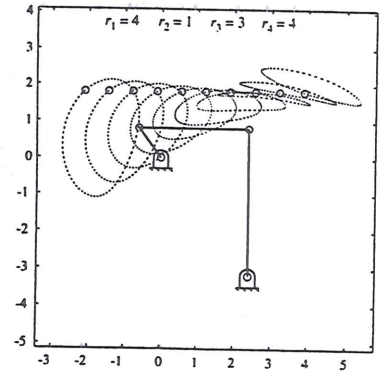

Figure 4.52 Coupler curves for Example 4.4.

gives a set of curves generated with the program *hr_crankrocker.m* when $r_1 = 4$, $r_2 = 1$, $r_3 = 3$, and $r_4 = 4$. From the curves displayed, we will select the curve shown in Fig. 4.53.

2. After a coupler curve is identified, find the center of the circle that best fits the circular region identified in step 1. The radius of the circle will be the length of link 5. Identify explicitly the beginning and end of the circular portion of the curve. The center of the circle arc will be one extreme position for point *F*. This is shown in Fig. 4.54, where the mechanism has been redrawn so that the frame link (r_1) is horizontal.
3. Point *F'* corresponds to the second extreme position of *F*. To locate *F'*, identify the point on the coupler curve corresponding to 120° of crank rotation beyond the dwell. Locate a perpendicular line to the coupler point at this point, and locate *F'* on this line.
4. The pivot *G* must be located on the perpendicular bisector of the line *FF'*. Locate *G* such

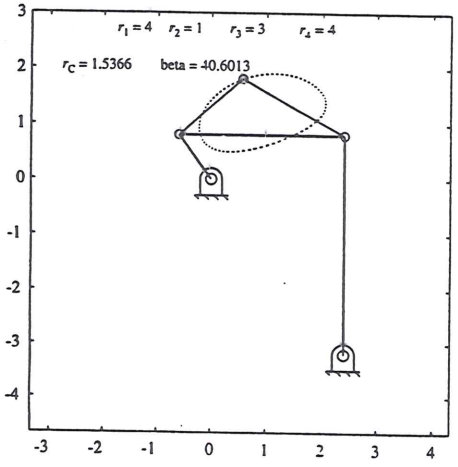

Figure 4.53 Coupler curve chosen for design.

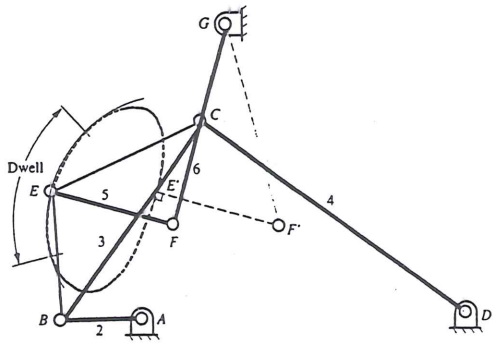

Figure 4.54 Design procedure for mechanism in Example 4.4.

that the angle *FGF'* is 30°. The parameters corresponding to the solution are

$r_1 = 4$ $r_5 = 1.682$ $BE = 1.537$

$r_2 = 1$ $r_6 = 2.694$ $\beta = 40.6°$

$r_3 = 3$ $G_x = 0.697$ $\theta_1 = 0$

$r_4 = 4$ $G_y = 3.740$

5. Compute and plot the motion of link 6 relative to link 2 to evaluate the design. The resulting mechanism is simply a four-bar linkage with the addition of two more links (Watt's six-bar

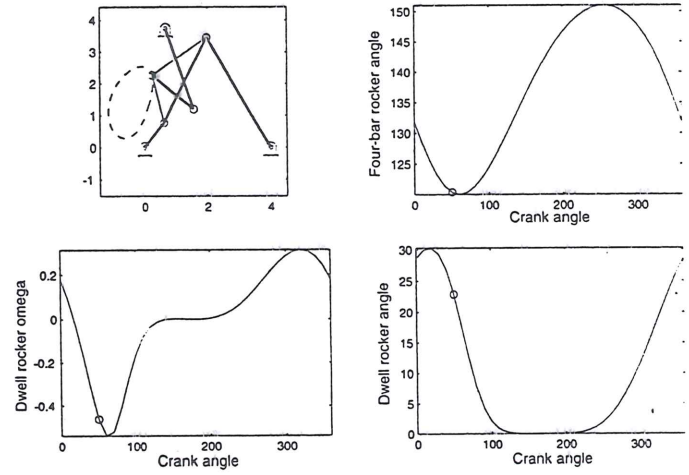

Figure 4.55 Analysis of linkage designed in Example 4.4. The velocity plot is based on a crank velocity of 1 rad/s.

mechanism). The two additional links are called a dyad and can be easily analyzed using the procedures given previously. A MATLAB routine (*sixbar.m*) for a six-bar linkage analysis based on the four-bar and dyad routines is provided on the disk with this book. Part of the analysis from this program is given in Fig. 4.55. The results are close to the design specifications, and the basic design is acceptable. Note in Fig. 4.55 that the angular velocity of link 6 is approximately zero during the dwell. The input (crank) velocity was 1 rad/s. ■

This design procedure can yield a large number of candidate designs. The best designs can be chosen by using some kind of evaluation criterion. Typical criteria are linkage size, force transmission characteristics, and acceleration characteristics.

EXAMPLE 4.5 ***(Design of a Six-Link Mechanism for Double Oscillation)***

ROBLEM A mechanism of the type shown in Fig. 4.51 is to be designed such that link 6 will make two complete 30° oscillations for each revolution of the driving link.

OLUTION For this problem, no timing information is required. Therefore, we need only ensure that the output link makes two complete oscillations for one oscillation of the input crank. Again, we will use the four-bar program (*hr_crankrocker.m*) to generate candidate coupler curves. The first step is to visualize the shape of coupler curve that can be used to drive links 5 and 6. One curve that will work for this type of problem is a figure-8 curve. The design procedure is shown in Fig. 4.56 and described in the following:

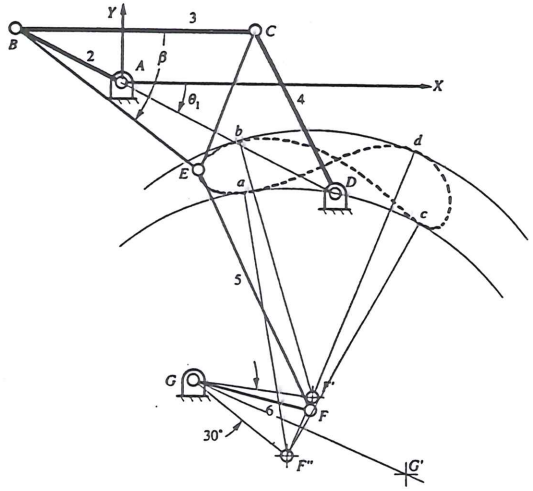

Figure 4.56 Procedure for designing linkage for Example 4.5.

1. Select a coupler curve that is a figure-8 curve with roughly equal lobes. The coupler curve selected is displayed in Fig. 4.57.

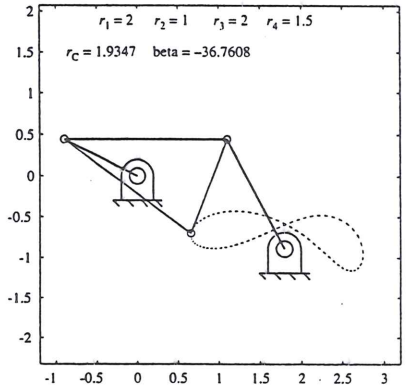

Figure 4.57 Curve that can be used for Example 4.5.

2. After the coupler curve is identified, select the length of link 5 and draw a circle or circle arc with a radius equal to the length of link 5 and tangent to the coupler curve at the two points *b* and *d*. The center, *F'*, of this circle is one extreme position of point *F*. Draw another circle or circle arc of the same radius tangent to the coupler curve at points *a* and *c*. The center, *F''*, of this circle is the second extreme position of *F*.
3. The pivot point, *G*, must be located on the perpendicular bisector of the line *F'F''*. Locate *G* such that the angle *F'GF''* is 30°. Link 6 is the link from *F'* to *G* (or from *F''* to *G*). Note that there are two possible locations for point *G*. The location *G* is chosen in this example over *G'* because it will result in better transmission characteristics. If point *G'* is chosen, the linkage will lock up before it traverses its entire range of motion because the distance *G'b* is slightly larger than (*EF* + *FG*). The parameters corresponding to the solution are

$r_1 = 2$	$r_5 = 2.231$	$BE = 1.929$
$r_2 = 1$	$r_6 = 1.010$	$\beta = -36.44°$
$r_3 = 2$	$G_x = 0.633$	$\theta_1 = -26.57°$
$r_4 = 1.5$	$G_y = -2.292$	

4. Compute and plot the motion of link 6 relative to link 2 to evaluate the design. This is done in Fig. 4.58 based on the program (*sixbar.m*) provided on the disk with this book. Again, the input (crank) velocity was chosen as 1 rad/s.

The results given in Fig. 4.58 are very close to the design specifications. If more accurate results are desired, the location of *G* or the lengths of r_5 or r_6 could be adjusted slightly. This can be done manually or by using an optimization program that minimizes the error created by the linkage. However, even if an optimization program is used, the graphical procedure, which is very simple and quick to apply, is a good means of generating an initial estimate of the optimum solution. ■

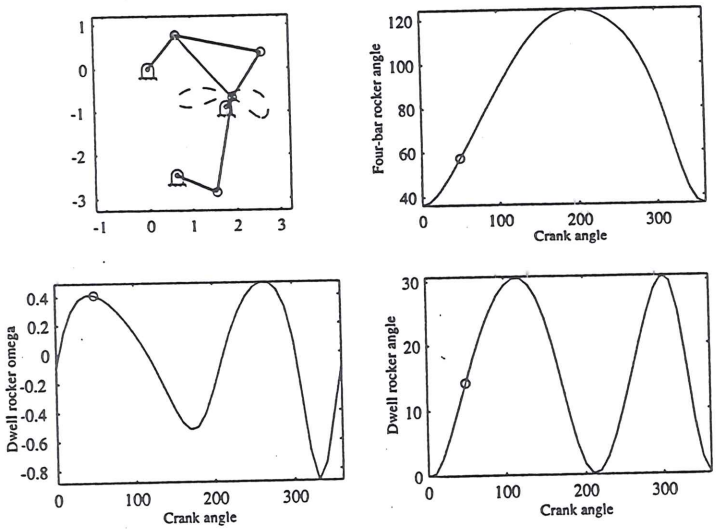

Figure 4.58 Analysis of mechanism designed for Example 4.5.

How to use and interpret the Coupler Curve and Centrode Atlas

In order to view the images, your browser must be able to interpret frames, and you will have to have Adobe Acrobat Reader installed on your computer. It is available for free download .

Once you have Acrobat working properly on your machine, the atlas page should work properly. You may peruse the images by varying the parameters in the left frame by obvious means. In order to obtain the best possible scale for your image in the right hand frame, I suggest that you go to Acrobat in a separate window, and excecute the following: File--> Preferences--> General--> Default Magnification--> Fit Page. Once you have a set of curves which appears interesting, you may zoom in or out using the soft buttons provided within your browser by Acrobat.

Each image has lines and curves of several different colors. Below is an explanation of the meaning of these colors as well as the four-bar linkage parameters which determine the shapes of the curves.

The image shown here is a four-bar mechanism with parameters labeled. The two double (concentric) circles represent pin joints located on a fixed link. This ground link is labelled *d*. Links *a* (the input link) and *c* (the output link) pivot about these pin joints. In turn, the coupler link (the blue triangle) is pinned to link *a* at A and to link *c* at B. The coupler point P is located at some interesting position on the coupler link. As link *a* is rotated, the coupler point will trace out a special path called the coupler curve.

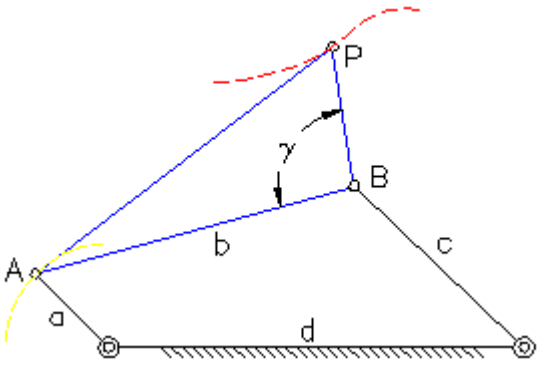

Four-bar mechanism (not to scale)

The following parameters are necessary to determine a unique four-bar mechanism coupler curve: the lengths *a*, *b*, *c*, *d*, and BP; and the angle gamma which line segment BP forms with line segment AB. In order to pack more information on each image, several values of BP are shown on each graph. In the atlas, they are all indicated by small black circles on the edge of the coupler triangle, all originally located along the x-axis.

To further reduce the number of images necessary, the value of *a* is set to 1 cm on all graphs. To obtain results for a different length *a*, simply scale the whole graph.

If the double circles represent fixed pivots, why are they shown in different positions on various pages of the atlas? For the purpose of easy comparison, the various coupler points in the mechanism's starting position are always plotted along the x-axis. The rest of the mechanism is rotated enough to be plotted in a congruent starting position.

The colors' meanings are below.

- The red lines are coupler curves.

- The yellow line is the path of point A (it may not make a full rotation).
- The green line is the fixed centrode.
- The magenta line is the moving centrode. It is an imaginary curve which describes the motion of the coupler in a meaningful way. As the moving centrode rolls on the fixed centrode, it moves with the same motion as the coupler link. Thus, the moving centrode could be considered to be fixed to the coupler.

Each dash in the curves mentioned above represents 5^{o} of rotation of line *a*, as does each of the gaps between the dashes.

Return to Four-bar Coupler Curve and Centrode Atlas main page.

If you beleive there are major omissions of information on this page you may contact:
thompson@cedarville.edu

http://www.cedarville.edu/cf/engineering/kinematics/ccapdf/fccca.htm

IL QUADRILATERO ARTICOLATO.

Regola di Grashof

Siano a il lato più corto, b il lato più lungo, c e d le aste intermedie.

a + b < c + d	quadrilateri di Grashof	(Figura 1: primo, secondo e quarto caso)
a + b > c + d	quadrilateri non di Grashof	(Figura 1: terzo, quinto e sesto caso)
a + b = c + d	caso limite (Figura 2)	

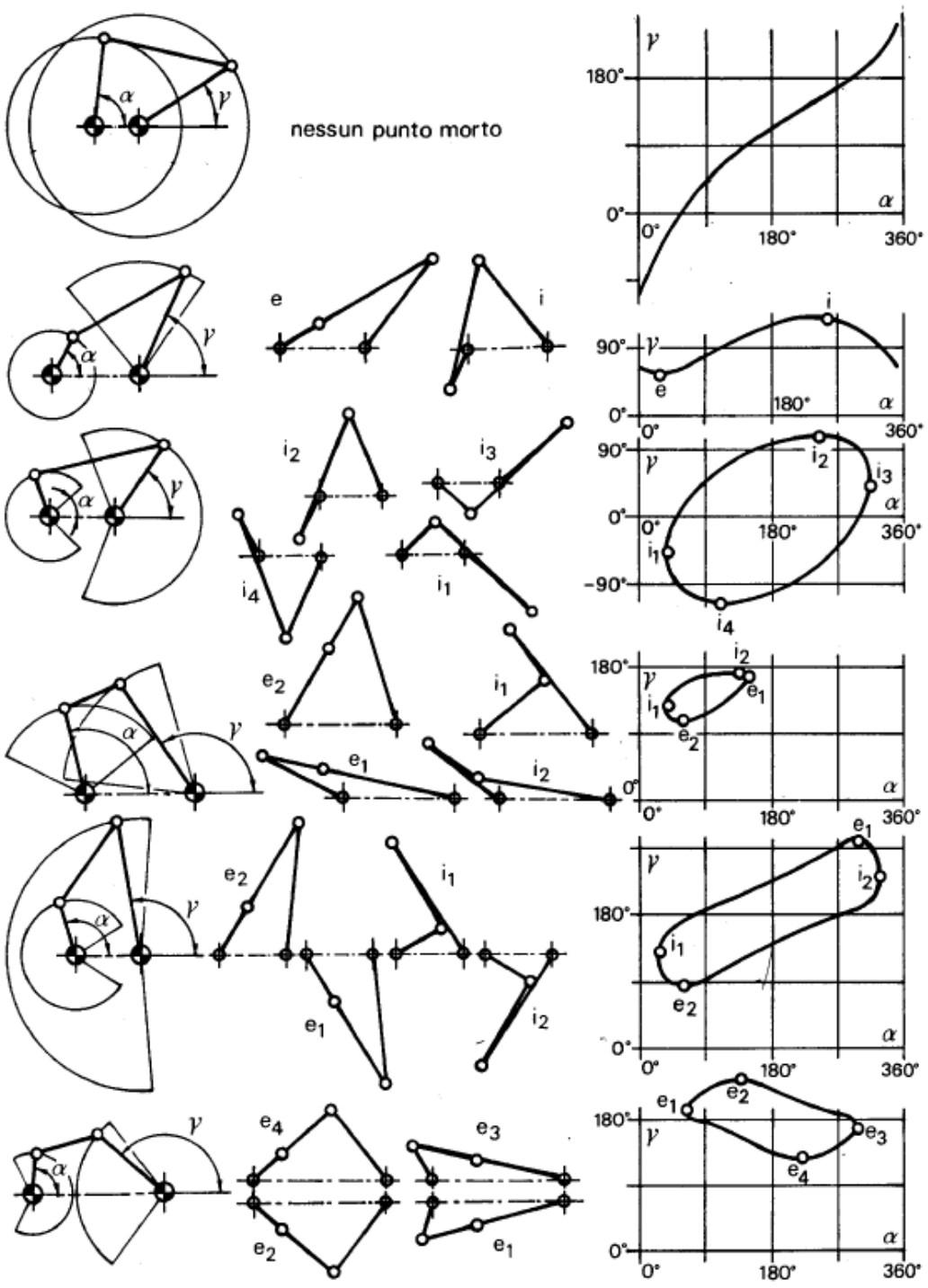

[8]